Mechanical Properties of Selectively Degraded Cartilage Explants: Correlation to the Spatiotemporal Distribution of Glycosaminoglycans

by

Ralph Gregory Allen

B.S., Mechanical Engineering
San Diego State University, 1992

Submitted to the Department of Mechanical Engineering
in partial fulfillment of the requirements for the degree of

Master of Science
at the
Massachusetts Institute of Technology

September 1996

Author.....
Department of Mechanical Engineering
August 1, 1996

Certified by.....
Martha L. Gray, Ph.D., Thesis Supervisor
J.W. Kieckhefer Associate Professor of Medical and Electrical Engineering

Accepted by.....
Ain A. Sonin, Ph.D.
Professor of Mechanical Engineering

Mechanical Properties of Selectively Degraded Cartilage Explants: Correlation to the Spatiotemporal Distribution of Glycosaminoglycans

by

R. Gregory Allen

Submitted to the Department of Mechanical Engineering in partial fulfillment of the requirements for the degree of Master of Science, August 1, 1996.

Abstract

The efficient operation of synovial joints in the human body depends upon the integrated performance of several physiological members, cartilage being one. Cartilage is the dense connective tissue covering the ends of long bones. It endows the synovial joints with the functional characteristics of load distribution, resiliency, and low-friction articulation. These properties are determined by the extracellular matrix of cartilage, which is a hydrated network composed principally of a heterogeneous distribution of collagen and aggregating proteoglycans. It is well known that the anionic dissacharides of proteoglycans, glycosaminoglycans, are important contributors to the mechanical integrity of cartilage. With relevance to diseases of cartilage (e.g., osteoarthritis) an immunomodulatory cytokine called interleukin-1ß has been implicated in eliciting glycosaminoglycan degradation. The action of interleukin-1ß has been demonstrated *in vitro* to elicit the production of matrix-degrading enzymes from perivascular cells.

The objective of this study was to examine the relationship between glycosaminoglycan content and equilibrium and dynamic stiffness over physiologically relevant frequencies. More specifically, it was the intention of this study to determine whether this relationship was affected by the spatial distribution of glycosaminoglycan degradation. This was accomplished by monitoring the mechanical properties of explanted cartilage samples subjected to selective enzymolysis. Two *in vitro* techniques of inducing different modes of spatial degradation were used: treatment with interleukin-1ß and the direct addition of proteolytic enzymes (like hyaluronidase, chondroitinase, or trypsin).

Epiphyseal cartilage was explanted from the distal ulna or femoropatellar groove of 1-2 week-old calves, cut into 2mm-thick plane-parallel slices and punched into 3 or 4mm diameter disks. Explants were cultured in radially-unconfined conditions for up to two weeks in an incubator-housed displacement-based mechanical spectrometer. A series of measurements of stiffness were performed to monitor the time-course effects of enzymolysis. The dimethylmethylene blue dye-binding assay was used to assess the glycosaminoglycan content remaining in the tissue explants and the amount released to the culture media over the incubation period.

The key findings were that (1) untreated control samples showed a monotonic decline of equilibrium stiffness and a slow, steady release of glycosaminoglycans; (2) direct enzymolysis produced an immediate and accelerated decrease in equilibrium stiffness whereas the effects of interleukin-1ß were similar, but sometimes delayed; (3) for each condition (with or without treatment), the trends for stiffness and glycosaminoglycan release were correlated, but the drop in equilibrium stiffness was earlier and of greater magnitude than the drop in glycosaminoglycan content; and (4) the drop in dynamic stiffness, at all frequencies tested and for all modes of degradation, followed a time course intermediate to that seen for equilibrium stiffness and glycosaminoglycan content, with the special mention that the "high" frequency stiffness (~1Hz) exhibited near-identical kinetics and proportions of change as the glycosaminoglycan content.

This thesis demonstrated that the spatial pattern of glycosaminoglycan depletion cannot be discerned from the correlated measurements of stiffness and glycosaminoglycan content. Interestingly, the relative changes in the 0.88Hz relative dynamic stiffness directly correlated with the changes in glycosaminoglycan content ($R^2 = 0.9233$), implying that mechanical measurements could be used to predict the relative glycosaminoglycan content, or vice versa.

Acknowledgments

The culmination of three years of arduous effort in the Continuum Electro*moo*chanics Laboratory are proudly inscribed in the pages that follow. This thesis is the greatest accomplishment of my life, and for this I acknowledge Professor Martha Gray. In addition to her enviable qualities of enthusiasm and patience, Martha's skillful guidance brought this thesis to fruition.

For their friendship and encouragement, I thank the members of my lab group for significantly ($p<.01$) contributing to my experiences at MIT. Dr., at last, Sandip Biswal; from my very first day in the lab through Appendix B of this thesis, Sandip shared his precious time without hesitation, without flinching, and always with a smile. He freely dispensed his knowledge of cartilage trivia and performed endless demonstrations of laboratory procedures. Not surprisingly, his work is heavily referenced throughout the following pages. Sharing lab space with Dan Sobek was very exciting, especially when he needed to work in the dark! Mr. Dan, the man with a plan to arrive in California ASAP! Red or white? Arthur Liu, where are you? For the many discussions/interpretations of experimental results I am indebted to Arthur. The incessant cheerfulness of Shelly-Ann Davidson brightened up the lab; her enthusiasm was very much appreciated, especially at the conclusion of my thesis writing when computers crashed and deadlines came rushing forward. Adil Bashir, who never really knew how close he was to sudden danger, was a constant provider of enthusiastic pessimism and *bald* comments. Well Adil, I hope all your hair falls out, too, and, oh yeah, thanks for the hat! Ann Black, who commanded the everyday laboratory operations with efficiency, provided endless encouragement and positive criticism to everyone, and guarded my chemicals with heroic tenacity. And on a serious note, thank you Ann for all your help (a phrase that I must have said at least a thousand times). I am thankful to Linda Bragman for her encouragement to persevere and providing psychological counseling on a moment's notice!

I shall always fondly remember Professor Alan Grodzinsky. In describing his several endearing qualities, of which decorum prevents me from complete enumeration, let it suffice that: first, my presence here is direct result of his limitless capacity to maintain an amicable faculty-student relationship (unlike someone else who I shall refrain from mentioning); and second, he is a pillar of high fashion which is evident through his efforts to enforce a high degree of dress-code professionalism in the lab. Even though Eliot Frank, Al's right hand man, was a tremendous resource for scientific discussion, his sense of humor and friendship were even more meaningful and appreciated. Where's my Electromechanics shirt? Words cannot express how grateful I am for becoming friends with Dr. Tom Quinn; a great experimentalist and theoretician who wouldn't bat an eye at the opportunity to disrobe for science. Thanks to fellow San Diegan Minerva Garcia

for her friendship and preserving the peace in the lab. I also thank Steve Treppo and Paula Ragan for their thoughtful considerations of my work.

I am grateful for having had the opportunity to discuss the art of cartilage squeezing to the Cochlear Physiology Group. In particular, their enthusiasm and willingness to momentarily set aside their research projects and critique my first conference talk (and then listen to it over and over and over and over ...) was wholeheartedly appreciated. Thank you Tom, Denny, AJ, Cameron, Quinton, and Zoher.

Working with Lisa Freed, Gordana Vunjak-Novakovic, Vicky and Predrag was, even up to the very last minute (!!), very exciting and rewarding. Passing on the hands-on knowledge is a crucial component of research, and I am grateful to have finally had the opportunity to do so.

I would have succumbed to this work if it were not for the emotional support of Jennifer Stinn, who carried me through the hectic pace of these final months. Raising my spirits by enforcing fun-filled weekend activities will forever I be grateful. I should mention that the absence of typos and clarity of the text in the main body of this thesis is due to Jen's editorial efforts and scientific critique. I promise to get some sleep and quit drinking coffee, ... well, we'll see!

The love and encouragement from my family provided the emotional nourishment to endeavor the frustrations of graduate school and gave me will to conquer MIT. Thank you Dad, Mom, Leslie and James! The same is true for my friends abroad who understood the months of silence and provided the ears to listen and the shoulders to lean on. Well, it's time to lock the doors and light the fires, it's nearly "wheels up" for my plane to San Diego!

Two closing comments that equivocate how I feel about cartilage and research in general: First, contrary to popular opinion, cartilage is NOT an avascular tissue. Second, on work ethics I offer a paraphrased USMC slogan: "First in, last out, kick ass while you're there ..."!

Financial support was provided by Proctor & Gamble, The National Science Foundation, The National Institutes of Health, and the J.W. Kieckhefer Foundation.

Table of Contents

List of Figures

INTRODUCTION

MATERIALS AND METHODS

RESULTS

DISCUSSION

List of Tables

MATERIALS AND METHODS

DISCUSSION

Introduction

Of the many splendid physical activities available for us to enjoy in this life, all demand the performance of a seemingly simple and passive connective tissue called *cartilage*. One of the many baseline operations that our bodies routinely perform is the smooth operation of articulating joints. Virtually a physiological concert, this process is orchestrated by the superposed contribution of several tissues, consisting of the skeletal, ligamentous, cartilaginous, and musculotendon systems. Controlled joint operation is realized in synovial joints by the relative motion of long bones. The musculotendon system provides the actuation for joint motion and the ligaments keep the skeletal system connected. Cartilage, which covers the ends of long bones, contributes to the normal function of these synovial joints. Its function is crucial in that it provides low-friction contact surfaces between apposed joints and it effectively bears, distributes, and reduces contact loads transmitted to the skeletal system. This becomes painfully obvious when the joint experiences such pathologies as rheumatoid arthritis or osteoarthritis. Characteristic of these diseases are varying degrees of joint dysfunction, all resulting from the destruction and degeneration of cartilage.

Therefore, cartilage functionality is, in part, defined as its ability to support a mechanical load. Clinically observed osteoarthritic lesions include fibrillation of the articular surface, degeneration of the bulk tissue, and deep running fissures exposing the underlying bone. Concomitant to these macroscopic defects is a compromised resiliency (Bullough 1992) manifested as a mechanical softening of the tissue.

Ideally, the mechanical integrity of cartilage should be quantifiable. Monitoring such mechanical properties as equilibrium and dynamic modulus would provide a descriptive characterization of functionality. The experimenter has several conditions from which to select as to how mechanical properties should be measured, all of which pose technical difficulties. Defining *challenging* as encompassing the actual act of acquiring information and subsequently interpreting that information, *in vivo* observation of mechanical properties is arguably the most challenging. While preserving the natural environment of the synovial joint, the physical application of mechanical stimuli as well as the elucidation of material properties are non-trivial. Retaining cartilage on its subchondral bone, or *in situ* observation, is a close runner-up. This experimental regime approximates *in vivo* conditions, but the joint capsule is opened and separated, with the exposed cartilage left intact on the end of the bone. Typical measurements of mechanical properties for *in situ* studies are performed with an indentor apparatus. Although this may lessen some experimental restrictions from the *in vivo* model, interpretation is hindered by the necessary assumptions of the properties of the underlying bone and boundary conditions of the

indentor and cartilage-bone interface. From an engineering perspective, the precise control of a sample's geometry is the first step towards straightforward measurement of mechanical properties. Dissecting cartilage into cylindrical disks and maintaining the disks in an explant culture system allows the information-rich mechanical properties to be readily assessed. Furthermore, *in vitro* organ culture affords more control over exogenously added perturbations to the tissue than *in vivo* and *in situ* systems.

Cartilage is essentially a porous gel of aggregating macromolecules, called proteoglycans, contained within a water-swollen network of collagen fibrils. Proteoglycans are constructed of linear polysaccharides termed glycosaminoglycans covalently attached to a protein core. Conceptually, the glycosaminoglycans behave like sponges, osmotically imbibing water into the tissue. The extent to which the tissue can swell is determined by the collagen, which entraps the proteoglycans. Under physiological conditions, this confinement prevents proteoglycans from realizing their full swelling capacity.

It is well known that glycosaminoglycan concentration is an important determinant of mechanical properties (Buckwalter et al. 1988). The variation in tissue stiffness observed in a single joint has been attributed to the non-uniform distribution of glycosaminoglycans (Jurvelin et al. 1988; Kempson et al. 1970). The available literature reveals that as early as 1944 there was an interest in the correlation of mechanical indentation properties to the chemistry of cartilage (Hirsch 1944). Since then, several studies have examined the effects on tissue mechanics by controllably inducing the release of glycosaminoglycans. The ubiquitously agreed upon effect of glycosaminoglycan extraction is too diminish the mechanical integrity of cartilage explants, observed as varying degrees of reduction in equilibrium and dynamic stiffness (Bonasser et al. 1994; Frank et al. 1987) and other mechanical indices of performance (e.g., compressive creep strain (Kempson et al. 1976), tensile creep strain (Schmidt et al. 1990), equilibrium "structural stiffness" and damping coefficient (Bader et al. 1992), and shear modulus (Parsons and Black 1987)). However, it is evident that knowledge of the glycosaminoglycan content is not sufficient for predicting material properties. Data in the literature indicates that cartilage from different species having the same glycosaminoglycan content have different mechanical properties.

However, it is interesting to consider that *changes* in glycosaminoglycan content within a given tissue sample are predictive of the *changes* in its mechanical properties. With this premise as its foundation, the objective of this study was to examine the relationship between tissue glycosaminoglycan content and mechanical stiffness (equilibrium and dynamic). More specifically, it was intended to determine whether this relationship is affected by the spatial distribution of degradation. In short, this was accomplished by investigating the kinetics and proportional change in stiffness (equilibrium and dynamic) and glycosaminoglycan content with respect to the mode of degradation as induced by treatment with (1) interleukin-1ß and (2) by direct

addition of proteolytic enzymes such as hyaluronate-lyase, chondroitinase-ABC, and trypsin. The aim of this study was conclusively addressed by combining this data, thereby correlating the relationship of stiffness to glycosaminoglycan content for the two spatially-distinct modes of glycosaminoglycan depletion.

Background

Although it is abundant in various other places in the body, the young epiphyseal cartilage of articulating joints was the object of study in this thesis. The term from which cartilage is derived, *cartilago* (L.), meaning gristle, conjures a mental image of texture with an ambiguous reference to function. To the eye, cartilage appears amorphous and translucent. However, the complexity of articular cartilage lies at a lower, microscopic level.

Cartilage structure

Articular cartilage, a type of hyaline cartilage, is the load bearing, near-frictionless covering of the ends of long bones in synovial joints. In young animals before the sub-chondral bones fully develop, the cartilaginous regions of these joints are comprised of two types of cartilage: articular cartilage on the surface, and the underlying epiphyseal cartilage. A schematic representation of articular-epiphyseal complex (Figure 1.1) highlights the articular surface, secondary bone-forming centers, progenitor cartilage (the type used in these experiments and is synonymously referred to as "epiphyseal cartilage"), and the underlying bone. Through maturation, the epiphyseal cartilage is transformed into bone. Epiphyseal cartilage found in the distal ulna and femoropatellar groove of young calves has a few distinct differences from adult articular cartilage, which motivated its use for our experiments. Most significantly, the abundance of epiphyseal cartilage allows experiments to use tissue from a single animal, reducing the effects of animal-to-animal biological variation.

Hyaline cartilage consists primarily of water and a sparse population of cells which reside in a plentiful matrix of various macromolecules. There are two principle macromolecular components of the extracellular matrix (ECM): collagen (Type II), which forms a fibrillar network that gives cartilage its tensile strength, and proteoglycans (PGs), which impart compressive strength. The collagenous network interacts with the proteoglycans and other noncollagenous proteins through chemical binding reactions or steric hindrances and this entire framework is filled with fluid.

The cells, called chondrocytes, are responsible for maintaining the mechanical integrity of the tissue by regulating the synthesis and degradation of the collagens, proteoglycans, and other structural components of the extracellular matrix. The active involvement of the cell in this continuous remodeling process is modulated by various exogeneous signaling mechanisms. The

biosynthetic and degradive potential of chondrocytes is influenced by mechanical signals (Gray et al. 1988; Quinn 1996) and chemical messengers like interleukin-1ß (discussed below).

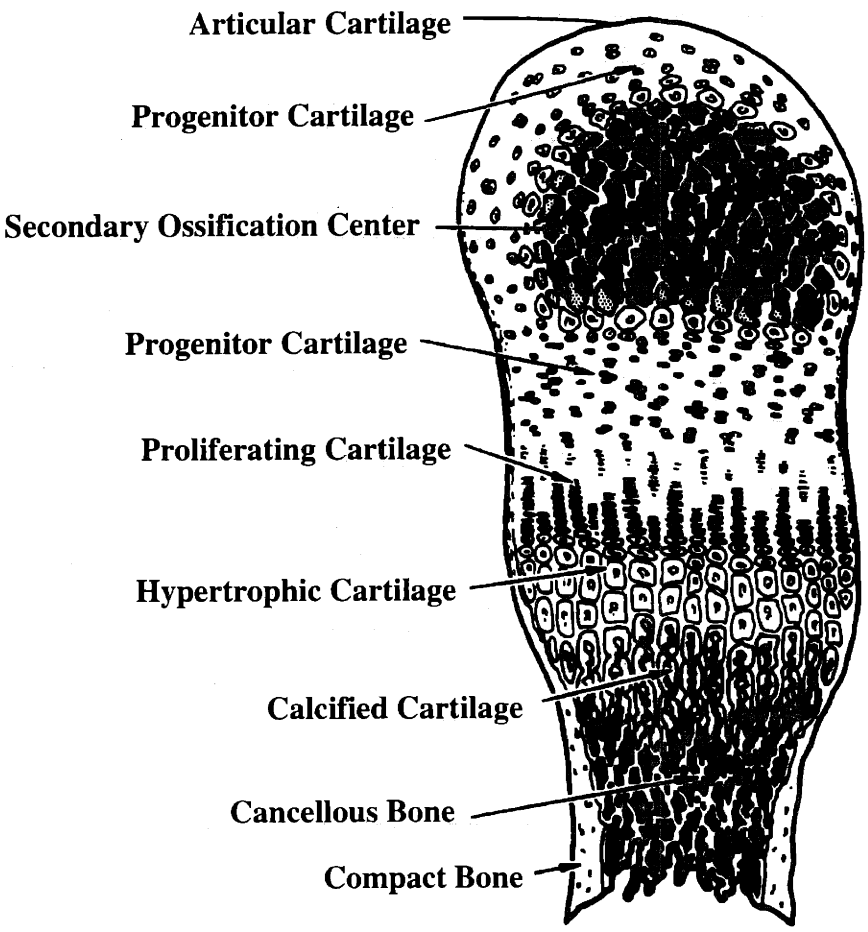

Figure 1.1: Diagrammatic representation of the epiphyseal apparatus (adapted from (Wuthier 1968). Tissue explants in this thesis were harvested from the "progenitor cartilage" region. The cartilage from this region, also called "epiphyseal cartilage", differs from that of the articular surface in that it is typically more plentiful in the young joint.

Cartilage biochemistry

The most important chemical component of cartilage, with respect to the scope of this thesis, is the glycosaminoglycan. It serves as a basic component of larger, more complicated structural elements that lend cartilage its poroelastic mechanical behavior.

In nature, six species of glycosaminoglycans have been identified in cartilaginous tissue: two types of chondroitin, keratin, hyaluronate, heparin, and dermatan (Figure 1.2). A glycosaminoglycan is a polyanionic carbohydrate that is comprised of a repeating disaccharide unit. This unit contains an amino sugar, which is typically sulfated, and an acidic sugar, which is ionized at physiological pH. The degree of sulfation varies, but its occurrence, combined with the titrated carboxyl group of the acidic sugars, gives glycosaminoglycans their highly negative electric charge.

The degree to which glycosaminoglycans are sulfated is not only important for their functionality, but is required for our biochemical measurement of glycosaminoglycan content. Spectrophotometric assays which use dimethylmethylene blue require several concatenated glycosaminoglycans and histological staining procedures utilizing *toluidine blue O* require negatively charged sulfate and carboxyl groups for positive results.

Glycosaminoglycans exist as unbound individual disaccharides or as disaccharides (or many repeating disaccharides connected in a linear fashion) covalently attached to a protein core (Figure 1.3). However, they are only mechanically relevant when present in the latter form, which is called a proteoglycan. Of course, there are several types of proteoglycans found in cartilage. The list includes the large aggregating proteoglycans called "aggrecan" and the smaller interstitial proteoglycans, biglycan, decorin, and fibromodulin.

Of principle relevance to this study is the structure and function of aggrecan. Aggrecan is composed of protein (7% by mass), chondroitin sulfate (87%), and keratan sulfate (6%) (Heinegard and Oldberg 1989). Figure 1.3 depicts the construction of a single aggrecan monomer as a protein core with covalently bonded keratin sulfate and chondroitin sulfate glycosaminoglycans. The 220kD core protein ranges from 180nm to 210nm in length and serves as the unifying element in these aggregating monomers. Specific regions along the core filament have been identified as keratan sulfate and chondroitin sulfate attachment sites. To these linkage points, linear chains of chondroitin sulfate, which may exceed 100 in number, radiate outward from the protein core. The glycosaminglycans remain separated from each other in three-dimensional space due to electrostatic interactions, giving aggrecan its "bottle brush" appearance.

Chondroitin-4-Sulfate

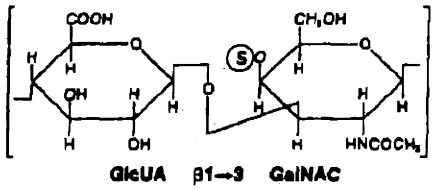

Chondroitin-6-Sulfate

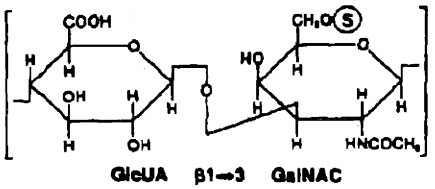

Keratan Sulfate

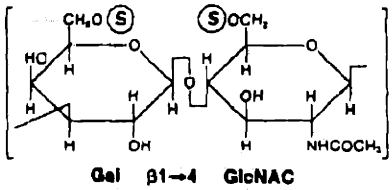

Hyaluronic Acid

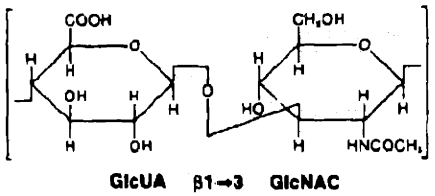

Heparin Sulfate

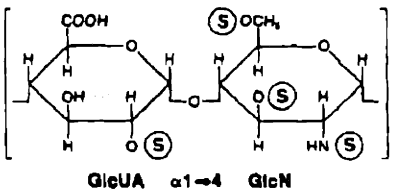

Dermatan Sulfate

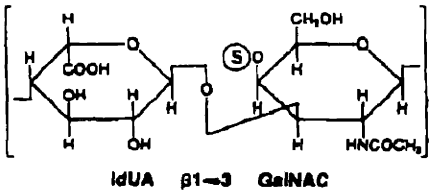

Figure 1.2: Glycosaminoglycan chemistry. The basic disaccharide repeating unit (GlcUA: glucuronic acid; GalNAC: N-acetylgalactosamine; GlcNAC: N-acetylglucosamine; Gal: galactose; IdUA: iduronic acid) and the sulfated moieties Ⓢ.

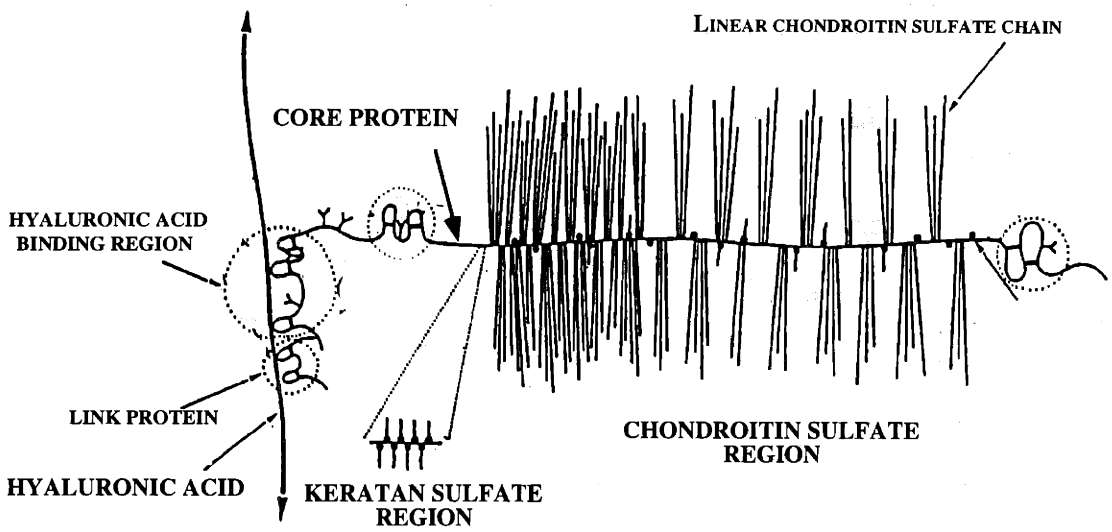

Figure 1.3: Aggrecan monomer. The chondroitin sulfate and keratan sulfate glycosaminoglycans are covalently bonded a single protein core, which noncovalently associates with a backbone filament of hyaluronic acid (Heinegard and Oldberg 1989).

The aggrecan monomers are subsequently assembled into larger proteoglycan aggregates. Through non-covalent interactions numerous aggrecan monomers assimilate onto a common carbohydrate backbone of hyaluronic acid. An unbranched, unsulfated glycosaminoglcyan, hyaluronic acid can extend from 40,000nm to 420,000nm in length and accommodate an aggrecan monomer approximately every 2500nm (Rosenberg et al. 1975). With a length scale of significant proportions, the filamentous hyaluronic acid intertwines with other matrix macromolecules, namely collagen, contributing to a massive structural scaffold.

The physicochemical properties of the aggregated proteoglycans contribute to the load-bearing, lubricating, and resilient aspects of cartilage. The highly anionic glycosaminoglycans give the aggregate macromolecule a signature "fixed" negative charge. The significance of this fixed charge density is two-fold: through electrostatic interactions the glycosaminoglycans resist mechanical compression and by the necessary presence of counter-ions in the interstitial fluid, water is osmotically entrained within the tissue. The swelling capacity of cartilage is enhanced by the density of fixed charges and restrained by the tensile forces of the collagen network. A

mechanical equilibrium state is achieved with the swelling pressure balanced by the restraining forces of the collagen. When cartilage is compressed, a series of events occur which define its resiliency. In response to a compressive load fluid is exuded from the extracellular matrix causing an increase in fixed charge density. The loss of water increases the tissue swelling potential, contributing to an increased resistance to compression (Maroudas 1979). Upon relaxation of the compressive load, the cartilage returns to its initial equilibrium state by imbibing water back into the tissue. Therefore, the contribution of aggregating proteoglycans (and the collagen network) is crucial to the normal function of cartilage and any circumstance in which the integrity of the glycosaminoglycans is diminished would result in decreased resiliency.

Role of interleukin-1ß in cartilage destruction

The interleukins belong to a family of soluble proteinaceous factors which are involved in the coordination of local and systemic immune responses. Any member of this family is non-specifically referred to as a cytokine, which implies a certain capacity for autocrine, paracrine, and/or endocrine effects. Enumerating the biological effects of interleukin-1 is a task of galactic proportions, therefore let it suffice that the incomplete set of traits exhibited by this cytokine are: inflammatory (i.e., immunomodulatory) (Goldring and Goldring 1991), metabolic (Bedard and Golds 1993; Morales and Hascall 1989), degradive (Arner and Pratta 1989; Smith et al. 1989), and protective (Dinarello 1991), and it has been implicated in the pathogenesis of vascular diseases (Clinton et al. 1991) and arthritis (Duff et al. 1988; Wood et al. 1985). Of the three known interleukin-1's in existence (Dinarello 1991), only a description of interleukin-1ß, the most potent and predominant variety (Biswal 1996; Demczuk et al. 1987), is necessary here.

The addition of interleukin-1ß to *in vitro* culture systems elicit the release of proteoglycan fragments (Campbell et al. 1986). However, the action of interleukin-1ß does not directly induce catabolic events, rather, it binds to specific cell-membrane receptor sites thereby inducing a multitude of intracellular processes. The result is the upregulation of the synthesis (MacNaul et al. 1990) of matrix metalloproteinase precursors and their subsequent secretion into the extracellular compartment. Although the mechanism of activation is unclear, these latent and inactive precursors (e.g., prostromelysin and procollagen) are transformed into highly efficient proteolytic enzymes (stromelysin and collagenase, respectively). Stromelysin exhibits a wide range of destructive capacity in that it degrades proteoglycans, collagens (including type II), and a wide variety of cartilaginous glycoproteins. Collagenase is well known for its efficiency in cleaving collagen (including type II) fibers, but it has also been found to digest proteoglycans (Hughes et al. 1991).

The effects of interleukin-1ß on cartilage explants have been studied in our laboratory. Interleukin-1ß has been shown to cause a dose-dependent release of glycosaminoglycans from

epiphyseal cartilage explants (Biswal 1996; Lai 1993). The concomitant decline in mechanical properties (static load and dynamic stiffness) and glycosaminoglycans content have been observed (Chang 1992). The spatiotemporal modality of glycosaminoglycan depletion has been characterized histologically and is described, in brief, in Appendix B.

Cartilage biomechanics

An understanding of the basic concepts of cartilage mechanics is important for the interpretation of its deformational behavior. This biomechanical behavior of cartilage is best described as "poroviscoelastic", a term which encompasses the viscoelastic qualities of the solid components (collagens and aggregating proteoglycans) and the fluidic resistance to deformation through the porous matrix.

Mechanical equilibrium (i.e., no fluid flow) is achieved when a compressive load is completely balanced by the swelling force, which has electrostatic and non-electrostatic contributions. The electrostatic contribution arises from the presence of sulfated glycosaminoglycans and the non-electrostatic component stems from the intrinsic stiffness of the solid phase. In this thesis, the term *equilibrium stiffness* is used to describe the resistance to compression exhibited by a cartilage sample and is defined as the incremental increase in equilibrium load in response to a small deformation.

Alternatively, significant fluid flows may result within the extracellular matrix in response to time-varying mechanical stimuli. The frictional drag introduced by the forced flow of tissue water around the solid components introduces an increased resistance to compression. The redistribution of the tissue fluid in response to an incremental step in displacement elicits a transient response. For time-varying displacements the mechanical response of cartilage exhibits a transient decline to an oscillatory steady-state. For the range of frequencies tested in this thesis (0.004Hz - 0.88Hz) the frequency response of cartilage has linear characteristics (Appendix A), which has also been demonstrated over a greater frequency window by Lee *et al* (1981).

The culture conditions used here specified that cartilage explants be prepared into cylindrical discs and cultured in radially unconfined, axially confined conditions. Measurements of equilibrium and dynamic stiffness were made by imposing uniaxial static and dynamic compressions, respectively, between two impermeable platens. This "unconfined" compression arrangement allows the tissue sample free to exude its fluid and/or expand in the radial direction. Complications arise at the cartilage-platen interface, where friction (or the lack thereof) influences the mechanical response of the tissue. The presence of friction would elevate the internal stresses of the tissue and result in a higher observed stiffness than when friction is absent.

An analytical expression has been developed that models the behavior of a "cartilage" sample compressed with frictionless boundary conditions (Armstrong et al. 1984). For a step in compressive displacement, the model-based solutions for internal deformations and externally observable stress relaxation indicate an instantaneous change in volume and that the material behaves as an incompressible solid. With time, the model demonstrates that the transient fluid flow diminishes the internal fluidic pressure gradients until equilibrium is achieved with the external fluid bath. Furthermore, this model illustrates that the extent to which the fluid flow (constrained to the radial direction) penetrates into sample is frequency dependent. However, this model has been shown to underpredict experimentally observed values of dynamic stiffness, presumably due to the frictionless boundary condition.

Subsequently, Kim developed numerical methods that included the effects of interfacial friction (Kim 1989). Compared to the frictionless model, the effect of the "adhesive" boundary condition on the predicted value of dynamic stiffness was minimal at low frequencies but resulted in significantly elevated values at high frequencies. These boundary conditions shifted the predicted frequency response closer to that observed empirically, indicating that interfacial friction is indeed an important factor in the unconfined compression of cartilage.

Both of these models are instructive, however, in their qualitative conceptualization of the physics of the dynamic stiffness. Low frequency displacements were demonstrated to induce the movement of large volumes of fluid. At high frequencies cartilage is approximately incompressible (very little relative motion of the fluid and solids). Most interestingly, there is a frequency dependent transition region characterized by the simultaneous decrease in fluid movement and increase in internal hydrostatic pressure. Although these models to not precisely agree with experimental data in magnitude, they do provide some insight as to the mechanisms by which the dynamic stiffness increases with frequency.

Objectives

The purpose of this thesis was to investigate the relationship between the mechanical properties and glycosaminoglycan content of explanted cartilage. Specifically, it was intended to determine if this relationship was affected by the spatial distribution of glycosaminoglycan degradation. This study was approached by following these three objectives:

1. To investigate the kinetics and proportions of change of stiffness (equilibrium and dynamic) and glycosaminoglycan content with respect to the mode of degradation as induced by treatment with interleukin-1ß.
2. Same, but treatment with the direct addition of proteolytic enzymes (such as hyaluronate lyase, chondroitinase-ABC, and trypsin).
3. To determine the relationship of stiffness (equilibrium and dynamic) to glycosaminoglycan content for both modes of degradation.

Materials and Methods

Introduction

In order to measure the mechanical properties of cartilage explants several methods and protocols had to be established and verified. Fortunately, some were already existent and were adapted to suit the objectives of this thesis. This section covers the details of harvesting and preparing cartilage for long-term culture, the specific culture/compression chambers used, the preparation of the enzymes and cell-regulator used to induce tissue degradation, the means by which the mechanical properties were determined, and the biochemical techniques employed to quantify the release of glycosaminoglycans.

Tissue explantation and preparation

All tissue used in this study was calf-bovine in origin and of 1-2 weeks in age. From a local abattoir, A. Arenas Co. of Hopkinton, MA, we obtained foreleg ulnar-metacarpal and hindleg femoropatellar groove joints. These joints were delivered cold, intact and completely encapsulated in periochondrium and musculature by tissue delivery professionals (Research 87, Boston). In the rare occurrence that dissection did not immediately follow delivery, the tissue was stored at 4°C (for a period of time that never exceeded 2 hours).

Ulna-derived tissue

Under *quasi*-sterile conditions aided by a biosafety cabinet, the ulnar-metacarpal joint was relieved of its surrounding musculature, periosteal, and perichondral connective tissues. Isolating the ulna from the radius facilitated the separation of the epiphysis from the metaphysis. This separation was accomplished by manually bending the ulna until it virtually "snapped" in half. This process consistently yielded separation at the interface of the *hypertrophic* cells of the growth plate and *calcified* cartilage region of the metaphysis. Discarding the remaining tissue, the epiphyseal "apparatus" (which includes articular cartilage, the underlying secondary center of ossification, epiphyseal cartilage {a.k.a. *progenitor* cartilage}, and growth plate) was immersed in Hank's Balanced Salt Solution containing 1% antibiotics/antimycotic (see below). By clamping the end of the epiphysis containing the articular cartilage and the secondary center of ossification in a device such that only the epiphyseal cartilage was exposed, tissue was sectioned with an

American Optical (Buffalo, NY) sledge microtome. The first slice boldly sectioned away ~1mm of tissue; simultaneously creating a flat surface and removing the growth plate. Subsequently, "plane-parallel" slices (of which two could be regularly obtained) were cut to 2mm-thickness. Five or six 3mm-diameter discs, often referred to as "plugs", were harvested from each slice by using a dermal punch. Plugs were placed separately into the wells of a culture dish and incubated in 1.0ml of culture medium. The culture medium was composed of Dulbecco's Modified Eagle Media (DMEM) supplemented with 10mM HEPES, 0.1mM non-essential amino acids, 0.4mM proline, 2mM glutamine, 1% (v/v) of an antibiotics/antimycotic cocktail (stock solution consists of 10,000U/ml penicillin, 10mg/ml streptomycin, and 25μg/ml amphotericin-B in 20ml of sterile, distilled and deionized water) 1% (v/v) heat inactivated fetal calf serum, and 50μg/ml ascorbate. The explant plugs were cultured in an incubator at 37°C, 5% CO_2, and ~95% humidity for up to two days before mechanical testing was initiated. The geometrically friendly ulnar-derived explants (3mm in diameter by 2mm in thickness) typically numbered in the five to twelve range, which was more than adequate for a single experiment.

Femoropatellar groove-derived tissue

Conveniently, the same abattoir was a source for the completely intact foreleg itself. Delivered under the same conditions, the leg arrived into the laboratory with intact musculature and perichondral connective tissues encapsulating the femoropatellar groove. The ensuing dissection was performed on the bench-top, being the only suitable space available for handling such a large package. Since the dissection was performed in the questionably sterile laboratory environment, the joint was frequently rinsed with Hank's Balanced Salt Solution supplemented with 1% by volume of the antibiotics/antimycotic solution. The musculature and periosteum were systematically removed, beginning from the proximal femur and working towards the groove. Care was taken not to penetrate the perichondrium prematurely. With the musculature removed, the joint capsule was exposed by cutting through the perichondrium and then the cruciate ligaments were severed; thereby isolating the femur and exposing the femoropatellar groove. Cutting the femur in half with a bone saw allowed for insertion into a clamp device. With the joint immobilized, several 3/8" "cores" were drilled from the lateral and medial sides of the groove by drilling directly into the chondyle at a near-perpendicular angle of attack. The drill press was configured to have a slow rotational speed and the drill bit was continuously lubricated with cold, sterile, Hank's Balanced Salt Solution supplemented with 1% antibiotics/antimycotic. Again, the bone saw was used to free the cores from the underlying trabecular bone by severing the chondyles. Thus, numerous 3/8"-diameter cylinders (cores) were explanted, each with

approximately 5mm of cartilage atop 10mm of subchondral bone. These cores were clamped into the sledge microtome for sectioning. As with the ulnar-derived tissue, the material was faced off by removing the first ~1.0mm (which included the articular surface). The remaining underlying epiphyseal cartilage was sectioned into 2mm-thick discs from which were promptly punched to yield either four 3mm-diameter plugs or three 4mm-diameter plugs (depending upon the experiment). As above, the abundance of epiphyseal cartilage, characteristic of young joints, yielded a venerable cornucopia of plugs; five of which were cultured in supplemented media for up to two days before mechanical testing.

Culture conditions: media preparation

Throughout the course of every culture experiment in this thesis the culture media was changed on a regular basis depending upon the frequency of mechanical testing (typically once a day, but this was not the case for every experiment). Old media was collected and frozen at -20°C for further biochemical analysis. For ongoing cultures, the old media was replenished with fresh media. This being the case, it was necessary to have a large volume of culture medium at hand during an experiment. Base culture media was prepared in 500ml batches and stored at 4°C. Fresh media refers to the supplementation of the base media with certain substances (e.g. 1% by volume of ascorbate, L-glutamine, heat inactivated fetal calf serum, and antibiotics/antimycotic) that are presumably unstable in solution at culture conditions and begin to break down. The base media formulation was as follows:

Table 2.1: Formulation of Base Media

Amount (ml)	Base Media Constituent
200	25mM HEPES DMEM
300	DMEM
5	10 mM NEAA
2	100 mM Proline

The supplemented media was typically prepared in 10ml volumes and consisted of:

Table 2.2: Formulation of Supplemented Media

Amount (ml)	"Fresh" Supplemented Media Constituent
0.100	2mM L-Glutamine
0.100	20mg/ml ascorbate dissolved in 0.5 ml of base media
0.100	antibiotic/antimycotic
0.100	heat inactivated fetal calf serum
9.6	base media

Culture conditions: culture-compression chambers

Cartilage explants were cultured for up to two weeks during the course of mechanical testing in special chambers. Machined from polysulfone (Westlake Plastics, Lenni, PA), an autoclavable plastic, these chambers allowed for the long-term culture of cartilage explants in the incubator-housed mechanical spectrometer. The construction of these chambers satisfied the culture requirements by retaining up to 2.0ml of culture media, venting to the atmosphere of the incubator (allowing for gas exchange and maintaining the culture medium at atmospheric pressure) and by being equipped with a syringe coupling for the exchange of culture media. The compression chamber, as its name implies, facilitates the mechanical compression of cartilage plugs. The cylindrically-shaped test specimen, surrounded by fluid, rests on the bottom of the compression chamber with a quartz compression post located superiorly and in axial alignment. The vertical translation of the post, guided through the chamber lid, transmits relative displacements from the TCS (see below) to the tissue sample. The observed stiffness of the entire compression apparatus (in the absence of cartilage) ranges from 0.2-0.4MN/m, whereas a 4mm-diameter by 2mm-thick cartilage disc generally exhibits an equilibrium stiffness of approximately 3.0kN/m. Since the *system* is two orders-of-magnitude stiffer than the *cartilage* it was presumed that any observed equilibrium or low-frequency displacements corresponded solely to tissue deformation. However, the dynamic stiffness of cartilage increases with frequency in the range of 0.05Hz to 1.0Hz, such that system compliance may need to be considered (Appendix A).

The compression post and chamber material are impermeable to aqueous media. Therefore, this axially-confined, radially-unconfined loading configuration of cartilage restricts fluid transport and solute diffusion to the radial direction only.

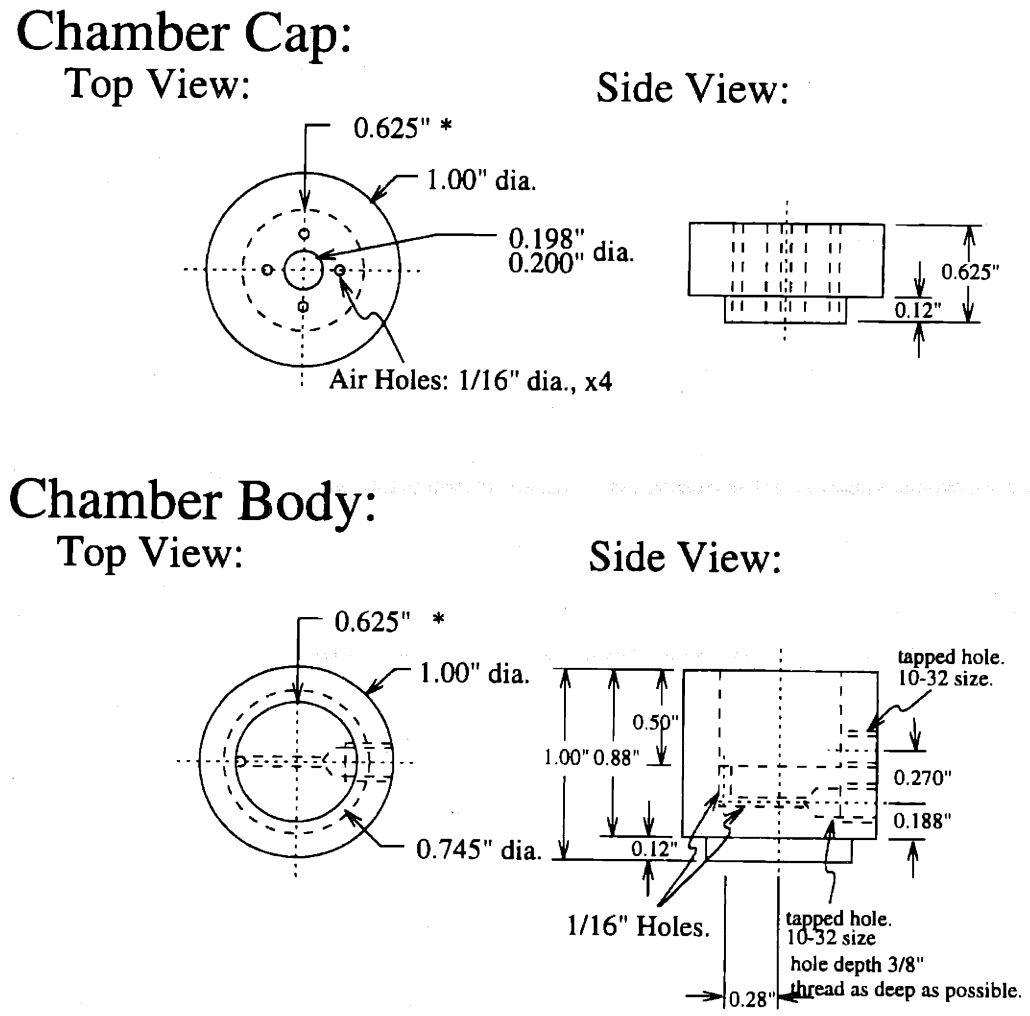

Figure 2.1: Culture-Compression Chamber Design.
Schematic drawing of compression chamber components (cap and body). Machined out of polysulfone, an autoclavable plastic, each chamber allows for the long term culture of a single cartilage explant. A quartz compression post slides through the cap and axially confines a cartilage "plug" with the base. The seat of the base fits into a clamp in the lower platen of the TCS, thereby anchoring the compression chamber. The quartz compression post is brought into contact with the thrust button of a load cell. Capillary ports, drilled and tapped into the base, allow for the exchange of culture media. Adapted from the original design drawings of Stephen Lin.

Enzymes: hyaluronate lyase, trypsin, and chondroitinase-ABC

Streptomyces hyaluronate lyase was received as a lyophilized powder. In the manufacturer's ampule, the enzyme was reconstituted with 400µl base media. The mixture incubated at room temperature for fifteen minutes to ensure that all the powder dissolved into solution. The enzyme solution was dispensed in 80µl aliquots into microcentrifuge tubes (yielding an activity of 100 TRU/tube) for long-term storage at -80°C. For experimental usage, 100µl of enzyme solution was added to 9.90ml of supplemented media, giving a total volume of 10ml and an enzyme activity of 10TRU/ml. Tissue samples were fed 1.0ml.

Lyophilized trypsin was reconstituted with Hank's Balanced Salt Solution (HBSS) and stored at 4°C. For *in situ* degradation studies, this stock preparation, designated 10X[1], was diluted to 0.0025X with HBSS supplemented with 1% (v/v) antibiotic/antimycotic. Tissue samples were fed 1.0ml.

Lyophilized chondroitinase-ABC, protease-free and purified from *Proteus vulgaris*, was reconstituted in the manufacturer's ampule with 1.0ml of base media. Similar to the preparation of hyaluronate lyase, the mixture incubated at room temperature for fifteen minutes to ensure that all the powder dissolved into solution. The enzyme solution was dispensed in 200µl aliquots into microcentrifuge tubes (yielding an activity of 0.2 Units/tube) for long-term storage at -80°C. For experimental usage, 200µl of enzyme solution was added to 1.80ml of supplemented media, giving a total volume of 2ml and an enzyme activity of 0.1 Units/ml. Tissue samples were fed 0.5ml.

Interleukin-1ß

Copious amounts of purified human wild-type interleukin-1ß (IL-1ß) were graciously provided Professor Lee Gehrke. Purification techniques, established by Professor Gerhke and Dr. Amy Lai, are described elsewhere (Lai 1993). The experimental efforts of Dr. Sandip Biswal and Daniel KH Chang consistently demonstrated successful tissue degradation over relevant (5-8 days) time periods with 100ng/ml (Biswal 1996; Chang 1992). Aliquots of 1µg/ml IL-1ß in 17.2µl of Hank's Balanced Salt Solution with 2% (v/v) antibiotics were stored at -20°C.

---

[1] Sigma packages trypsin in an ampule as a lyophylized powder consisting of trypsin and sodium chloride. "10X trypsin" refers to the reconstitution of said powder with 20ml of sterile, distilled, deionized water, yielding 25g/L trypsin (and 8.5g/L sodium chloride).

Mechanical testing

An incubator-housed, displacement-based mechanical spectrometer, affectionately referred to as the "Tissue Compression System" (TCS), enabled *in situ* measurements of equilibrium and dynamic stiffness. The TCS allows for long-term culture of cartilage explants in such a fashion that facilitates the elucidation of the tissue load-displacement relationship. In short, five cartilage discs can be cultured separately and the specific load-displacement relationship of each plug can be observed independently. The utility of this contraption has been previously established (Chang 1992; Cho 1996) and the results of further verification studies are reported in Appendix A.

Cartilage plugs were selected from the pool of harvested explants for mechanical properties' measurements based upon gross appearance. Samples which did not exhibit plane-parallel faces were discarded. Likewise, samples which did not retain cylindrical shape or had visible damage incurred during the explantation process were discarded. A digital micrometer was used to measure the thickness of acceptable plugs to the nearest 0.01mm; note that all explanted plugs swelled by at least 10% of their originally prepared thickness. Five plugs which were similar in thickness were sterily placed into freshly autoclaved compression chambers. The compression chambers were loaded into their respective positions in the TCS. The upper platen was positioned such that the LVDT was in its linear range (-0.2 to 0.2 inches) and that the thrust buttons of the load cells were close to, but not touching, the compression posts. A contact tare load of less than 5g was established by positioning each compression chamber with its micrometer. It was assumed that the tare load elicited negligible compressive strain, thereby establishing a "0%-strain" level of contact. A tare load of 5g would give an estimated offset strain of 1.4% and .8% for 3mm diameter and 4mm diameter cartilage samples, respectively (assuming an equilibrium modulus of 0.5MPa, which is typical of epiphyseal cartilage explants). At this point the incubator door was closed and the interior environment was allowed to reach culture conditions (37°C, >90% humidity, and 5% CO_2).

All mechanical measurements were made from the 15% level of compressive strain. From this static offset were imposed either a step-wise series of small compressive strains to measure the equilibrium stiffness or set of periodic displacement waves of small peak-to-peak strains to measure the dynamic stiffness. This is consistent with the literature (Frank and Grodzinsky 1987; Sah et al. 1992) and in accordance with the generally accepted methodology of extracting linear measurements from inherently non-linear materials (Ferry 1970). Over a period of three hours, the upper platen was lowered to establish this offset. This was accomplished by driving the platen down, which was set to a maximum strain rate of 1.0%-strain per second, in four successive steps separated by 45 minutes. Mechanical measurements were initiated after stress-relaxation was complete.

Equilibrium stiffness measurements

Equilibrium stiffness measurements were made from the 15%-strain static offset level. The protocol consisted of four sequential steps of approximately 20μm each (i.e., 0.91% compressive strain for a plug 2.20mm in thickness) imposed at intervals which allowed for the complete stress-relaxation of the tissue. For untreated tissue samples, this relaxation was typically thirty minutes for 3mm diameter plugs and one hour (sometimes more) for 4mm diameter plugs. Note that the derived (Armstrong et al. 1984) unconfined compression stress relaxation time constant,

$$t \approx \frac{a^2}{H_a k}$$

is proportional to the square of the plug radius, a, and inversely proportional to the equilibrium confined compression modulus, H_a, and hydraulic permeability, k. Figure 2.2 illustrates the physical measurement of equilibrium stiffness on a 3mm diameter cartilage plug: an imposed displacement of 20μm at a 1.0%/s strain-rate elicits an immediate resistance to deformation followed by a period of stress-relaxation which converges upon a steady *equilibrium* load. The unconfined equilibrium stiffness, M, is defined as the net incremental increase in stress normalized by the imposed strain:

$$M \equiv \frac{Lg/\pi r^2}{\delta/l_o}$$

where L is the measured increase in equilibrium load, g is the gravitational constant, r is the plug radius, δ is the incremental step in displacement, and l_o is the thickness of the plug. The average unconfined equilibrium modulus, as reported in this thesis, is the arithmetic mean and standard deviation of the mean of four measurements.

Dynamic stiffness measurements

Like the equilibrium stiffness, measurements of dynamic stiffness were performed at the 15% static offset level. Depending upon the experiment, a series of five or six periodic displacement waves, ranging from 0.004Hz or 0.02Hz through nearly 1Hz in frequency and approximately 1% peak-to-peak strain in magnitude, were applied and the load-response was

observed. Previous work has identified that these frequencies and magnitudes elicit a linear mechanical response from cartilage (Lee et al. 1981), which has been verified for this testing system (Appendix A). Furthermore, it is over this frequency range that fluid transport effects become significant and enhance the dynamic stiffness of the tissue (refer to the biomechanics section of the introduction or to (Armstrong et al. 1984; Kim 1989; Lee et al. 1981).

The unconfined dynamic stiffness, D_f, is defined for any particular frequency, f, as the steady-state peak-to-peak stress divided by the imposed strain:

$$D_f \equiv \frac{L_{pp} g / \pi r^2}{\delta_{pp} / l_o}$$

where L_{pp} is the steady-state peak-to-peak load and δ_{pp} is the peak-to-peak displacement. Figure 2.2, exhibiting a 0.5Hz displacement wave, defines the variables for the determination of the dynamic stiffness.

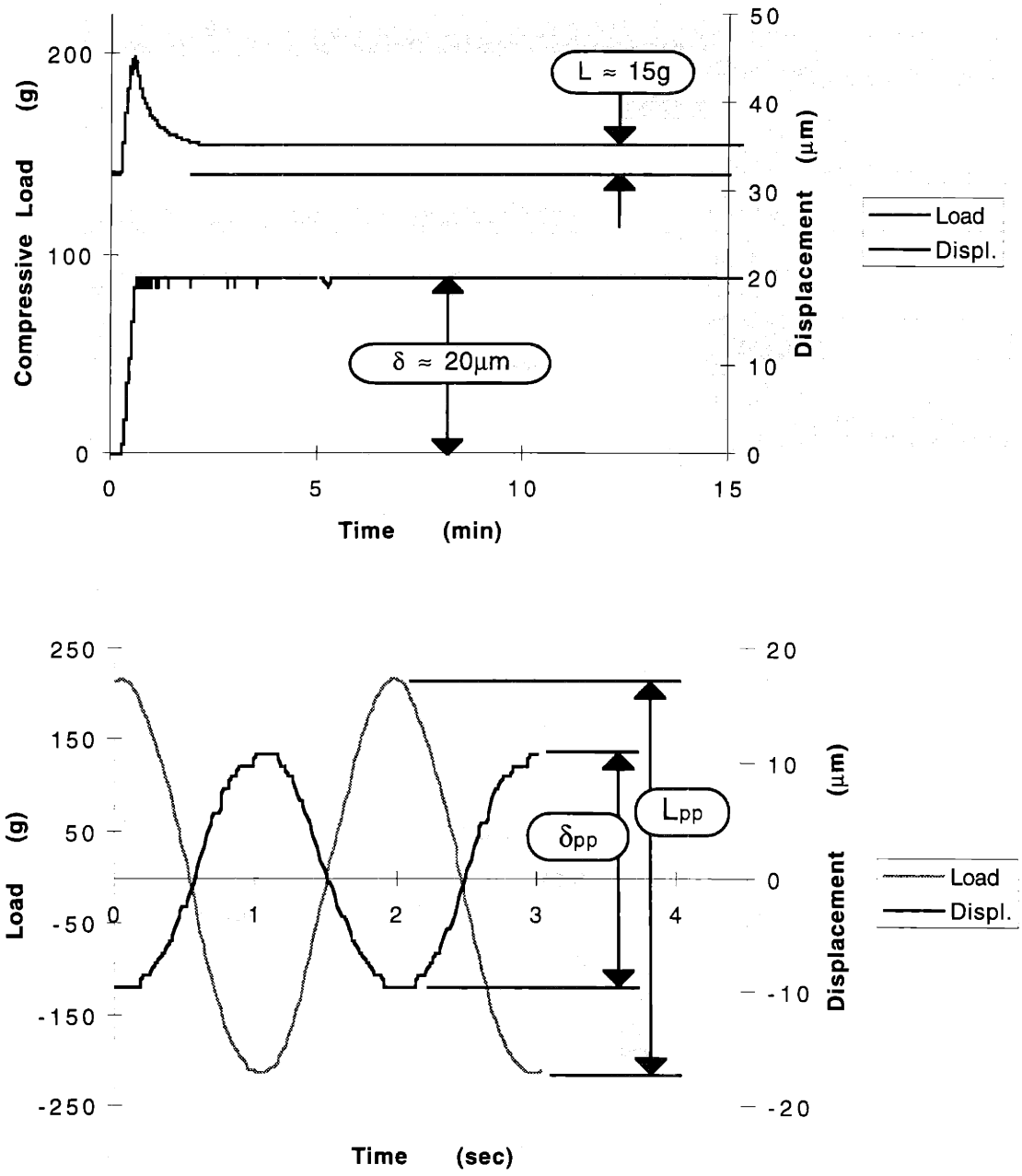

Figure 2.2: Example Measurements of Equilibrium and Dynamic Load and Displacement

The definition of measured parameters used to calculate the equilibrium (top) and dynamic (bottom) stiffness. Note that the arbitrary polarity of the transducer outputs, seen in the bottom plot, may be misleading; the compression cycle of the imposed displacement (plotted as increasingly negative) induces a positive increase in observed load.

Biochemistry: the assessment of sulfated glycosaminoglycan content

Biochemical analysis of the amount of sulfated glycosaminoglycans remaining in the explant plugs and released to culture media was performed in accordance with the dye-binding spectrophotometric methods as described by Farndale (Farndale et al. 1986). Tissue samples were lyophilized and subsequently digested in 0.5ml of 125μg/ml papain in PBE at 40°C for twenty-four hours. Glycosaminoglycan content was determined by adding 2.0ml of DMB solution to 20μl aliquots of the digest solution in polystyrene cuvettes and measuring the absorbance at 525nm in a Perkin Elmer Model λ3B spectrophotometer (Perkin Elmer, Norwalk, CT). The absorbance was compared to that of standards of known concentration. Standards were serial dilutions of chondroitin sulfate in PBE. Analysis of glycosaminoglycan content in media samples was performed in a similar fashion, except that the standards were diluted with unsupplemented media.

Histology: tissue fixation, sectioning, staining, and photomicroscopy

Histological preparations of tissue samples were prepared for the purpose of visualizing the tissue morphology and spatial distribution of matrix-intact glycosaminoglycans. We utilized the methods developed by Hunziker et al. (Hunziker et al. 1982; Hunziker et al. 1983) to circumvent the aqueous extraction of proteoglycans during the fixation process. Selected time-points, representing the gamut of induced tissue degradation, were chosen to elucidate the kinetics and proportions of glycosaminoglycan release. Tissue explants were chemically fixed in a 1.0ml cocktail of 0.7% ruthenium hexamine trichloride (RHT), 2.0% glutaraldehyde, 0.05M sodium cacodylate (pH 7.4, 330mosmol) for four hours at room temperature and then for twelve hours at 4°C. Next, the explants were placed in a RHT-free fixative for forty-eight hours at 4°C. The fixation process concluded by washing the explants in 0.1M sodium cacodylate buffer (pH 7.4, 330mosmol) with four consecutive 1.0ml rinses, each one hour in duration. Fixed samples were stored in 70% ethanol at 4°C. Previous work has demonstrated the feasibility of this method (Biswal 1996) for similar culture conditions.

Fixed tissue was embedded in paraffin, sectioned to thicknesses of 4, 5, or 10μm (depending upon the experiment), and mounted on glass slides by either Mike Fredrickson, chief pathologist at the Massachusetts General Hospital, Boston, MA, or Pathology Services, Cambridge, MA. The slides were then returned for staining and cover-slip-mounting by yours-truly. Slides were deparaffinized by total immersion for ten minutes in xylenes followed by serial rehydration in 100%, 90%, 80%, 40%, and 0% ethanol (percentage ethanol diluted in distilled, deionized water). After deparaffinization and rehydration, the sections were stained with 0.1% toluidine blue-O in distilled, deionized water for one minute followed by one minute wash in

distilled, deionized water. The sections were then dehydrated with ten minute serial immersions in 70%, 80%, 90%, 100% ethanol, 1:1 ethanol:xylenes, and xylenes. Immediately following immersion in xylenes, 25 x 50mm coverslides were mounted on the slides with Permount. The staining protocol was adapted from Johnson's Toluidine Blue-O Technique (Thompson 1966). Toluidine blue-O is a cationic dye which associates preferentially with negatively-charged, large molecular weight substances. There exists a minimum density of electronegative charges for which the dye will associate, below which an apparent threshholding effect is observed.

A Nikon Diaphot-TMD inverted phase microscope and Nikon N2000 camera were used to take photomicrographs of the sections. Bright field images were captured on Kodak Gold 100 speed film with the microscope configured at 10X magnification and lamp intensity set between 9-11 and the camera set for auto shutter speed. Some diffusion and neutral density filtering was performed on a few samples to selectively augment contrast.

Table 2.3: Source of Materials

Provider	Material
Sigma, St. Louis, MO	L-proline, non-essential amino acids (NEAA), papain, chondroitin sulfate (from whale/shark cartilage), hyaluronate lyase (i.e., hyaluronidase; from Streptomyces hyalurolyticus), toluidine blue-O, and penicillin-streptomycin-amphotericin-B (antibiotics/antimycotic)
Gibco, Grand Island, NY	Dulbecco's Modified Eagle Medium (DMEM), Hank's Balanced Salt Solution (HBSS), N-2-hydroxyethylpiperazine-N'-2-ethanesulfonic acid (HEPES), L-glutamine, L-ascorbate, and trypsin
EM Science, Cherry Hill, NY	L-cysteine hydrochloride
Mallinckrodt, Paris, KY	Ethylene-diamenetetraacetic acid (Na_2EDTA), xylenes, and n-propyl alcohol
Polysciences, Warrington, PA	Dimethylmethylene blue chloride (DMB), ruthenium hexamine trichloride (RHT), and 8% glutaraldehyde
Fisher Scientific	Hydrochloric acid (HCL) and Permount
Professor Lee Gerhke, MIT, Cambridge	Human wild-type interleukin-1ß (IL-1ß)
Hyclone, Logan, UT	Fetal calf serum (FCS); heat inactivated by incubation in a hot water bath for one-hour at 37°Cwas
INC Biomedicals, Inc, Costa Mesa, CA	Chondroitinase-ABC (from *proteus vulgaris*)
Bio-Rad, Cambridge, MA	Sodium cacodylate

Results

Control Studies:

Baseline measurements of equilibrium stiffness, dynamic stiffness and glycosaminoglycan content of cartilage samples cultured in the absence of induced degradation.

Control studies of both calf epiphyseal cartilage and femoropatellar groove cartilage explants cultured *in situ* were specifically designed to facilitate the quantification of equilibrium stiffness, dynamic stiffness, and glycosaminoglycan content of each explant. The ulnar cartilage was prepared into 3mm-diameter, 2mm-thick cylindrical plugs. In a departure from the previously described methods, the ulna-derived tissue was cultured at a 0%-strain offset (effectively constraining the plugs axially) throughout the course of the experiments. The plugs were compressed to a 15%-strain static offset prior to the measurements of equilibrium and dynamic stiffness. Subsequent to the measurements of equilibrium and dynamic stiffness, the plugs were returned to the initial 0% level of strain for continued culture.

In contrast, femoropatellar groove explants were prepared into 4mm-diameter, 2mm-thick plugs. These discs were initially brought to a 15%-strain compressive static offset and were maintained at this level during quiescent periods throughout the culture. In some cases, measurements were made of dynamic stiffness at 0.004Hz, and under other circumstances, equilibrium stiffness measurements were not taken.

The absolute magnitude of the mechanical and biochemical measurements are reported in Appendix C. The data reported in this section has been non-dimensionalized. A non-dimensionalization technique was utilized in order to clarify the measurement trends. Measurements made just prior to induced degradation (denoted as DAY 0) were defined as "100%". All subsequent measurements of stiffness and glycosaminoglycan content were referenced to their respective values just prior to treatment. By presenting the data in this relative fashion the variability introduced from sample to sample biological variation was removed. The *relative* values of equilibrium stiffness, dynamic stiffness, and glycosaminoglycan content are designated as RES, RDS, and RGC, respectively. For clarity, the RDS acronym comes equipped with a subscript to indicate frequency, i.e., $RDS_{0.88}$ symbolizes the relative dynamic stiffness at 0.88 Hz.

Mechanical properties and glycosaminoglycan content of cultured cartilage explants

Figures 3.1 and 3.2, depicting the results of experiments using ulna-derived and femoropatellar groove explants, respectively, both exhibit a monotonic decline of all measurements. For ulna-derived tissue, the drop in RES was statistically less than the $RDS_{0.88}$ and

RGC on Days 3, 4, and 5, but that the $RDS_{0.88}$ was never statistically different from the RGC. For the femoropatellar groove-derived tissue, statistical analysis revealed that the measurements of $RDS_{0.02}$, $RDS_{0.88}$, and RGC, on any given day, were never different from one-another. Therefore, the diminishing stiffness measurements were statistically consistent with the release of glycosaminoglycans.

The dynamic stiffness of all untreated samples demonstrated a frequency dependence. The increase in dynamic stiffness with frequency, characteristic of poroelastic materials, exhibited a significant drop with time in culture. The dynamic stiffness of a single sample as observed initially and after four days of culture is shown in Figure 3.3; where it can be seen that the data shifts downward in time, but the general trends remains the same.

Histology of untreated, cultured cartilage explants

Histological samples were prepared from a separate study conducted under similar conditions. Cartilage explants, cultured in static compression chambers, were axially confined with a 15%-strain static offset and cultured for five days with daily media changes. Figure 3.4 shows a section representative of a typical explant cultured for five days in the absence of induced degradation. The homogeneous distribution of toluidine blue-O indicates a spatially uniform distribution of glycosaminglycans. Histological sections of the explants were prepared by chemical fixation in glutaraldehyde and ruthenium hexamine trichloride (RHT), sectioned to 5μm, and stained with toluidine blue-O. The circular-sections were sliced from the mid-region of the cylindrically-shaped explant. There are three key morphological features of these sections: the pervading vasculature, characterized by large areas devoid of stain; the homogeneously distributed chondrocytes, the comparatively minuscule areas devoid of stain; and the vast proteoglycan-rich extracellular matrix, for which toluidine blue-O preferentially stains. Note that toluidine blue-O associates with the negatively-charged glycosaminoglycans causing its characteristic metachromatic shift towards a purple hue. For reference, the radial edge was the sole interface to the culture medium, therefore the diffusion of solutes, nutrients, etc., in the bulk tissue was constrained to the radial direction only.

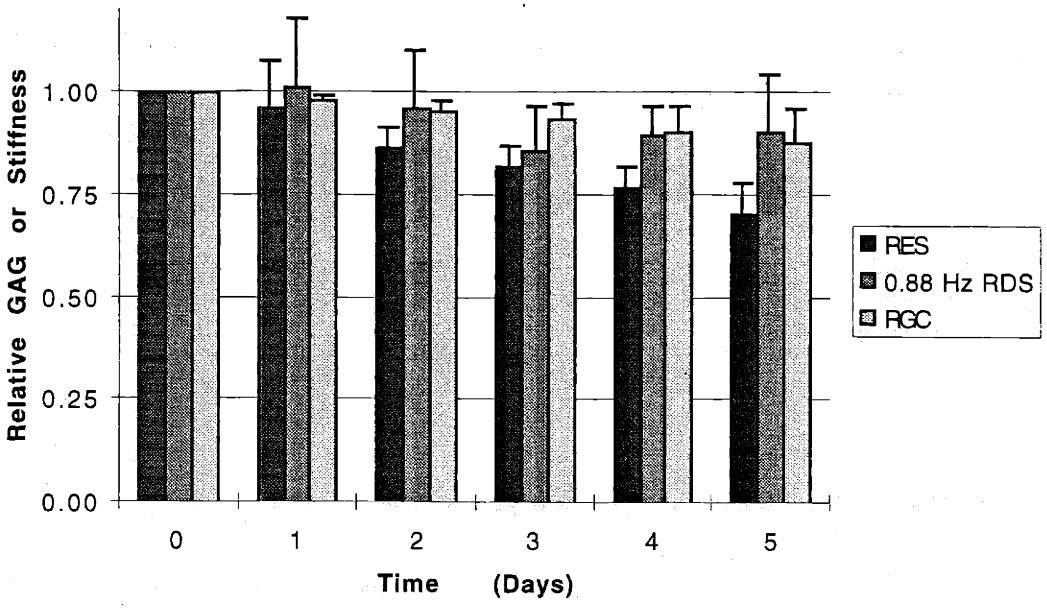

Figure 3.1: Untreated Control
The relative equilibrium stiffness (RES), relative dynamic stiffness ($RDS_{0.88}$), and relative glycosaminoglycan content (RGC) of explants harvested from the calf distal ulna and cultured in the TCS for five days. The data are reported as the arithmetic mean of ten samples plus the standard deviation of the mean.

- Analysis of variance (ANOVA, two-factor without replication, α=0.05) testing the hypothesis that all measurements are significantly different from their respective initial values on Day 0 indicates that all measurements decline with significance, with the three exceptions of RES and $RDS_{0.88}$ on Day 1 and $RDS_{0.88}$ on Day 2.
- Analysis of variance (ANOVA, single-factor, α=0.05) testing the hypothesis that for any given day the mean RES, $RDS_{0.88}$ and RGC are statistically equivalent indicates that: the RES is less than both the $RDS_{0.88}$ and RGC on Days 3, 4, and 5; and the $RDS_{0.88}$ and RGC are never statistically different.

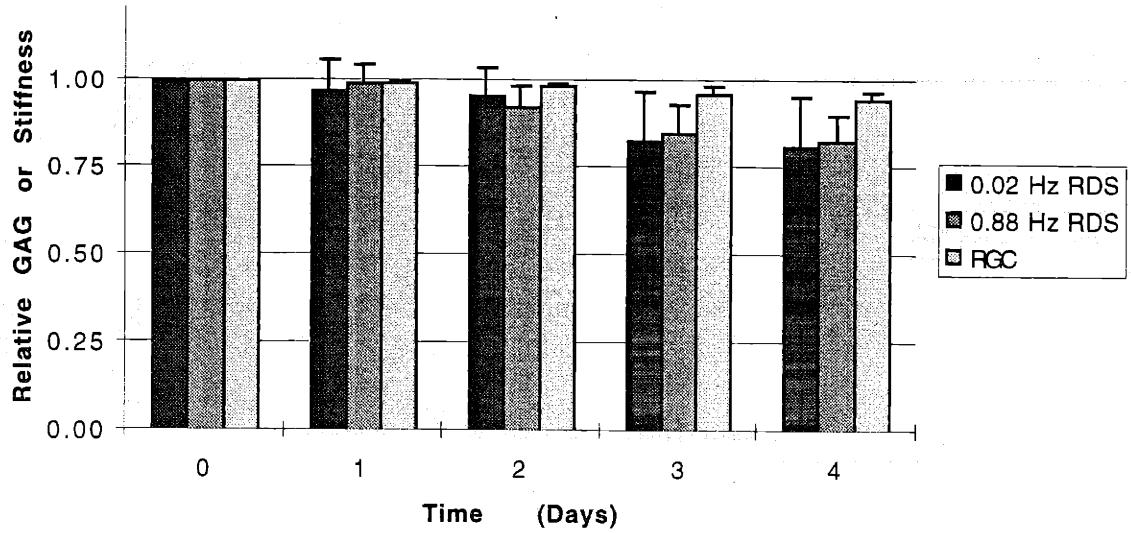

Figure 3.2: Untreated Control
The relative dynamic stiffness ($RDS_{0.02}$ and $RDS_{0.88}$) and relative glycosaminoglycan content (RGC) of explants harvested from the calf femoropatellar groove and cultured in the TCS for four days. The data are reported as the arithmetic mean of four samples plus the standard deviation of the mean.

- Analysis of variance (ANOVA, two-factor without replication, α=0.05) testing the hypothesis that all measurements are significantly different from their respective initial values on Day 0 indicates that all measurements decline with significance everyday, with the two exceptions of $RDS_{0.02}$ and $RDS_{0.88}$ on Day 1.
- Analysis of variance (ANOVA, single-factor, α=0.05) testing the hypothesis that for any given day the mean $RDS_{0.02}$, $RDS_{0.88}$ and RGC are statistically equivalent indicates that all three measurements are never statistically different.

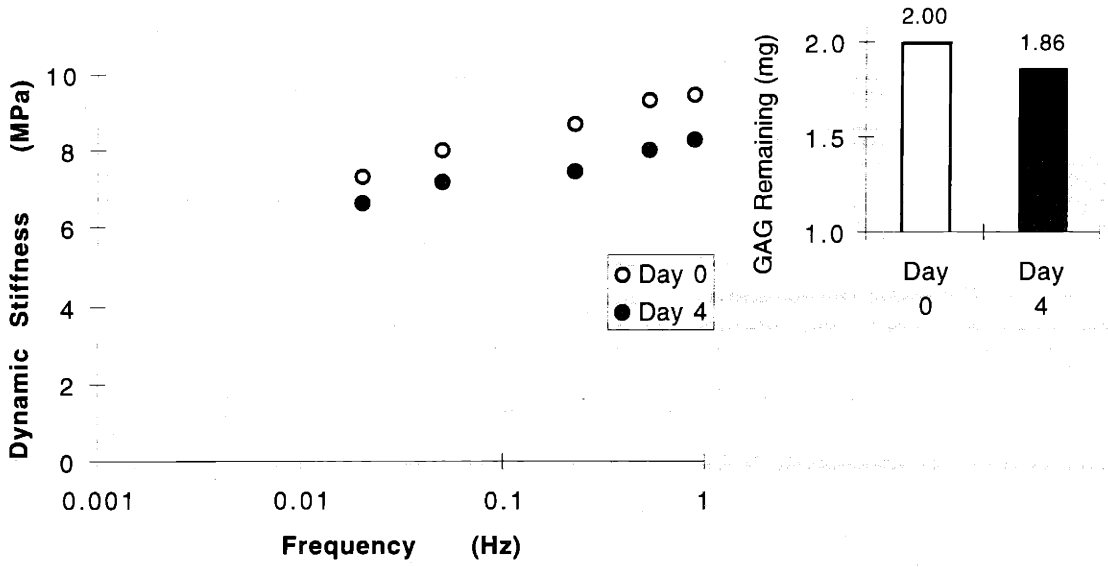

Figure 3.3: Untreated Control

1. The frequency dependence of the absolute dynamic stiffness exhibits a downward shift with time in culture. The data is of a single femoropatellar groove explant, but it is representative of the entire set of untreated controls. The equilibrium stiffness was not measured.
2. The histogram plots the absolute glycosaminoglycan content of the explant at the time when the mechanical measurements were performed. The initial dynamic stiffness dropped by 12±2% and the initial GAG content declined by ~7% over four days. This particular sample had a relatively high initial GAG content; typical values were 1.21±0.37mg (n=20) for explants (4mm-diameter, 2mm-thick) from the femoropatellar groove.

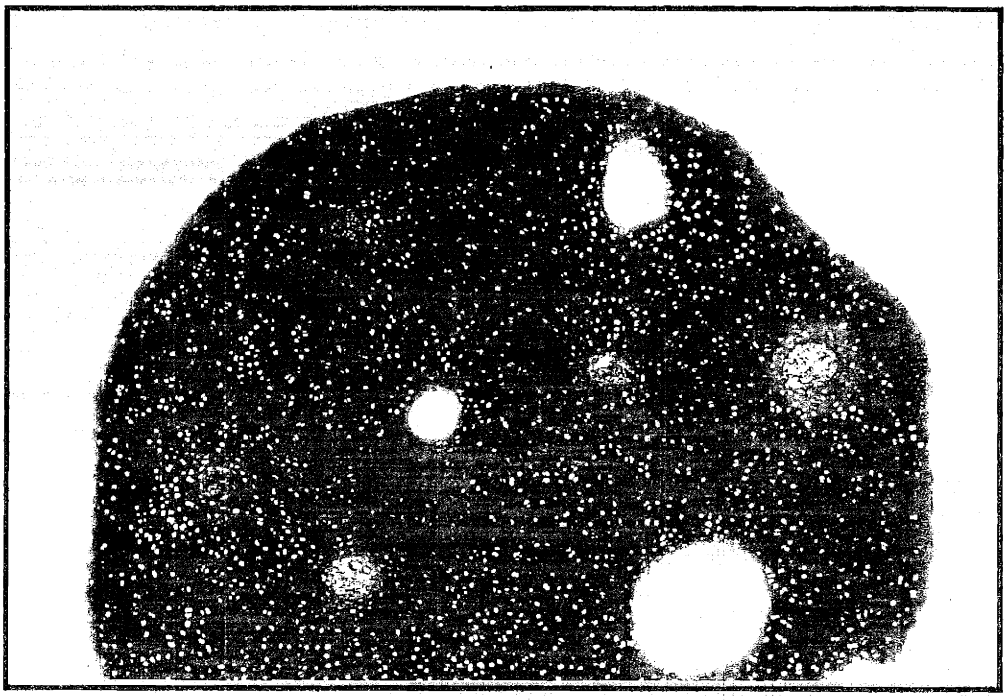

Figure 3.4: Untreated control
Histologic section of epiphyseal cartilage obtained from the calf distal ulna; explant dimensions are 3mm in diameter and 2mm in thickness. Explant was axially confined with a 15%-strain static offset and cultured for five days with daily media changes (two days in free-swelling conditions and three in confinement). This sample released 30μg of GAG over the three days in confinement. This photomicrograph is typical of samples cultured in the absence of induced degradation. This sample was chemically fixed with glutaraldehyde and RHT, sectioned at 5μm, and stained with toluidine blue-O. Photomicrographs were taken at 10X magnification and exhibit only a portion of the entire circular section. Note the presence of vasculature and the sparse distribution of cells.

The effect of interleukin-1ß on the mechanical properties and glycosaminoglycan content of cartilage explants (addressing objective 1)

The presence of interleukin-1ß (IL-1ß) has been demonstrated to cause the net release of sulfated glycosaminoglycans (Arner and Pratta 1989; Hubbard et al. 1988). Presumably, the increased presence of glycosaminoglycans detected in the culture media of tissue cultured in the presence of interleukin-1ß is caused by the upregulation of matrix-metalloproteinase (MMP) production or by the inactivation of MMP-inhibitors, or a combination of both. Through histological methods, it has been shown that the effect of adding IL-1ß to epiphyseal cartilage explants in culture is to elicit glycosaminoglycan release which is initiated in the perivascular regions and proceeds radially outward (see Appendix B for selected histological photomicrographs) (Biswal 1996). With relevance to *Objective 1* of this thesis, it has been established that IL-1ß-induced degradation provides a spatial pattern of degradation that is distinctly different from that of direct enzymolysis. Specifically, the spatial pattern of IL-1ß-induced degradation in axially-confined (radially-unconfined) explant culture systems is reminiscent of point-source initiation followed with an outwardly progressing, front-like, path.

The mechanical properties and glycosaminoglycan content of the *treated* samples were determined and are reported in Figures 3.5 and 3.6. The key findings are (1) a delayed effect of IL-1ß for the femoropatellar groove-derived explants (note that treatment began following DAY 0 but the onset of degradation was not observed biochemically until DAY 4); (2) an accelerated diminishment of both the relative equilibrium stiffness (RES) and 0.004Hz-relative dynamic stiffness ($RDS_{0.004}$) was the obvious effect of IL-1ß; (3) for each condition (±IL-1ß), the trends for stiffness and glycosaminoglyan-loss were highly correlated, but the drop in RES was consistently earlier and of greater magnitude than the drop in relative glycosaminoglycan content (RGC); and (4) the RDS, at all frequencies tested, followed a time course intermediate to that of the RES and RGC except that the $RDS_{0.88}$ was in proportion to the RGC.

The frequency dependence of the dynamic stiffness (of a single representative sample) is reported in Figure 3.7. The delayed mechanical effect, as seen throughout the experiment frequency window, of IL-1ß spanning two days of treatment is consistent with the biochemistry. After five days of treatment there is an obvious decrease in stiffness which is characterized by a high-frequency plateau region reduced by 50% in magnitude (with a cutoff in the vicinity of 0.05Hz) and a diminished ascent "slope" of the lower-frequency measurements.

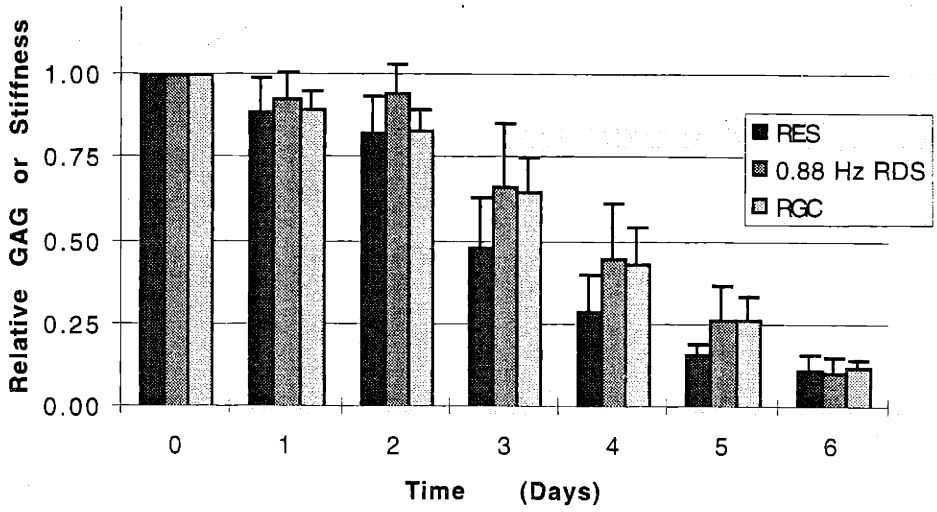

Figure 3.5: Treatment with 100ng/ml IL-1ß
The relative equilibrium stiffness (RES), relative dynamic stiffness ($RDS_{0.88}$), and relative glycosaminoglycan content (RGC) of explants harvested from the calf distal ulna and cultured in the TCS for six days in the presence of 100ng/ml IL-1ß. The data are reported as the arithmetic mean of five samples plus the standard deviation of the mean.

- Analysis of variance (ANOVA, two-factor without replication, α=0.05) testing the hypothesis that all measurements are significantly different from their respective initial values on Day 0 indicates that all measurements are significantly different from their respective initial values on Day 0. Furthermore, in comparing the observed decrease of a particular measurement from one day to the next: the RGC declines each day with statistical significance; the $RDS_{0.88}$ does not decline with statistical significance until Day 3 (from this point it drops with significance through Day 6); and the RES drops with significance on Day 2 through Day 5, but not to Day 6.
- Analysis of variance (ANOVA, single-factor, α=0.05) testing the hypothesis that for any given day the mean RES, $RDS_{0.88}$ and RGC are statistically equivalent indicates that the RES, $RDS_{0.88}$ and RGC are never statistically different, except that on Day 5 (note that on Days 3 and 4: (1) the F statistic for RES:RGC is marginally less than F_{CRIT}; and (2) the RES is significantly less than the RGC for α=0.079 and α=0.064 on Days 3 and 4, respectively).
- Analysis of variance (ANOVA, single-factor, α=0.05) testing the hypothesis that the RGC of treated samples is different from that of untreated samples indicates that the RGC, beginning on Day 1, of these treated explants is statistically different than that of untreated controls.

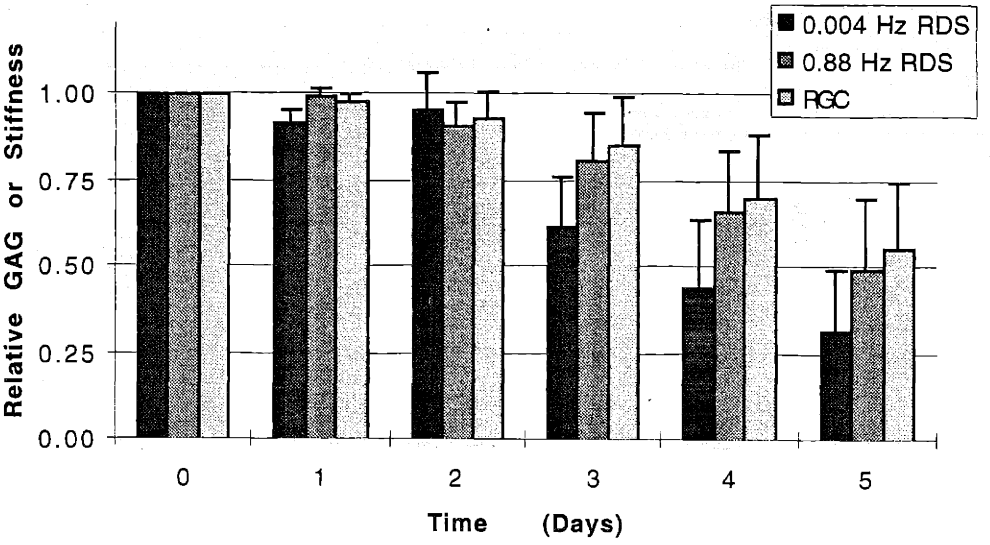

Figure 3.6: Treatment with 100ng/ml IL-1ß
The relative dynamic stiffness ($RDS_{0.004}$ and $RDS_{0.88}$) and relative glycosaminoglycan content (RGC) of explants harvested from the calf femoropatellar groove and cultured in the TCS for five days in the presence of 100ng/ml IL-1ß. The data are reported as the arithmetic mean of five samples plus the standard deviation of the mean.

- Analysis of variance (ANOVA, two-factor without replication, α=0.05) testing the hypothesis that all measurements are significantly different from their respective initial values on Day 0 indicates: the RGC does not decline with significance until Day 4; the $RDS_{0.004}$ declines with significance everyday, except Day 2; and the $RDS_{0.88}$ declines with significance from Day 2 forward.
- Analysis of variance (ANOVA, single-factor, α=0.05) testing the hypothesis that for any given day the mean $RDS_{0.004}$, $RDS_{0.88}$ and RGC are statistically equivalent indicates that all three measurements are not statistically different, except on Days 1 and 3 where the $RDS_{0.004}$ is significantly less than the $RDS_{0.88}$ and RGC.
- Analysis of variance (ANOVA, single-factor, α=0.05) testing the hypothesis that the RGC of treated samples is different from that of untreated samples indicates that the RGC does not statistically decrease, relative to controls, until Day 4.

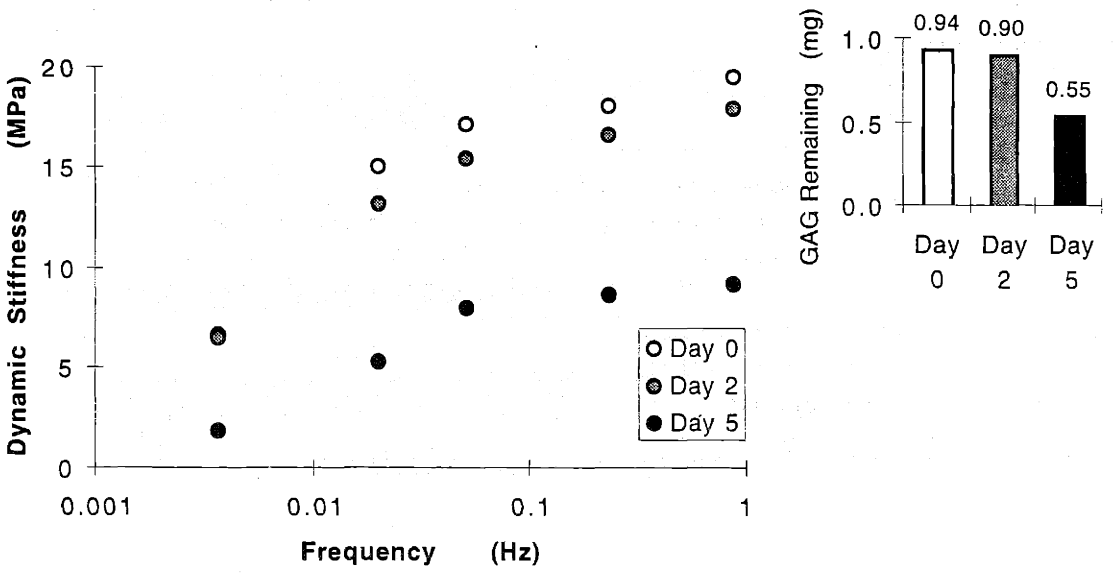

Figure 3.7: Treatment with 100ng/ml IL-1ß

1. The frequency dependence of the absolute dynamic stiffness as observed immediately prior to treatment, and two and five days, respectively, afterwards. The data is of a single femoropatellar groove explant, but it is representative of the entire set of interleukin-1ß-treated samples. The equilibrium stiffness was not measured.
2. The histogram plots the absolute glycosaminoglycan content of the explant at the time when the dynamic stiffness was measured.

The effects of enzymolysis (addressing objective 2)

Proteolytic enzymes induce the release of specific matrix macromolecules (or portions thereof) in a controlled manner. Cartilage explanted and cultured as described above, was systematically treated with specific catabolic agents to induce a "radially-inward" mode of glycosaminoglycan degradation. Experimental protocols were developed to monitor the time-course of change of mechanical properties and glycosaminoglycan content of *treated* cartilage explants. Several experiments were performed such that the individual effects of hyaluronate lyase, trypsin, and chondroitinase-ABC digestion could be studied.

The effect of hyaluronate-lyase on the mechanical properties and glycosaminoglycan content of cartilage explants

The enzyme hyaluronate lyase of *Streptomyces hyalurolyticus* origin acts only on hyaluronate (in contrast to testicular hyaluronidase which also acts on chondroitin sulfates A and C). The action of hyaluronate lyase is to specifically cleave the hyaluronic acid backbone of aggrecan, thereby releasing entire proteoglycan complexes (charged polysaccharides remaining covalently bound to the protein core of the proteoglycan). The 84kD enzyme has a pI between 7.4 and 7.9, and thus is presumably neutral at the pH of the culture medium. Femoropatellar groove- and ulna-derived explants were cultured in the presence of 10TRU/ml hyaluronate lyase.

The effect of hyaluronate lyase on the biochemical and mechanical properties of ulna-derived tissue is depicted in Figure 3.8. The key findings are (1) an immediate effect of the enzyme; (2) that the RES diminishes faster than the RGC; but that (3) the $RDS_{0.88}$ declines with the near-identical kinetics and proportions as the RGC.

Further experiments utilized 4mm-diameter calf femoropatellar groove explants. The data presented in Figure 3.9, depicting RES and RGC, indicates that (1) the effect of hyaluronate lyase is immediate, (2) the diminishment of the RES preceded that of the RGC in time and (3) was of greater proportion. Dynamic stiffness measurements were not performed in this experiment, but were made in a follow-up experiment; for which the high-frequency stiffness and glycosaminoglycan content is reported in Figure 3.10. Again, (1) the high frequency relative dynamic stiffness diminished with identical proportions and kinetics as the relative glycosaminoglcyan content and (2) the low frequency relative dynamic stiffness (0.02 Hz - not shown) dropped with marginally greater proportions.

The frequency dependence of the dynamic stiffness (of a single representative sample) is reported in Figure 3.11. The decrease in dynamic stiffness after one day of treatment appears to have diminished with greater proportions in the low-frequency range whilst the drop in high-

frequency stiffness is marginal. After eight days of treatment the drop in stiffness is apparent at all frequencies tested.

Epiphyseal cartilage explants that were cultured under similar conditions and treated with 10TRU/ml hyaluronate lyase were prepared for histological examination. Figure 3.12 presents photomicrographs of two samples, treated for one and three days. The absence of stain initiates in the periphery of the explant and progresses inwards with time.

The apparent lack of stain in the perivascular regions is somewhat difficult to interpret. However, this phenomenon has described previously (Biswal 1996) and has been found in *untreated* tissue (Figure 4.1) as well as in tissues treated with other catabolic enzymes (Figure 3.17b).

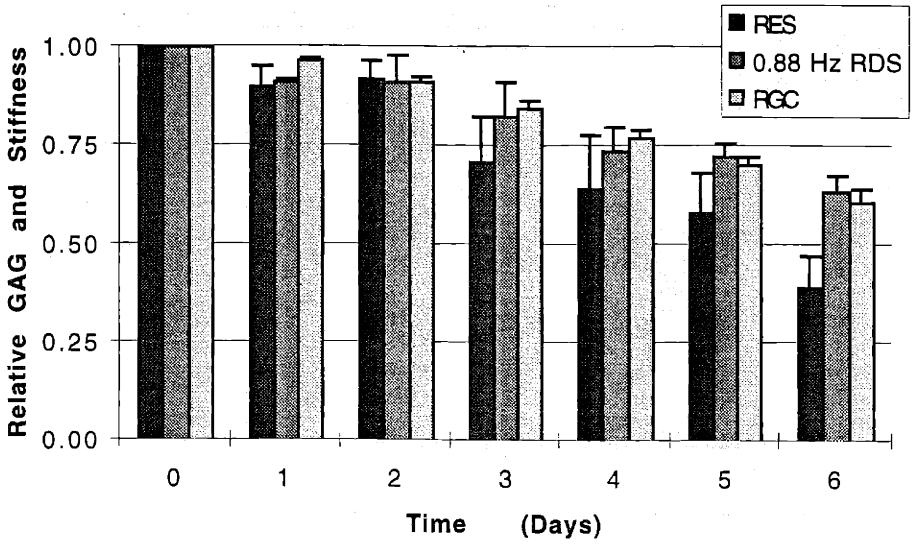

Figure 3.8: Treatment with 10TRU/ml hyaluronate lyase
The relative equilibrium stiffness (RES), relative dynamic stiffness ($RDS_{0.88}$) and relative glycosaminoglycan content (RGC) of explants harvested from the distal ulna and cultured in the TCS for six days in the presence of 10TRU/ml hyaluronate-lyase[2]. The data are reported as the arithmetic mean of five samples plus the standard deviation of the mean.

- Analysis of variance (ANOVA, two-factor without replication, α=0.05) testing the hypothesis that all measurements are significantly different from their respective initial values on Day 0 indicates that beginning on Day 1, the RGC, RES, and $RDS_{0.88}$ all have diminished significantly. Furthermore, each successive measurement of the RGC declines with significance, whereas $RDS_{0.88}$ declines with significance on Days 1, 4, and 6, and the RES on days 1, 3, and 6.
- Analysis of variance (ANOVA, single-factor, α=0.05) testing the hypothesis that for any given day the mean RES, $RDS_{0.88}$ and RGC are statistically equivalent indicates that: on Days 1, 3, 5, and 6 the RES is significantly less than the RGC; and $RDS_{0.88}$ differs from the RGC only on Day 1.
- Analysis of variance (ANOVA, single-factor, α=0.05) testing the hypothesis that the RGC of treated samples is different from that of untreated samples indicates that the RGC is statistically less than that of control at all times, beginning on Day 1.

[2] The units of hyaluronate lyase activity are expressed as "turbitity reducing units per volume", hence TRU/ml T. Ohya and Y. Kaneko, "Novel hyaluronidase from streptomyces," *Biochim. Biophys. Acta*, pp. 607-609, 1970.

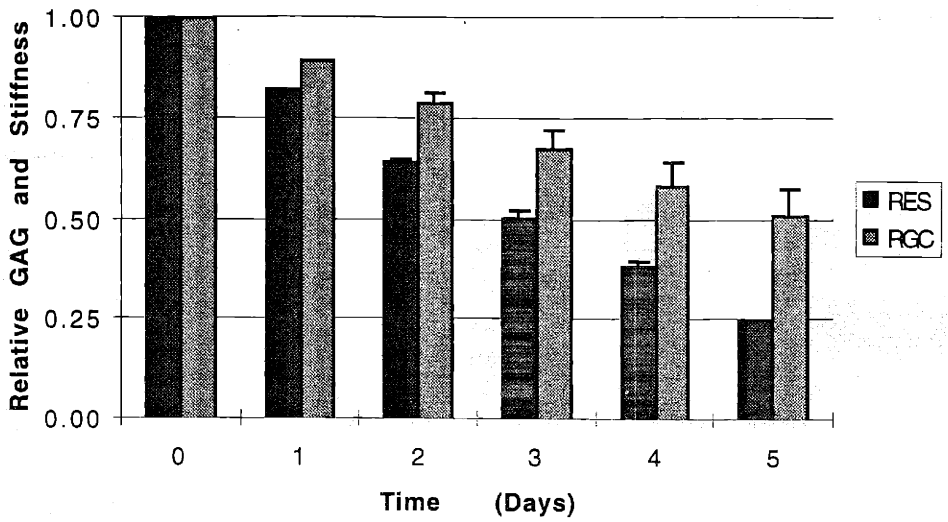

Figure 3.9: Treatment with 10TRU/ml hyaluronate lyase
The relative equilibrium stiffness (RES) and relative glycosaminoglycan content (RGC) of explants harvested from the calf femoropatellar groove and cultured in the TCS for five days in the presence of 10TRU/ml hyaluronate-lyase. The data are reported as the arithmetic mean of two samples plus the standard deviation of the mean.

- Analysis of variance (ANOVA, two-factor without replication, α=0.05) testing the hypothesis that all measurements are significantly different from their respective initial values on Day 0 indicates that beginning on Day 1, the RGC and RES both decline with significance.
- Analysis of variance (ANOVA, single-factor, α=0.05) testing the hypothesis that for any given day the mean RES and RGC are statistically equivalent indicates that every day the RES is significantly less than the RGC.
- Analysis of variance (ANOVA, single-factor, α=0.05) testing the hypothesis that the RGC of treated samples is different from that of untreated samples indicates that the RGC is statistically less than that of control at all times, beginning on Day 1.

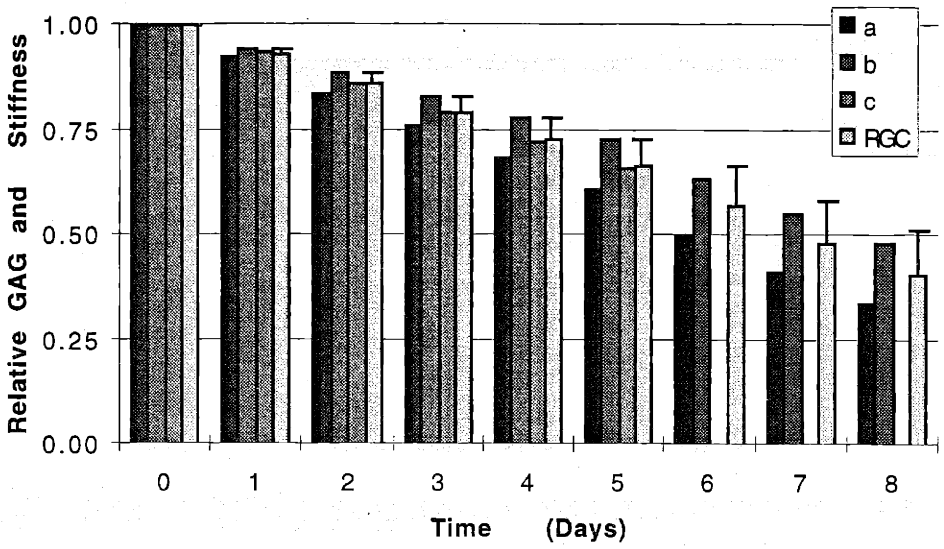

Figure 3.10: Treatment with 10TRU/ml hyaluronate lyase
The relative dynamic stiffness ($RDS_{0.88}$) and relative glycosaminoglycan content (RGC) of explants harvested from the calf femoropatellar groove and cultured in the TCS for eight days in the presence of 10TRU/ml hyaluronate-lyase. The stiffness data of three samples are reported individually, whereas the glycosaminoglycan content is reported as the arithmetic mean plus the standard deviation of the mean. After the exchange of culture media on Day 5, the compression chamber for sample C developed a leak which resulted in media release, rendering the sample unfit for further testing.

- Analysis of variance (ANOVA, two-factor without replication, α=0.05) testing the hypothesis that all measurements are significantly different from their respective initial values on Day 0 indicates that beginning on Day 1, the RGC and $RDS_{0.88}$ both decline with significance.
- Analysis of variance (ANOVA, single-factor, α=0.05) testing the hypothesis that for any given day the mean $RDS_{0.88}$ and RGC are statistically equivalent indicates that the hypothesis is correct.
- For data not shown, the mean $RDS_{0.02}$ and $RDS_{0.88}$ are statistically equivalent at every time point, except on Day 1.
- Analysis of variance (ANOVA, single-factor, α=0.05) testing the hypothesis that the RGC of treated samples is different from that of untreated samples indicates that the RGC is statistically less than that of control at all times, beginning on Day 1.

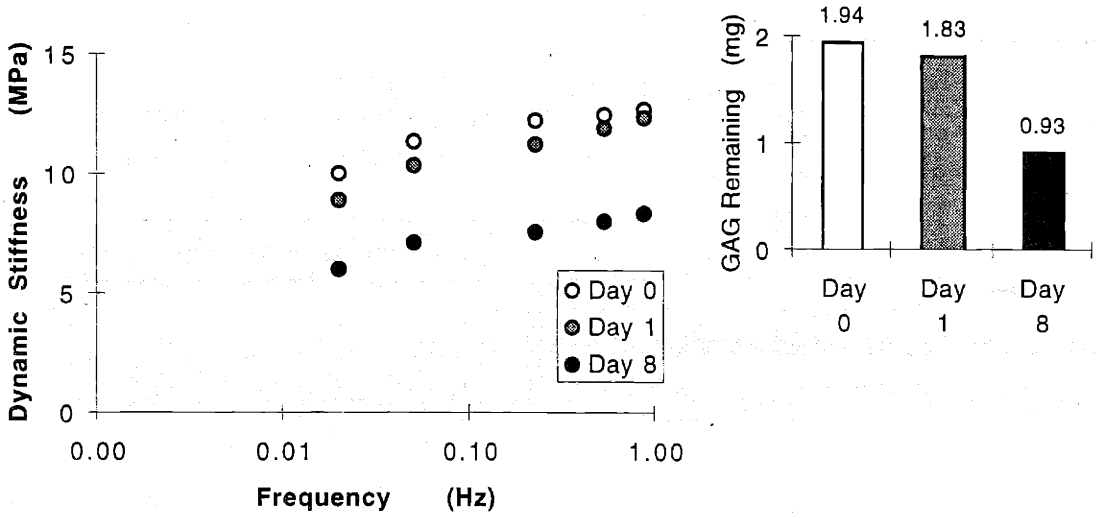

Figure 3.11: Treatment with 10TRU/ml hyaluronate lyase

1. The frequency dependence of the absolute dynamic stiffness as observed immediately prior to treatment, and one and eight days, respectively, afterwards. The data is of a single femoropatellar groove explant, but it is representative of the entire set of hyaluronate-lyase-treated samples. The equilibrium stiffness was not measured.
2. The histogram plots the absolute glycosaminoglycan content of the explant at the time when the dynamic stiffness was measured.

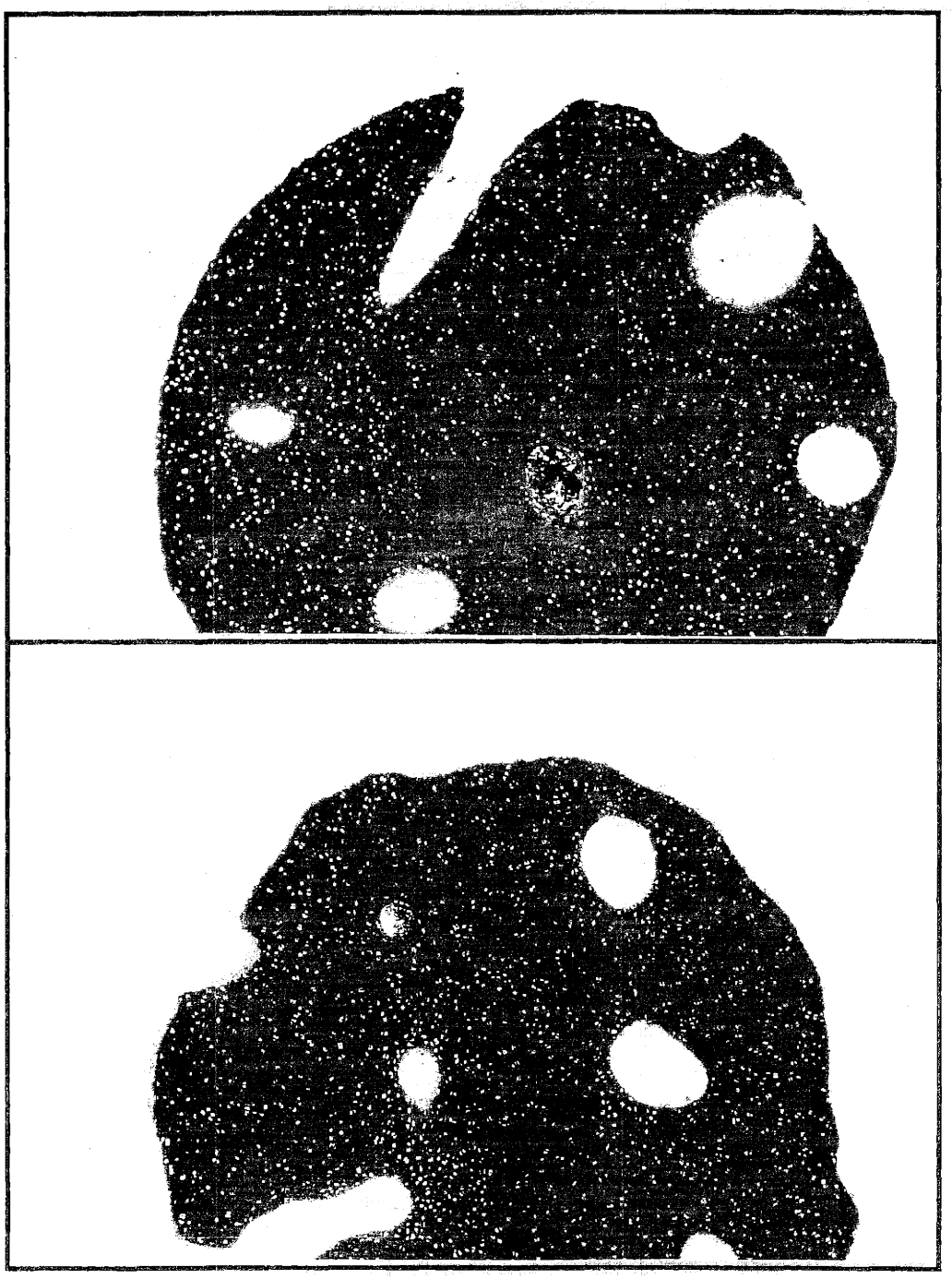

Figure 3.12: Treatment with Hyaluronate Lyase
Histologic section of epiphyseal cartilage explants (2mm-thick, 3mm-diameter) obtained from the calf distal ulna. Explants were cultured (free-swelling) for two days and then were axially confined with a 15%-strain static offset and cultured for one (top) and three (bottom) days with 10TRU/ml hyaluronate lyase. Fixed with glutaraldehyde and RHT, sectioned at 5μm, and stained with toluidine blue-O. Photomicrographs were taken at 10X magnification and exhibit only a portion of the entire circular section. Note that with time the peripheral region devoid of stain progressively advances inward.

The effect of trypsin on the mechanical properties and glycosaminoglycan content of cartilage explants

Glycosaminoglycan digestion in the presence of trypsin provided an alternative method of experimentally inducing "radially-inward" degradation. Femoropatellar groove explants were cultured in saline (HBSS) supplemented with 0.0025X trypsin. Dynamic stiffness measurements over a range of 0.004 - 0.88 Hz were made prior to treatment, 24 hours after initial treatment, and then at 12 hour intervals for the duration of the experiment. The results, in Figure 3.13, indicate that (1) this concentration of trypsin, although very low, induces an immediate, highly active, and steady release of glycosaminoglycans; (2) that the mean $RDS_{0.004}$ diminishes in greater proportion and faster, initially, than the measured glycosaminoglycan release; and (3) the mean $RDS_{0.88}$ *follows* the decline of RGC.

The dynamic stiffness (of a single sample) plotted against frequency is reported in Figure 3.14. The immediate effect of trypsin is to elicit a uniformly proportional decrease in dynamic stiffness. The general trends in the frequency-dependence are retained. After three days of treatment the dynamic stiffness is significantly reduced and, in contrast, the response appears to be nearly independent of frequency.

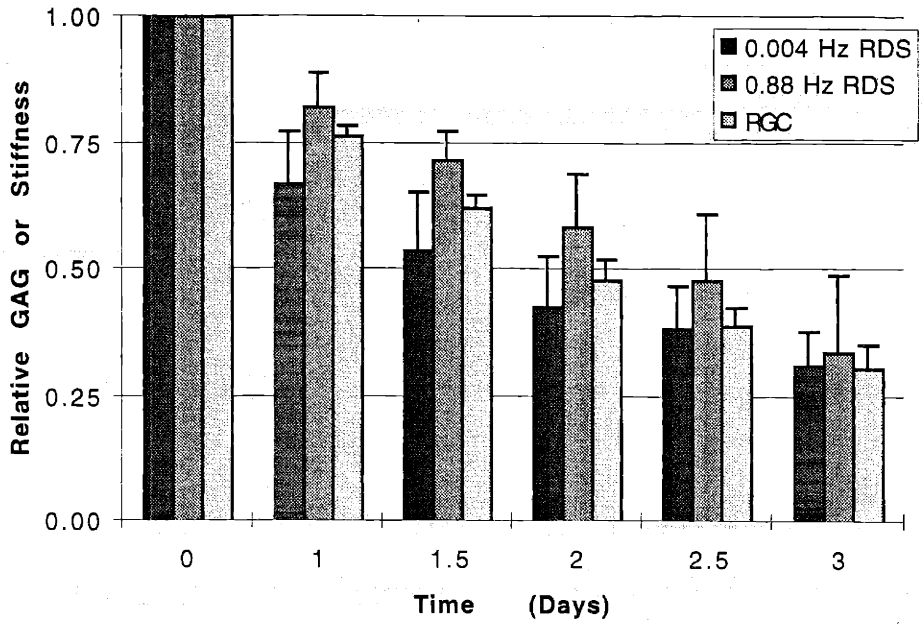

Figure 3.13: Treatment with 0.0025X trypsin.
The relative dynamic stiffness ($RDS_{0.004}$ and $RDS_{0.88}$) and relative glycosaminoglycan content (RGC) of explants harvested from the calf femoropatellar groove and cultured in the TCS for eight days in the presence of 0.0025X trypsin. The data are reported as the arithmetic mean of five samples plus the standard deviation of the mean.

- Analysis of variance (ANOVA, two-factor without replication, α=0.05) testing the hypothesis that all measurements are significantly different from their respective initial values on Day 0 indicates that beginning on Day 1, the $RDS_{0.004}$, $RDS_{0.88}$, and RGC all decline with significance.
- Analysis of variance (ANOVA, single-factor, α=0.05) testing the hypothesis that for any given time point the mean $RDS_{0.004}$, $RDS_{0.88}$, and RGC are statistically equivalent indicates: on Days 1, 1.5, and 2 the $RDS_{0.004}$ is less than $RDS_{0.88}$; on Day 1.5 the $RDS_{0.88}$ is significantly greater than the RGC; and that at all other time points the three measurements are not statistically different.
- Analysis of variance (ANOVA, single-factor, α=0.05) testing the hypothesis that the RGC of treated samples is different from that of untreated samples indicates that the RGC is statistically less than that of control at all times, beginning on Day 1.

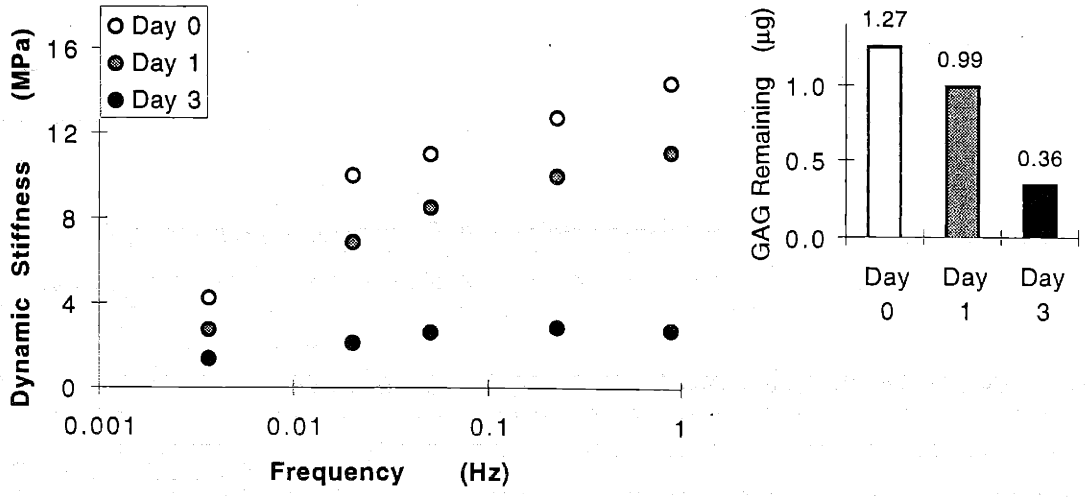

Figure 3.14: Treatment with 0.0025X trypsin

1. The frequency dependence of the absolute dynamic stiffness as observed immediately prior to treatment, and one and three days, respectively, afterwards. The data is of a single femoropatellar groove explant, but it is representative of the entire set of trypsin-treated samples. The equilibrium stiffness was not measured.
2. The histogram plots the absolute glycosaminoglycan content of the explant at the time when the dynamic stiffness was measured.

The effect of chondroitinase-ABC on the mechanical properties of cartilage explants

Explants from the calf distal ulna (2mm-thick by 3mm-diameter) were cultured in media supplemented with 0.1U/ml chondroitinase-ABC for four days. Measurements of mechanical properties were performed daily. Figure 3.15 reports the observed low- and high-frequency dynamic stiffness. The key findings were that chondroitinase-ABC elicited an immediate effect on the mechanical properties; the initial decline in lower-frequency dynamic stiffness preceded that of the higher-frequency stiffness; however, this trend changed after three days of treatment as the relative stiffness measurements were measurably similar in magnitude. The dimethylmethylene blue dye binding assay for glycosaminoglycan release was unable to detect the enzymatically degraded glycosaminoglycans, thereby making it impossible to correlate the mechanical properties to glycosaminoglycan content. The enzyme chondroitinase-ABC has been demonstrated to digest the chondroitin sulfate glycosaminoglyan polysaccharides into dissaccharides, which escape detection presumably due to threshholding effects. It has been reported in the literature that hyaluronic acid, when participating in the proteoglycan aggregate, is safe from degradation (Thurston et al. 1975); therefore the specific action of chondroitinase-ABC is quite different from that of hyaluronidase and trypsin.

Figure 3.16 reports the observed dynamic stiffness over a frequency range. A downward translation of the data is apparent after one day of treatment. But after four days the frequency response is significantly diminished in magnitude and "flat", indicating a departure from the previously witnessed frequency dependence.

Histological preparations of cartilage explants treated with 01.U/ml chondroitinase-ABC for one and two days, respectively, are presented in Figure 3.17. Identical to the effects of hyaluronate-lyase treatment (Figure 3.12) and in contrast to that of IL-1ß (Appendix B), the spatial mode of stain-depletion is along the prescribed diffusion path of the enzyme.

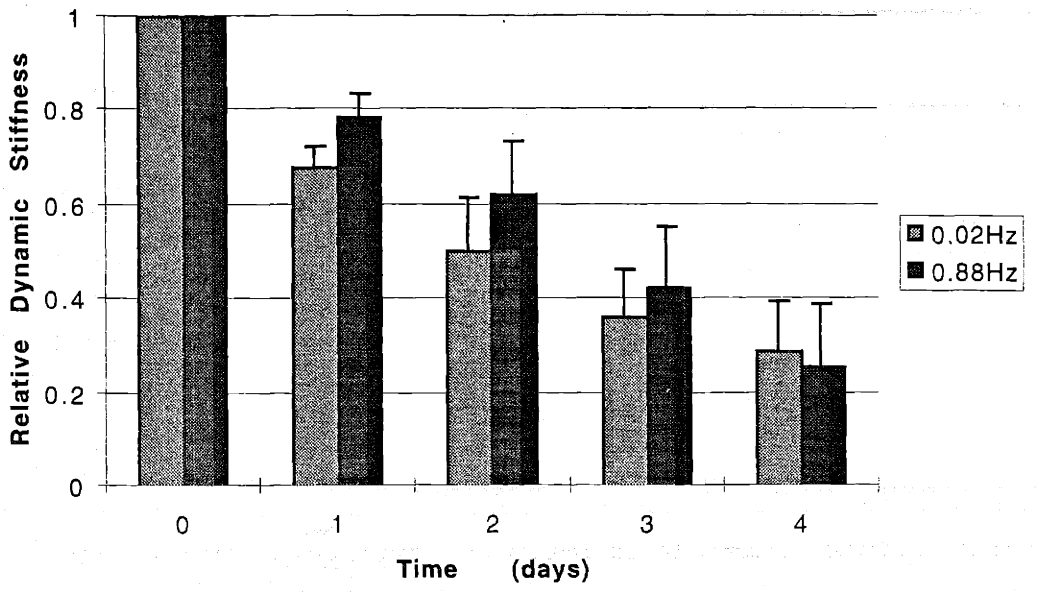

Figure 3.15: Treated with 0.1U/ml Chondroitinase-ABC
The relative dynamic stiffness ($RDS_{0.02}$ and $RDS_{0.88}$) of three explants harvested from the calf distal ulna and cultured in the TCS for four days in the presence of 0.1U/ml chondroitinase-ABC. The data are reported as the arithmetic mean of three samples plus the standard deviation of the mean.

- Analysis of variance (ANOVA, two-factor without replication, α=0.05) testing the hypothesis that all measurements are significantly different from their respective initial values on Day 0 indicates that beginning on Day 1, the $RDS_{0.02}$ and $RDS_{0.88}$ all decline with significance.
- Analysis of variance (ANOVA, single-factor, α=0.05) testing the hypothesis that for any given time point the mean $RDS_{0.02}$ and $RDS_{0.88}$ are statistically equivalent indicates that at all times they are never statistically different.

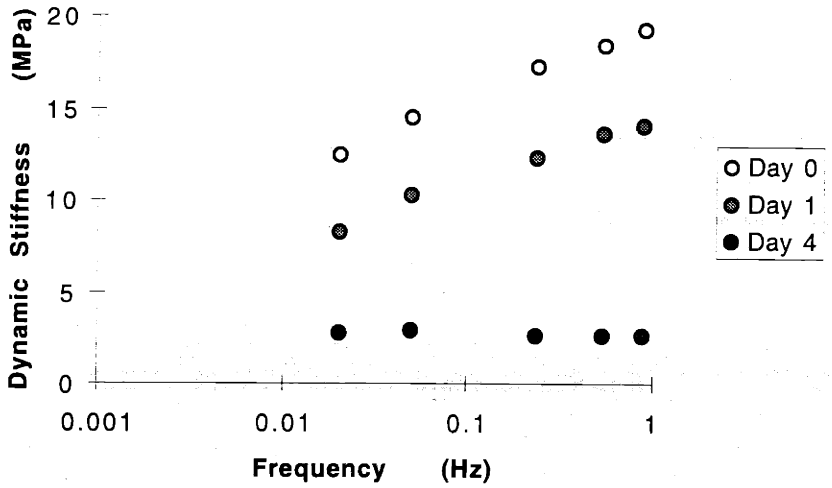

Figure 3.16: Treatment with 0.1U/ml Chondroitinase-ABC The frequency dependence of the absolute dynamic stiffness as observed immediately prior to treatment, and one and four days, respectively, afterwards. The data is of a single femoropatellar groove explant, but it is representative of the entire set of trypsin-treated samples. The equilibrium stiffness was 0.71Mpa, 0.61Mpa, and 0.06Mpa on Days 0, 1 and 4, respectively.

Glycosaminoglycan content could not be determined. The degradation products of this enzyme could not be detected with the dimethylmethylene blue assay. An alternative assay for glycosaminoglycan content, which tests for uronic acid content, was also defeated due to the presence of phenol red (a pH indicator) in the culture medium.

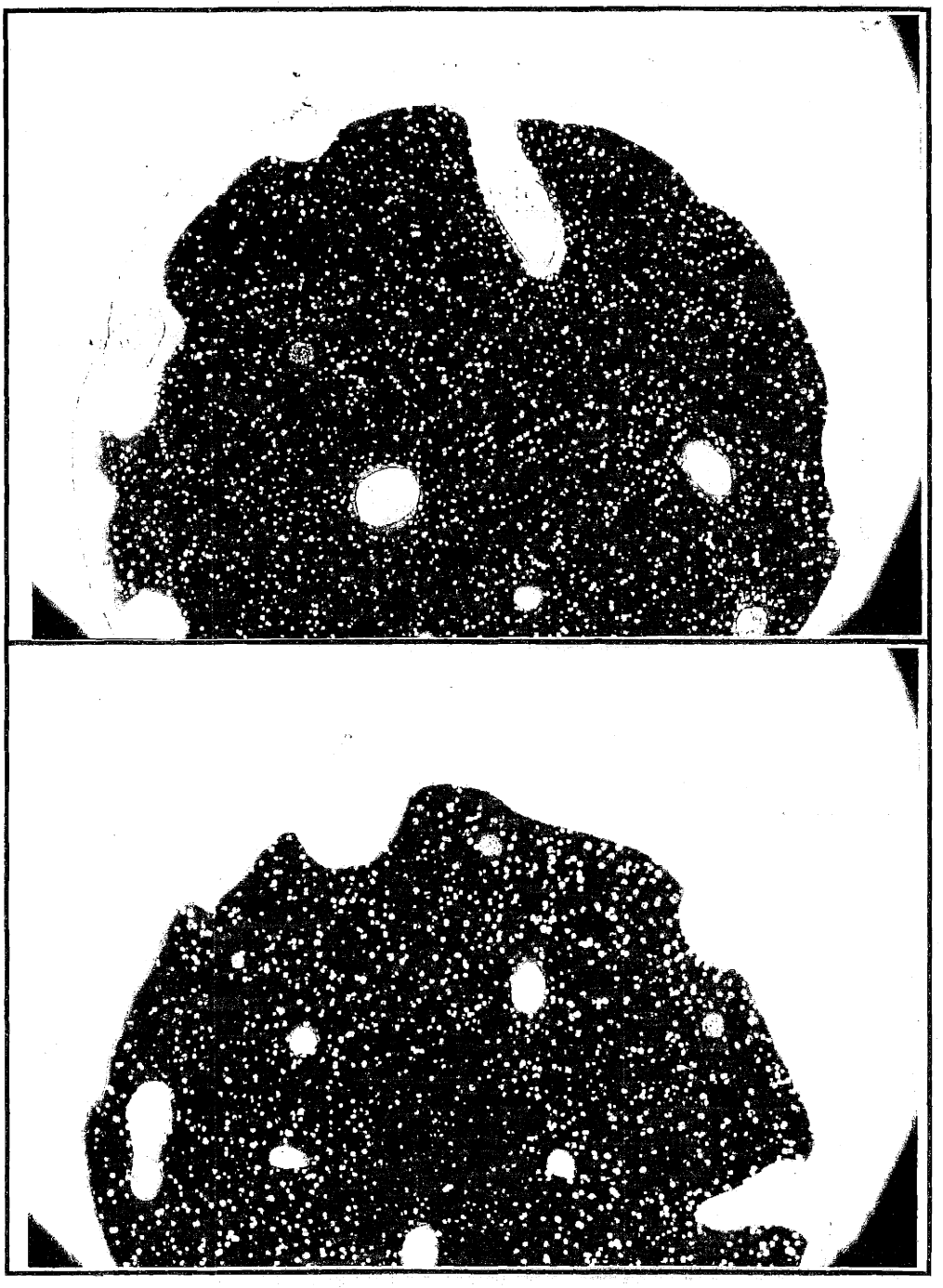

Figure 3.17: Treatment with Chondroitinase-ABC.
Histologic section of epiphyseal cartilage explants (2mm-thick, 3mm-diameter) obtained from the calf distal ulna. Explants were cultured for four days in free-swelling conditions and then axially confined with a 15%-strain static offset and cultured for one (top) and two (bottom) days 0.1Units/ml chondroitinase-ABC (protease-free, from *Proteus vulgaris*.). Fixed with glutaraldehyde and RHT, sectioned at 5μm, and stained with toluidine blue-O. Photomicrographs taken at 10X magnification and exhibit only a portion of the entire circular section. Similar to the effect exhibited by treatment with hyaluronate-lyase, with time the peripheral region devoid of stain progressively advances inward.

Discussion

Introduction

This discussion considers the effects of induced glycosaminoglycan degradation on the kinetics and proportions of change in equilibrium stiffness, dynamic stiffness and glycosaminoglycan content. The following conclusions have been drawn:

- Degradation of glycosaminoglycans causes a decrease in mechanical stiffness. For untreated tissue samples and samples treated with enzymes or interleukin-1ß, the decrease in stiffness is highly correlated with the decrease in glycosaminoglycan content.
- There is evidence from all three experimental regimes (control, enzyme, interleukin-1ß) that the drop in relative equilibrium stiffness and relative low-frequency (0.004Hz) dynamic stiffness leads the relative change in glycosaminoglycan content.
- Combining the data for enzyme-treated or interleukin-1ß-treated tissue relating the relative changes in stiffness to relative glycosaminoglycan content, indicates that the stiffness-glycosaminoglycan relationship is independent of the spatial pattern of glycosaminoglycan release.

The release of glycosaminoglycans is correlated with the decrease in mechanical properties.

Effects of "endogenous" degradation

The release of glycosaminoglycans occurs in conjunction with the decline in equilibrium and dynamic stiffness at all frequencies tested. The loss of glycosaminoglycans from tissue samples cultured in the absence of induced degradation is well documented for the culture techniques utilized in our laboratory (Biswal 1996; Chang 1992; Lai 1993) as well as for those of other investigators (Bonasser et al. 1994; Hubbard et al. 1988; Parsons and Black 1987). A review of the literature indicates that up to ~4% per day of the total glycosaminoglycan content in an explant can be released. For culture conditions that were essentially identical to those found in this thesis (3mm diameter, 800µm-thick, ulna-derived epiphyseal cartilage), Biswal observed a release rate of 2% per day. Furthermore, he found that the effects of static compression, ranging from 0% through 50% compressive strain, on the release of glycosaminoglycans were statistically insignificant. Chang noted that cartilage samples that were cyclically freeze-thawed, a process which promotes chondrocyte necrosis, released glycosaminoglycan at a rate of 1.25% per day. Lai noted a release rate of 2.5% per day for cultured explants (2mm-diameter, 800µm-thick, ulna-

derived epiphyseal cartilage). The upper limit of glycosaminoglycan release, established by Hubbard *et al*, for "live" cartilage was 4.3% per day (35±2% total loss after 8 days) and 3.6% per day (29±2% after 8 days) for "dead" (i.e., freeze-thawed) tissue.

Based upon initial sample glycosaminoglycan content, it was found that ulna-derived control samples cultured in the TCS released 2.4±1.6% (n=10) of their glycosaminoglycans per day and femoropatellar-groove samples released 1.5±0.8% (n=4) per day. The reason for this statistically significant (α=0.03) discrepancy between the two tissue sources is unclear. Recall the difference in culture protocol for these two tissues when mechanical measurements were not being performed; the ulna- and femoropatellar groove-derived samples were cultured with 0% and 15%-strain axial confinements, respectively. Although compression results in the consolidation of the extracellular matrix (a process which reduces the effective pore size and decreases the cartilage:medium interfacial surface area), the effects of stearic hindrances on glycosaminoglycan release are a subject of debate. Biswal and Lai observed no effect of static compression on the rate of "endogenous" glycosaminoglycan release, whereas Maroudas suggests (but does not report any empirical evidence) that matrix compaction would be expected to limit the release of cleavage products (Maroudas 1979). Biswal presented a hypothesis which considers the presence of the vasculature and its effect on glycosaminoglycan release. Paraphrasing, "it appears that the cells that are initially susceptible to {endogenous} degradive forces are those that reside in the perivascular or vascular region." (Biswal 1996). There is some histological evidence supporting his claim; Figure 4.1 indicates that glycosaminoglycans are released from the perivascular regions of samples cultured in the absence of induced degradation. This specimen exhibits a lack of stain, hence an absence of glycosaminoglycans, about a single blood vessel.

Also worthy of note in Figure 4.1 is the hint of degradation along the periphery of the sample. Interestingly, this coincides with the absence of viable cells observed at the peripheral interface of cartilage discs. Figure 4.2 is a result of a cell-viability study (methods described in Appendix D), demonstrating that as early as one hour post explantation there is a high density of propidium iodide (orange) stained cells, indicating defective cell membranes (i.e., "dead" cells), at the punched-edge. In contrast, the vast population of cells in the bulk extracellular matrix are fluorescein diacetate (green) stained, indicative of non-pathological esterase activity (i.e., "live" cells). A conclusion is that the damage to the tissue incurred by the explantation process disturbs the chondrocytes which presumably results in the release of proteolytic enzymes into the extracellular space. An alternative hypothesis is that the disruption of the peripheral collagen network reduces stearic obstructions, allowing the disentanglement of aggregating proteoglycans and their subsequent release into the bathing medium. The absence of stain at the radial edge does not occur routinely; a vast amount of histological evidence gathered in our laboratory does not exhibit this loss (e.g., the edges of the explants in Appendix B are positively stained).

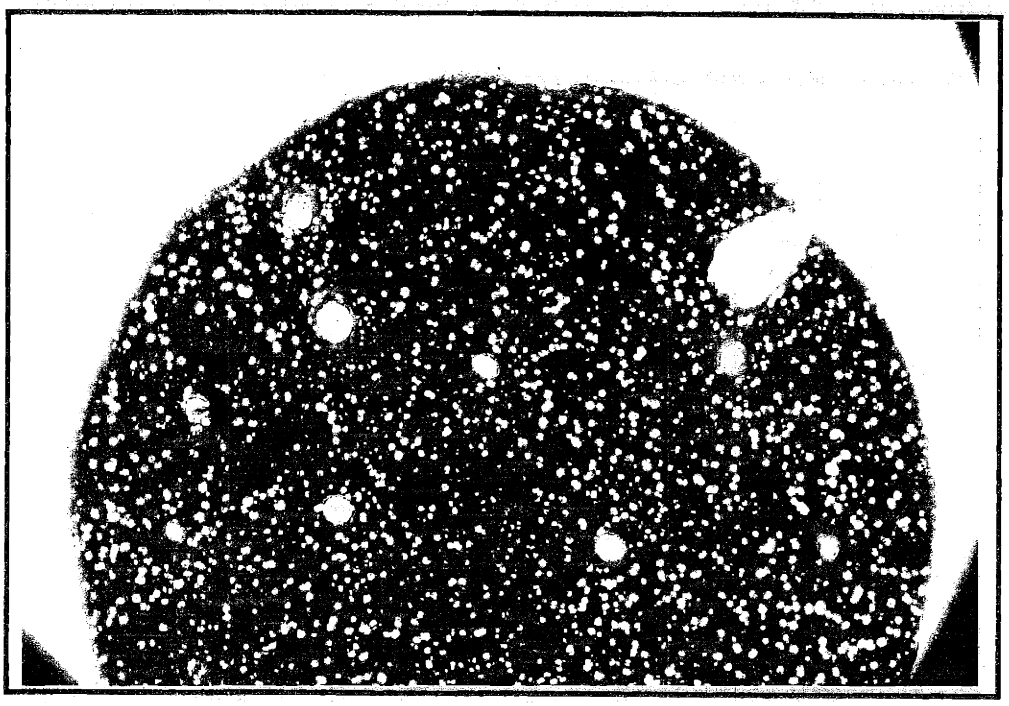

Figure 4.1: Untreated Control
Evidence of perivascular and peripheral glycosaminoglycan release in a cartilage explant cultured in the absence of induced degradation. The lack of toluidine blue O in the immediate extracellular matrix of the large blood vessel as well as the lack of stain in the periphery of the disc is indicative of glycosaminoglycan depletion. This sample of calf epiphyseal cartilage was harvested from the distal ulna, prepared into a disc (3mm-diameter, 2mm-thick) and cultured for five days in axial confinement with a time-invariant 15% compressive strain. The sample was fixed in glutaraldehyde and RHT, sectioned to 5μm, and stained with toluidine blue O. Photomicrograph was taken at 10X magnification.

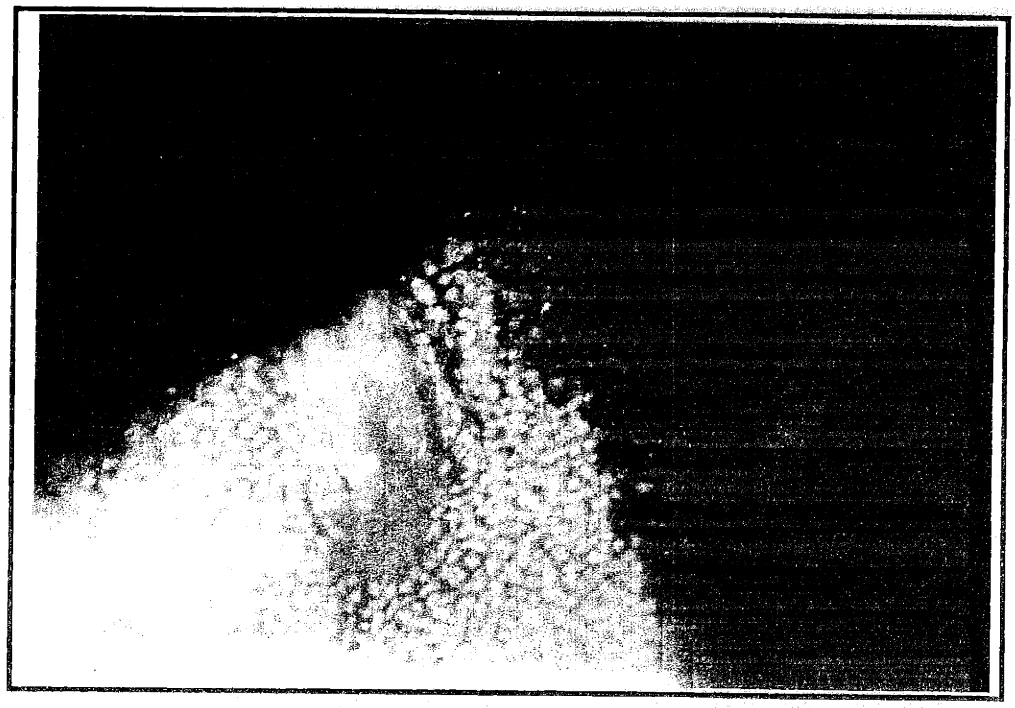

Figure 4.2: Chondrocyte Vitality
Evidence of necrotic chondrocytes at the cartilage:bath interface. Propidium iodide (PI) is essentially impermeable to the cell membrane over the time scale of exposure in this protocol, therefore a positive stain is indicative of a compromised cell membrane (i.e., the cell is dead). PI stains the nuclei orange by intercalating the bases of DNA. In contrast, fluorescein diacetate (FDA) is lipid soluble, thereby membrane permeable. FDA is not fluorescent in its nascent form, but in the presence of non-specific esterases the acetate moieties of FDA are enzymatically removed eliciting a green fluorescence. As a result of the explantation process the peripheral cells are ruptured, presumably releasing degradive enzymes into the surrounding extracellular matrix. It is proposed that this is a mechanism by which glycosaminoglycans are released at the explant's periphery (Figure 4.1).
The cartilage sample was harvested from the calf femoropatellar groove, prepared into a disc (3mm-diameter, 2mm-thick) and cultured in free-swelling conditions for one hour in supplemented DMEM. A circular section was removed from the mid-region of the disc and bisected into two semi-circles. The curvilinear edge with cells exhibiting intense orange staining was created with a dermal punch approximately one hour prior to staining, whereas the straight edge without orange staining was prepared with a razor blade about six minutes prior to staining. Apparently the effects of cutting the tissue are evident after one hour but are not immediate. The semi-circular section was immersed in 5ng/ml FDA for one minute, then 5μg/ml PI for one minute, and placed in a bath of 5ml of HBSS for microscope observation. The photomicrograph was taken at 25X magnification.

Effects of interleukin-1ß

The dynamic stiffness of ulna-derived tissue dropped in proportion to the glycosaminoglycan content; the relative drops in either measurement decreased with time (with statistical significance) in culture (with the exception of the 0.88Hz relative dynamic stiffness on Day 1) but were never statistically different from one-another over the experimental time-course. Likewise, the femoropatellar groove-derived tissue behaved in a statistically similar fashion; the 0.88Hz relative dynamic stiffness and relative glycosaminoglycan content dropped with significance, except on Day 1, and were never statistically different.

This study has clearly shown that interleukin-1ß-induced glycosaminoglycan release leads to a decrease in equilibrium and dynamic stiffness. The action of the cytokine was immediate in the case of the ulna-derived tissue, and delayed for the femoropatellar-groove-derived tissue. After the first twenty-four hours of treatment with IL-1ß the relative glycosaminoglycan content dropped below that of the untreated controls with statistical significance. The same was observed by Lai. However, a statistical difference in relative glycosaminoglycan content between untreated and treated femoropatellar groove-tissue was not observed until the fourth day of treatment. This delay may be attributable to the 15% static confinement of the explants. Unlike the glycosaminoglycan release rates of untreated tissue, Biswal noted that interleukin-1ß-induced degradation is inhibited by increasing static compression. However, the degree to which a 15%-strain static compression mediates the induced degradation is unclear because he found no statistically significant difference in glycosaminoglycan release for samples constrained to 0% and 10%-strain.

The drop in high-frequency dynamic stiffness was always in proportion to the drop in glycosaminoglycan content. Chang also witnessed this result; he reports that for cartilage explants treated with 150ng/ml IL-1ß the 0.046Hz dynamic load diminished in proportion with the relative glycosaminoglycan content. Although treatment clearly changed the magnitude of the equilibrium and dynamic stiffness, it did not measurably influence the response versus frequency. A high-frequency limit in stiffness was reached at ~0.2 Hz for both control and treated samples.

The action of interleukin-1ß requires the presence of viable chondrocytes. The ability of the established culture system to maintain cell viability was assessed and a representative section is presented in Figure 4.3. Here, viable cells (green-staining) are detected throughout the entire section. (Note: at this time the protocol did not include staining with propidium iodide to localize dead cells.)

Effects of enzymolysis

The individual effects of hyaluronate lyase, chondroitinase-ABC, and trypsin on cartilage explants were to induce glycosaminoglycan degradation. Although the methods used to quantify

glycosaminoglycan release products in the culture media were insufficient to account for chondroitinase-ABC-degraded glycosaminoglycans, histological methods did successfully indicate glycosaminoglycan depletion. Enzymolysis with hyaluronate lyase and trypsin both showed a steady monotonic release of glycosaminoglycans with statistically significant drops at every time point for both tissue types. Attendant to the loss of the glycosaminoglycans was the decrease in equilibrium and dynamic stiffness. The decline in dynamic stiffness directly correlated with the release of glycosaminoglycans and was never (with only one exception) statistically different from the relative changes in glycosaminoglycan content.

Although treatment with hyaluronate lyase clearly changed the magnitude of the equilibrium and dynamic stiffness, it did not measurably influence the response versus frequency. The frequency-dependence of the dynamic stiffness was identical for control and treated samples. In contrast, treatment with trypsin and chondroitinase-ABC altered the frequency dependence of the dynamic stiffness. The results after one day of treatment with either enzyme showed a greater reduction in the high-frequency stiffness than at low frequencies. Furthermore, after continued treatment the dynamic stiffness became nearly independent of frequency.

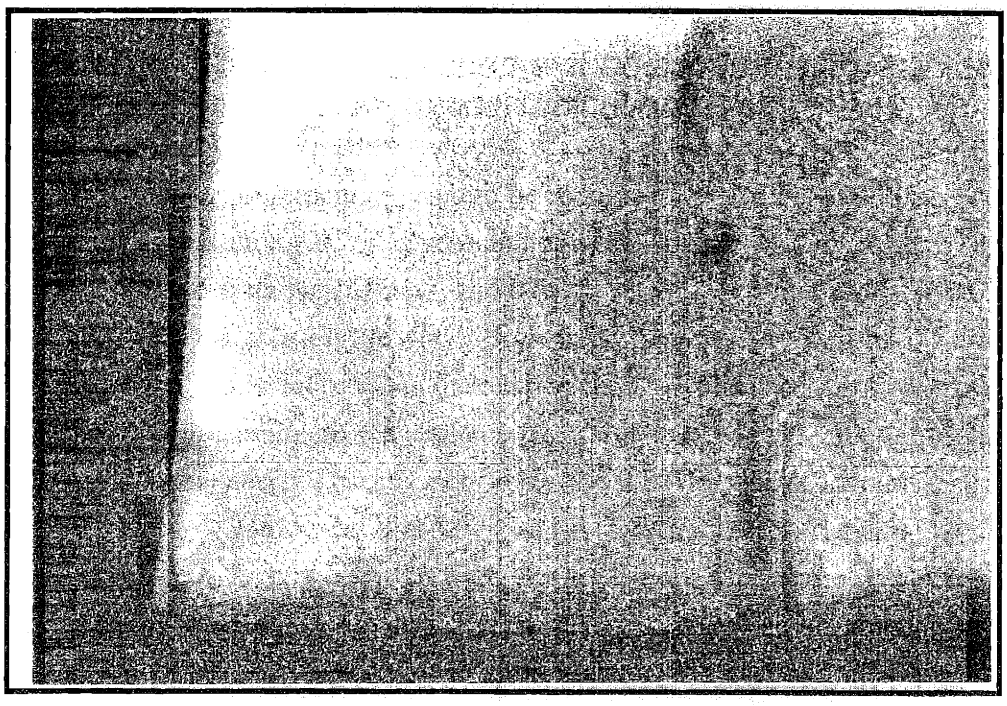

Figure 4.3: Chondrocyte Vitality
This explant, treated with 100ng/ml interleukin-1ß and cultured in static compression for five days, exhibits evidence of viable chondrocytes throughout the entire section. Explanted from the calf femoropatellar groove, this disc was cultured for two days in free-swelling conditions. Then it was confined with a 15%-strain static offset and cultured for five days in the presence of 100ng/ml IL-1ß. Mechanical properties were measured once a day. See Appendix D for discussion on fluorescein diacetate staining methods.

For induced degradation, measurements of equilibrium stiffness suggest tissue degradation prior to biochemical indications.

The equilibrium stiffness measurement appears to be more sensitive to induced tissue degradation than the biochemical measurement of glycosaminoglycan release. The relative equilibrium stiffness, 0.004Hz relative dynamic stiffness, and 0.88Hz relative dynamic stiffness from Figures 3.5 and 3.6 were combined into Figure 4.4. Both tissue sources, as well as different sample dimensions, are included in this data. When the relative change in mechanical properties is plotted against the fractional glycosaminoglycan content for tissue treated with 100ng/ml IL-1ß there appears to be a direct correlation between changes in the 0.88Hz relative dynamic stiffness and glycosaminoglycan loss. However, the changes in low-frequency dynamic stiffness and equilibrium stiffness do not directly correlate with changes in the glycosaminoglycan content; they appear to diminish faster than the drop in glycosaminoglycan content. This result has been previously alluded to by Chang, where he demonstrated that for cartilage explants treated with 150ng/ml IL-1ß the equilibrium static offset load declined with faster kinetics than the loss in glycosaminoglycan content.

Similarly, the relative equilibrium stiffness and 0.88Hz relative dynamic stiffness from Figures 3.8, 3.9 and 3.10 were combined into Figure 4.5. The equilibrium stiffness measurements of hyaluronate lyase-treated samples appear to be more sensitive to tissue degradation than measurements of glycosaminoglycan release. Figure 4.5 shows that the high frequency dynamic stiffness diminishes with near-identical kinetics and proportions as the measurement of glycosaminoglycan release but the equilibrium stiffness diminishes in greater proportion than the drop in glycosaminoglycan content.

The data of Figures 4.4 and 4.5 suggest that (1) there is a trend of low frequency dynamic stiffness and equilibrium stiffness measurements predicting tissue catabolism faster than the measurement of glycosaminoglycan release, (2) measurements of higher frequency dynamic stiffness correlate directly with glycosaminoglycan content, and (3) the source and diameter of the explants do not effect these trends.

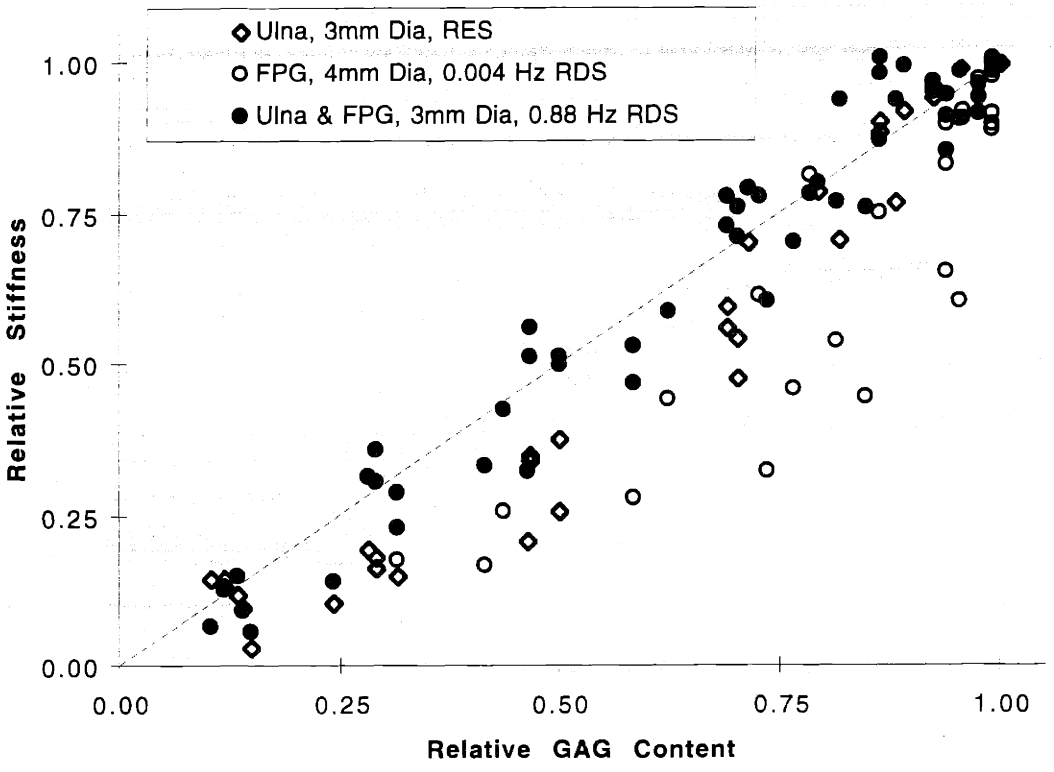

Figure 4.4: Stiffness vs. GAG for IL-1ß Treated Tissue
Relative stiffness vs. fractional glycosaminoglycan content for interleukin-1ß-treated tissue. The relative equilibrium stiffness (RES) and relative dynamic stiffness ($RDS_{0.004}$ and $RDS_{0.88}$) are plotted against the relative glycosaminoglycan content for ulna-derived and femoropatellar groove (FPG)-derived explants. Each point represents the stiffness of a specific sample plotted against its own glycosaminoglycan (GAG) content to highlight the dependence of stiffness on glycosaminoglycan content. A unity-slope line is provided as an eye-guide only, and is not intended to imply a "fit". However, a slope of m=1.0361 for the 0.88Hz relative dynamic stiffness data was calculated (R^2=0.9635).

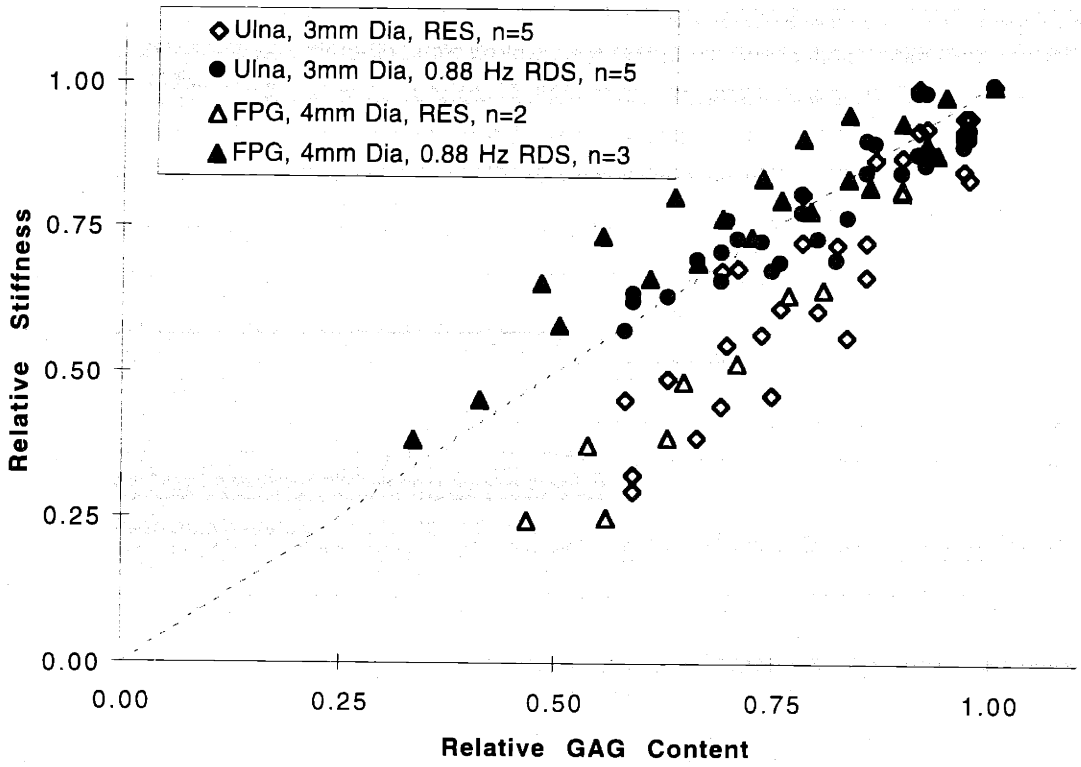

Figure 4.5: Stiffness vs. GAG for Hyaluronate Lyase Treated Tissue
Relative stiffness vs. fractional glycosaminoglycan content for hyaluronate lyase-treated tissue. The relative equilibrium stiffness (RES) and relative dynamic stiffness ($RDS_{0.88}$) are plotted against the relative glycosaminoglycan content for ulna-derived and femoropatellar groove (FPG)-derived explants. Each point represents the relative stiffness of a specific sample plotted against its own relative glycosaminoglycan (GAG) content to highlight the dependence of stiffness on glycosaminoglycan content. Note that irregardless of tissue source the high-frequency relative dynamic stiffness directly correlates with the changes in relative glycosaminoglycan content and the changes in relative equilibrium stiffness precede the changes in glycosaminoglycan content. A unity-slope line is provided as an eye-guide only, and is not intended to imply a "fit". A slope of m=0.8097 for the 0.88Hz relative dynamic stiffness data was calculated (R^2=0.8518).

The relative changes in stiffness elicited by altering the glycosaminoglycan fraction are independent of the spatial modality of glycosaminoglycan release (addressing objective 3).

The spatial patterns of glycosaminoglycan release induced by treatment with interleukin-1ß and by the direct action of enzymolysis have been established. For interleukin-1ß, the initial site of glycosaminoglycan release is in the perivascular regions. With continued treatment, the path of glycosaminoglycan release has been observed to progress radially outward from initiation sites in a front-like fashion. Biswal verified that the cytokine's diffusion path clearly does not coincide with the spatial pattern of glycosaminoglycan release (Biswal 1996). This "point-source" modality of degradation is quite different from that of direct enzymolysis. Because treatment with proteolytic enzymes is not cell-mediated, the action of proteolytic enzymes induces immediate degradation in the periphery of the explanted cartilage discs. Further treatment is characterized by the "concentric, radially-inward" path of glycosaminoglycan release.

The effect of the spatial pattern of glycosaminoglycan release can be studied by plotting the mechanical properties against glycosaminoglycan content for both modes of degradation. The relative equilibrium stiffness, 0.004Hz relative dynamic stiffness, and 0.88Hz relative dynamic stiffness adapted from data presented in the Results section were combined into Figures 4.6, 4.7 and 4.8, respectively. There is no apparent difference in equilibrium stiffness and 0.88Hz relative dynamic stiffness between interleukin-1ß and enzyme induced degradation. Comparing the linear regression of the high frequency stiffness results, a *Student's t* test indicates that that there is no statistical difference in regression coefficients (α=0.05). Therefore, changes in the relative dynamic stiffness directly infer changes in glycosaminoglycan release, and vice versa.

Figure 4.7 suggests that a difference exists at the low-frequency dynamic stiffness; however, the "enzyme" was trypsin and there may be a procedural caveat with trypsin-induced degradation. Glycosaminoglycans were released very quickly with this treatment (note the time scale in Figure 3.13) so that the biochemical measurement may reflect some error in accounting for glycosaminoglycan content. The actual amounts of glycosaminoglycans (GAGs) released to the bathing media due to the action of trypsin are presented in Table 4.1 (reported is the mean and standard deviation of the mean for five samples). Subsequent to the final measurement of mechanical properties the culture medium was collected (time point 5) and the samples were rinsed with a ~1.0ml volume (rinse duration of approximately two minutes). The data in Table 4.1 suggest that the amount of glycosaminoglycans detected in the rinse is not negligible compared to the amount released at time points 1-5. The unexpectedly large amount of glycosaminoglycans in the rinse volume suggests that the estimation of content throughout the experiment might be skewed. Thus, this may be reflected in Figure 4.7. Further experiments with slower acting

enzymes, like hyaluronate lyase, would clarify this caveat. Moreover, this procedural concern does not reject the conclusion that the relative changes in stiffness elicited by altering the glycosaminoglycan fraction are independent of the spatial modality of glycosaminoglycan release

Table 4.1: Trypsin-Induced GAG Release
Glycosaminoglycans released to the culture media and final rinse volume (mean ± standard deviation of the mean, n=5).

Time (time point)	GAGs Released (μg)
1	311±32
2	191±16
3	181±23
4	119±10
5	110±7
Rinse	24±8

Reality, it seems, obfuscates our simple conceptualizations of the "point-source" and "concentric, radially-inward" patterns of degradation beyond the degree we had hoped. It was thought that these terms conveniently and simply described the spatial pattern of glycosaminoglycan release as induced with interleukin-1ß or with direct enzyme treatment. It turns out that the communication of blood vessels with the bathing medium coupled with the apparent pervasiveness of the vasculature introduces effects. It is conceivable that the presence of a network of cartilage canals would facilitate the rapid advancement of exogenously added enzymes and allow for the expedited disbursement of degradive substances. Although it has been observed that a certain level of endogenous degradation occasionally occurs in the perivascular and peripheral regions of untreated explanted cartilage discs (e.g., Figure 4.1), the explant in Figure 4.9, treated with 10TRU/ml hyaluronate lyase for two days, clearly demonstrates a lack of stain about the blood vessels that exceeds that found in Figure 4.1. The explant in Figure 4.10, treated with the same dose of hyaluronate lyase for three days, depicts a more severe example of invasive degradation. However, this result is not unexpected since the vessel appears to be continuous with the periphery. On the other hand, there are several histological examples of hyaluronate lyase (and chondroitinase-ABC) treated tissue exhibiting no evidence of this invasiveness whatsoever. Thus, though the data in Figures 4.6, 4.7, and 4.8 suggest that there is no measurable difference in

mechanical properties for the two spatial degradation patterns, a conclusion is that the degree of difference in generating these spatial profiles may be immeasurable with the TCS.

Lastly, since interleukin-1ß induces the production and activation of a range of metalloproteinases, it remains unclear whether the changes in stiffness are purely a result of changes in tissue glycosaminoglycans or whether interleukin-1ß-induced effects on collagen or other matrix macromolecules play a role. The contribution of the collagen network to the mechanical properties of radially-unconfined explants is unknown at this time. Since collagen is a crucial structural constituent, future experiments addressing this issue would involve inducing alterations of the collagen fraction (e.g., with exogenously added collagenase).

Despite heterogeneity intrinsic to the cartilage explants and procedural complications of enzymolysis, the data presented (particularly in Figures 4.6 and 4.8) is very tight and completely endorses the conclusion that the release of glycosaminoglycans is correlated with the decrease in mechanical properties.

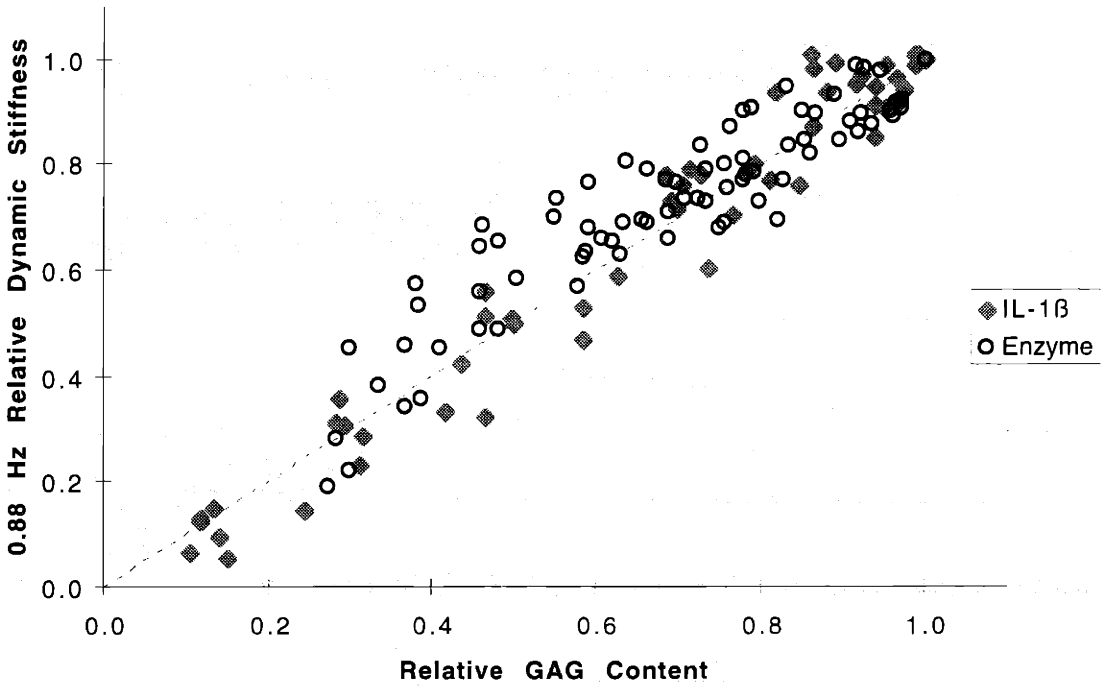

Figure 4.6: 0.88Hz Relative Dynamic Stiffness vs. GAG Content
The 0.88Hz relative dynamic stiffness plotted against the relative glycosaminoglycan (GAG) content for cartilage explants treated with either 100ng/ml interleukin-1ß or proteolytic enzymes (hyaluronate lyase or trypsin). By comparing the linear regression (not shown) of both sets of data it was determined that the slopes of the two lines were not significantly different at the 95% confidence interval. This result suggests that observations of high-frequency dynamic stiffness decrease in direct proportion to the decline in the relative glycosaminoglycan content, despite the apparent discrepancies in the spatial modality of glycosaminoglycan release. In contrast to Figure 4.5, the data for trypsin-treated tissue was included here, modifying the calculated slope of the "enzyme" data to 0.8542 (R^2=0.8816). Combining both data sets into a single data set and performing a linear regression analysis the correlation changed to R^2=0.9233, which is the value reported in the *Abstract*.

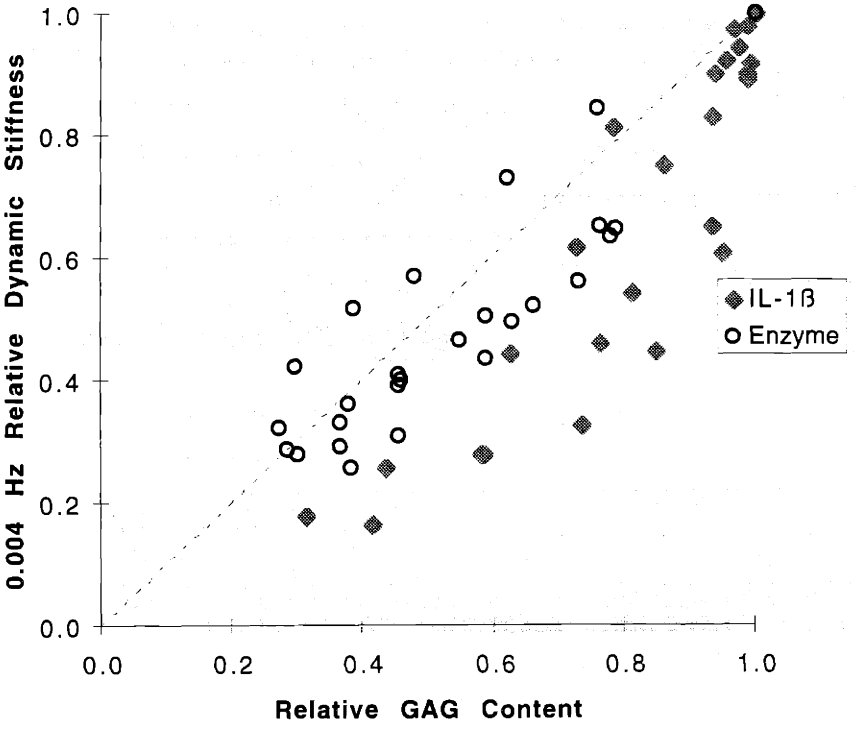

Figure 4.7: 0.004Hz Relative Dynamic Stiffness vs. GAG Content

The 0.004Hz relative dynamic stiffness plotted against the relative glycosaminoglycan (GAG) content for cartilage explants treated with either 100ng/ml interleukin-1ß or trypsin.

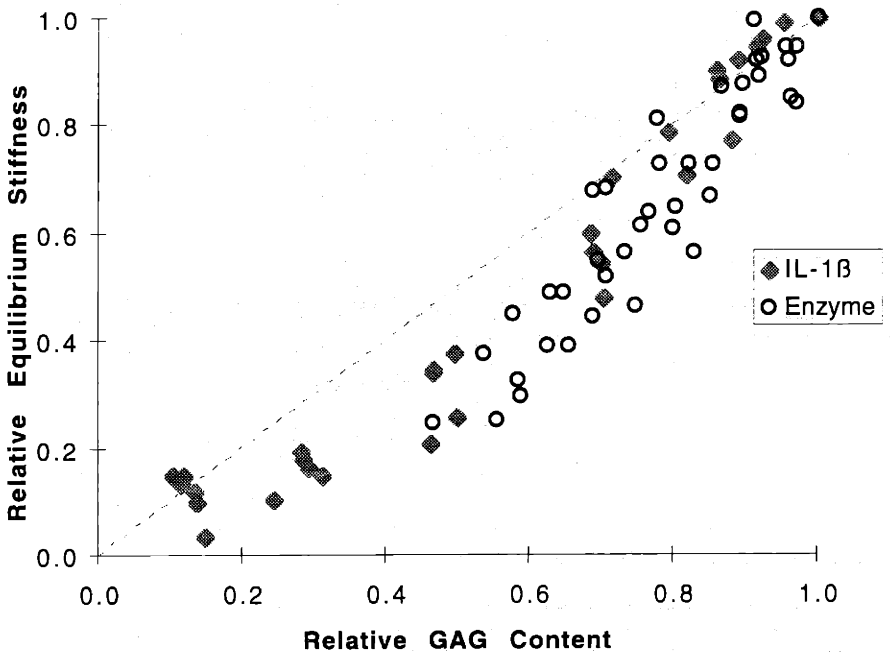

Figure 4.8: Relative Equilibrium Stiffness vs. GAG Content

The relative equilibrium stiffness plotted against the relative glycosaminoglycan content for cartilage explants treated with either 100ng/ml interleukin-1ß or hyaluronate lyase.

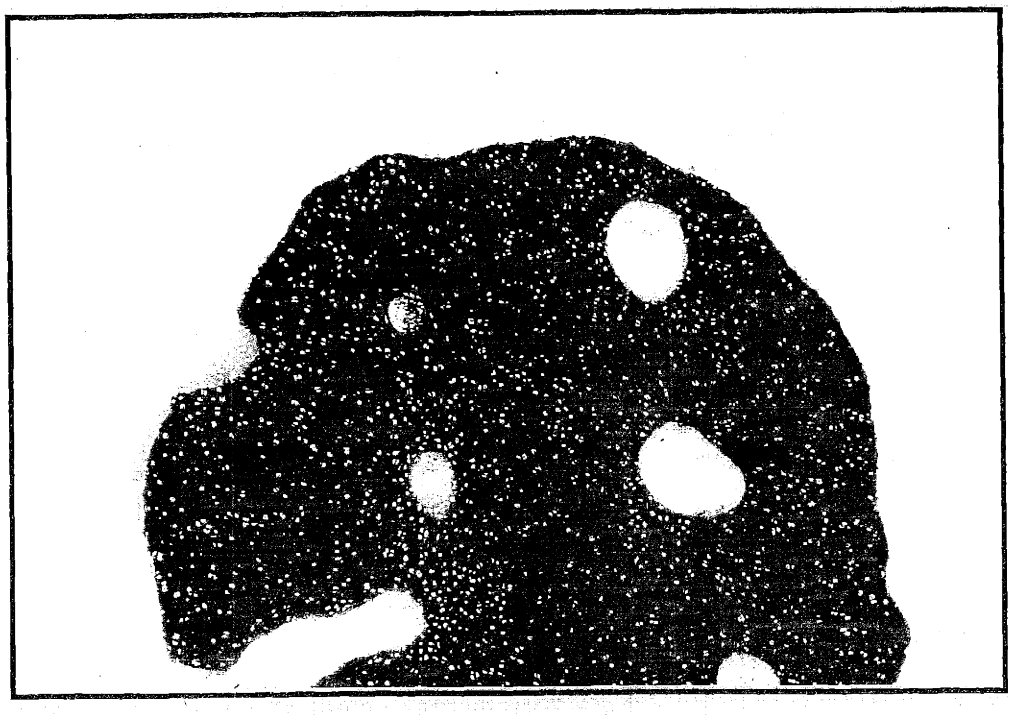

Figure 4.9: Treatment with Hyaluronate Lyase
Histological evidence of exogenously added enzymes entering the explant through the cartilage canals. Calf epiphyseal cartilage, explanted from the distal ulna and prepared into cylindrical disk (3mm-diameter, 2mm-thick). This sample was cultured in free-swelling conditions for two days. Then it was cultured two days in the presence of 10TRU/ml hyaluronate lyase while confined with a 15%-strain static offset. Fixed in glutaraldehyde and RHT, sectioned to 4μm, and stained with toluidine blue O. Photomicrograph taken at 10X magnification with a Quantaray 52mm, 80Å (blue) filter.

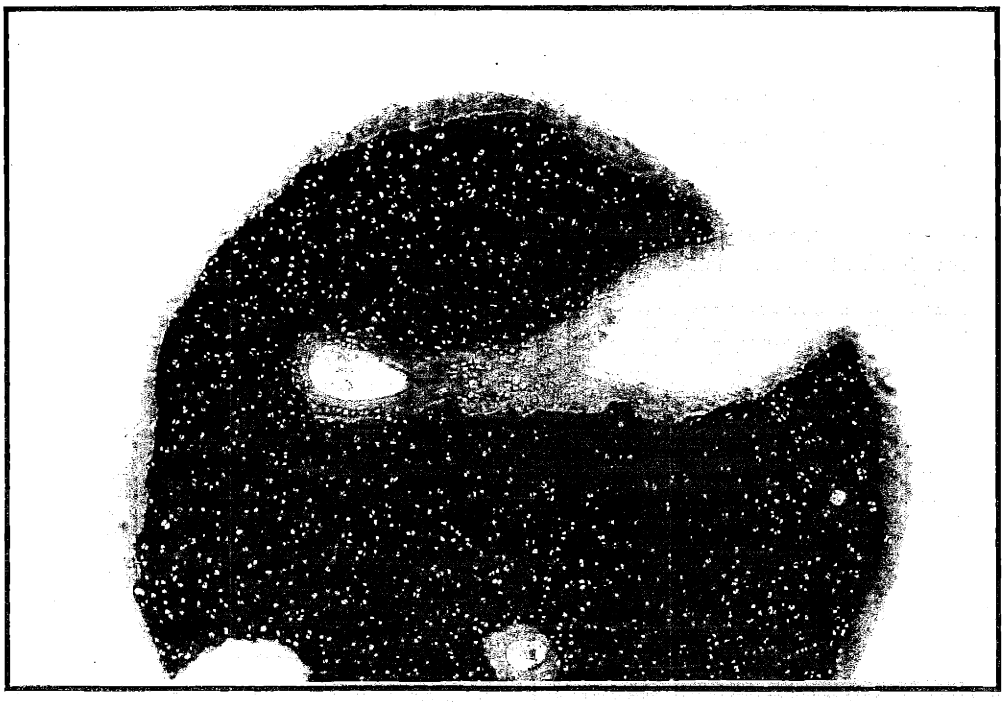

Figure 4.10: Treatment with Hyaluronate Lyase
Histological evidence of exogenously added enzymes entering the explant through the cartilage canals. Calf epiphyseal cartilage, explanted from the distal ulna and prepared into cylindrical disk (3mm-diameter, 2mm-thick). This sample was cultured in free-swelling conditions for two days. Then it was cultured two days in the presence of 10TRU/ml hyaluronate lyase while confined with a 15%-strain static offset. Fixed in glutaraldehyde and RHT, sectioned to 4μm, and stained with toluidine blue O. Photomicrograph taken at 10X magnification without filtering.

Appendix A

Frequency characterization of the Tissue Compression System (TCS) in the absence of cartilage and six displacement-based compression waves.

This appendix contains the results of several verification studies. Preliminary analyses of the TCS were undertaken to establish its credibility to accurately generate and measure small-amplitude, time-varying displacements. These displacements were imposed upon tissue samples in order to observe their dynamic stiffness.

The range of frequencies utilized in this study spanned two orders of magnitude (~0.004Hz through 0.86Hz), a frequency-window of sufficient limits to observe the effects of fluid flow and hydrostatic pressurization on dynamic stiffness (Lee et al. 1981). A 1.8mm-thick by 4mm diameter cartilage disc (from the femoropatellar groove) was the subject of Figures A.1 through A.6, which depict the measurements of the imposed displacement (as per the protocol described in the Methods section) and the load response and the fourier decomposition of those measurements. The dynamic stiffness was calculated by two methods: "manually", by measuring the peak-to-peak loads and displacements, and, more rigorously by using the fourier magnitudes of the load and displacement measurements at the fundamental frequency. Figure A.7 demonstrates that either method is sufficient for determining the dynamic stiffness of normal cartilage at any frequency. The dynamic stiffness reported in the Results section was obtained manually.

The dynamic stiffness of the TCS, in the absence of cartilage, was determined and is presented in Figure A.8. This "everything but the cartilage" experiment was designed to measure the compliance of all hardware directly associated with the containment and compression of cartilage samples, which included the upper- and lower- stainless steel platens, the load cells (Sensotec, Columbus, OH: Model 31, 4.53kg capacity), the polysulfone compression chambers, and the quartz compression post. Except for the load cells, all of these components are constructed of materials sufficiently stiffer than cartilage. The fundamental theory behind the load-sensing ability of these load cells requires certain internal deformations of a piezoelectric sensor. The manufacturer of the load cells specifies an inherent compliance of "0.001-0.003in. at full scale", or an equivalent "spring stiffness" range of 1.752MN/m - 0.584MN/m. The specific stiffness of each test-position of the TCS (numbered 1 through 5) was observed to vary from 0.24MN/m to 0.43MN/m. The system stiffness was less than the range of allowable load cell compliance, presumably attributable to manufacturer mis-specification or the "series-compliance" of the polysulfone chambers in addition to that of the load cells. Most importantly, however, the stiffness of each position in the TCS was found to be independent of frequency. Figure A.9 compares the stiffness of the cartilage sample mentioned above to the system stiffness of the test

position it was situated in. At high frequencies the cartilage sample resists deformation to the extent that the deformations of the systems are dominant. The stiffness values reported in this thesis were not corrected for system compliance. Although compensating for system compliance may effect the magnitude of high-frequency dynamic stiffness values, the interpretations of the *relative* results would not change.

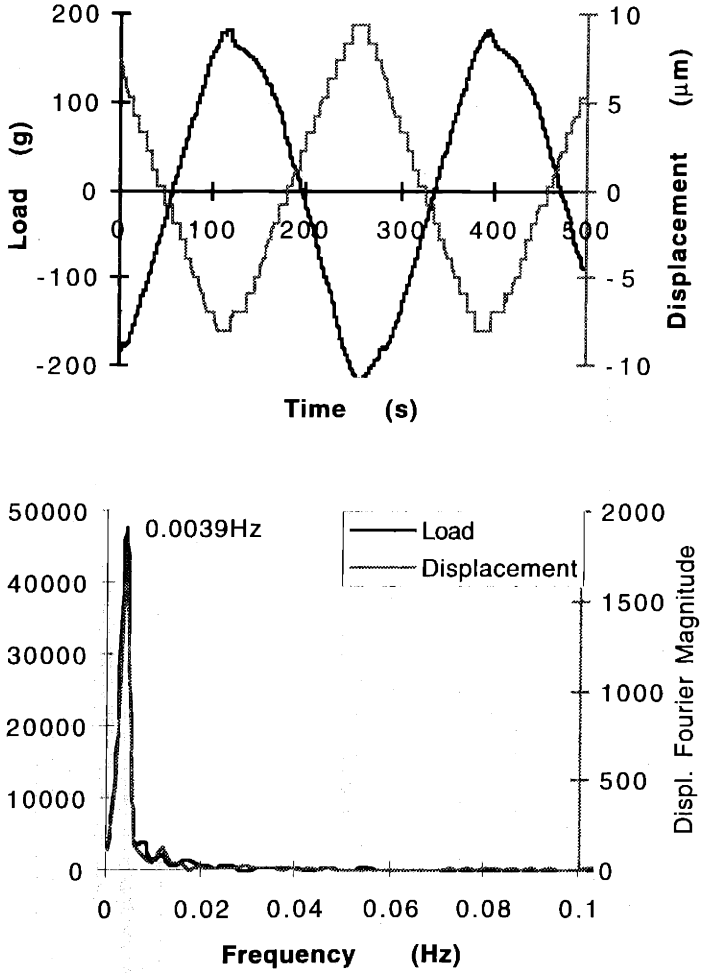

Figure A.1: Cartilage subjected to a 0.004Hz, 17.4μm peak-to-peak displacement wave
A. Load and displacement versus time.
B. 512-point Fourier magnitude versus frequency

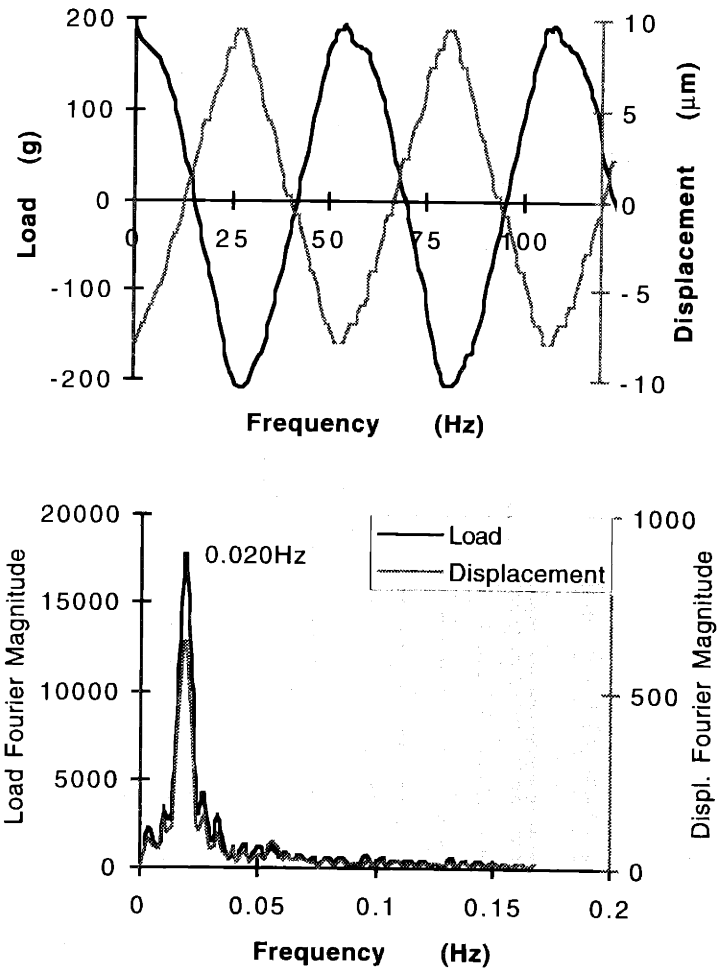

Figure A.2: Cartilage subjected to a 0.020Hz, 17.4μm peak-to-peak displacement wave
A. Load and displacement versus time.
B. 512-point Fourier magnitude versus frequency

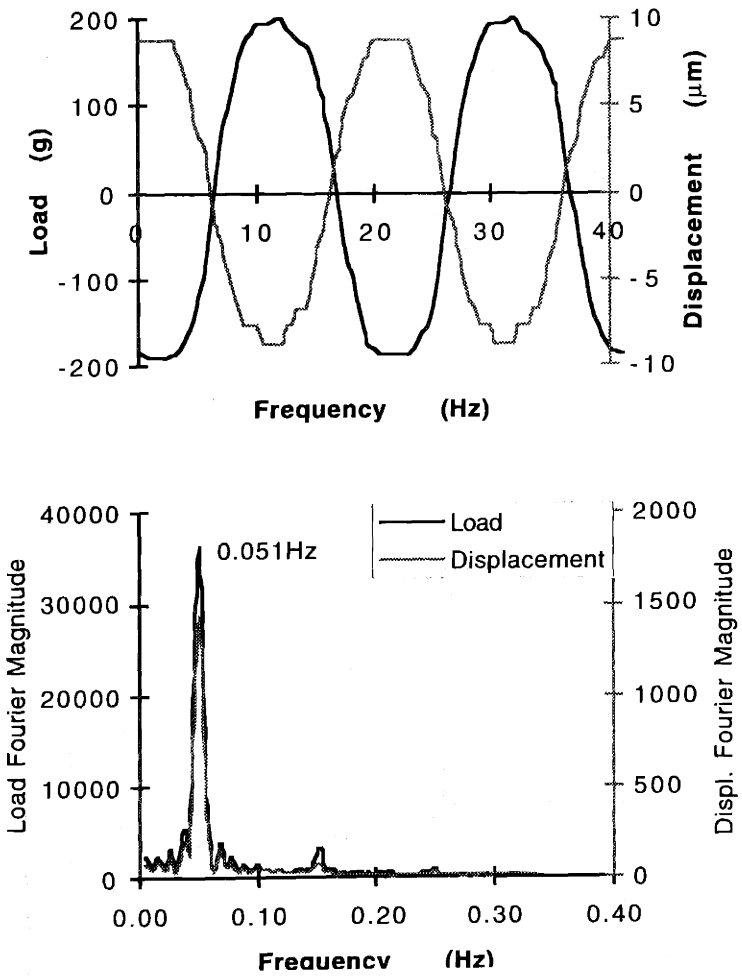

Figure A.3: Cartilage subjected to a 0.05Hz, 17.4μm peak-to-peak displacement wave
A. Load and displacement versus time.
B. 512-point Fourier magnitude versus frequency

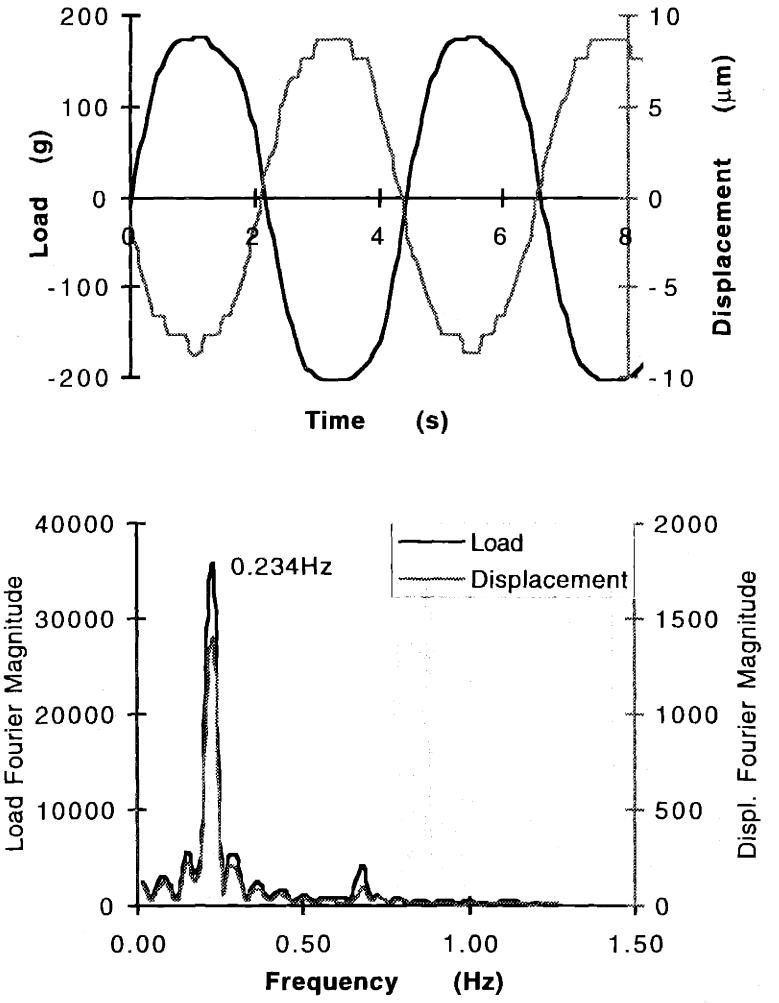

Figure A.4: Cartilage subjected to a 0.23Hz, 17.4μm peak-to-peak displacement wave
A. Load and displacement versus time.
B. 512-point Fourier magnitude versus frequency

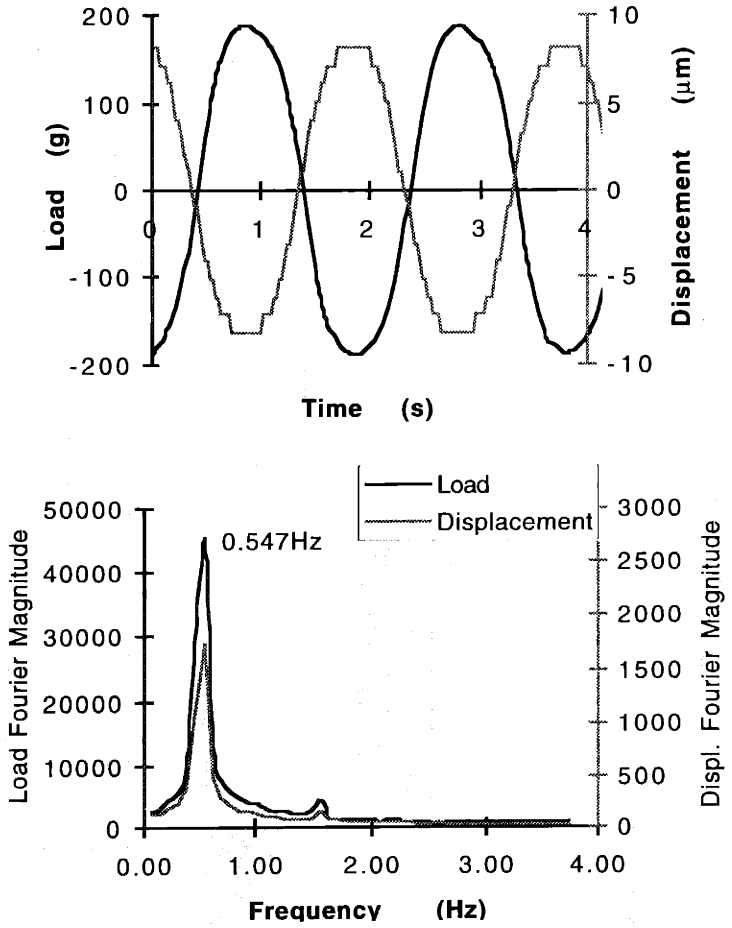

Figure A.5: Cartilage subjected to a 0.55Hz, 16.4μm peak-to-peak displacement wave
A. Load and displacement versus time.
B. 512-point Fourier magnitude versus frequency

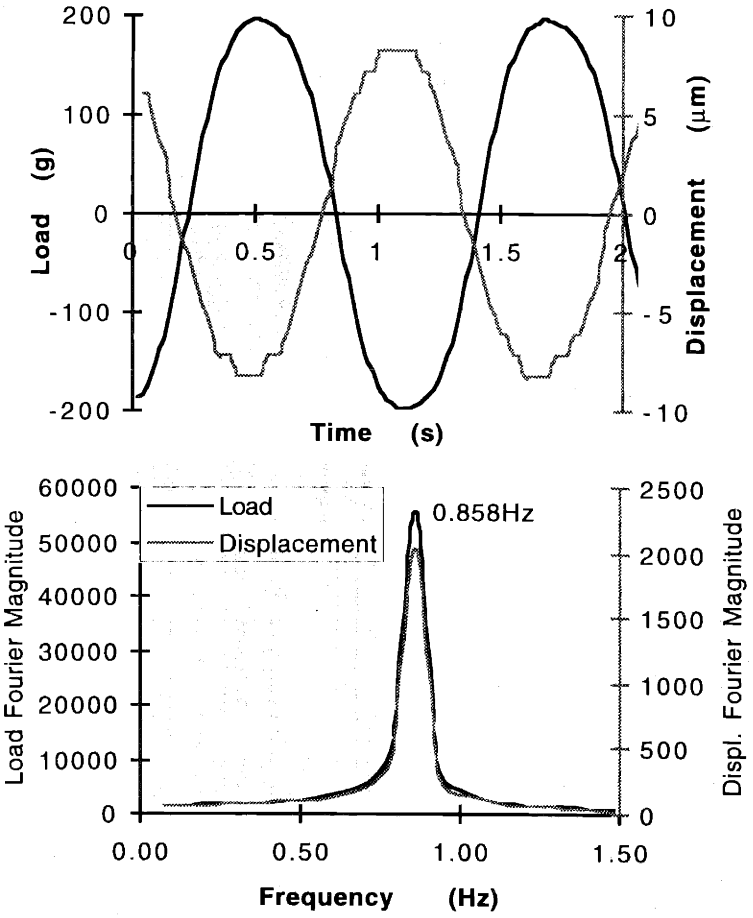

Figure A.6: Cartilage subjected to a 0.88Hz, 16.4μm peak-to-peak displacement wave
A. Load and displacement versus time.
B. 256-point Fourier magnitude versus frequency

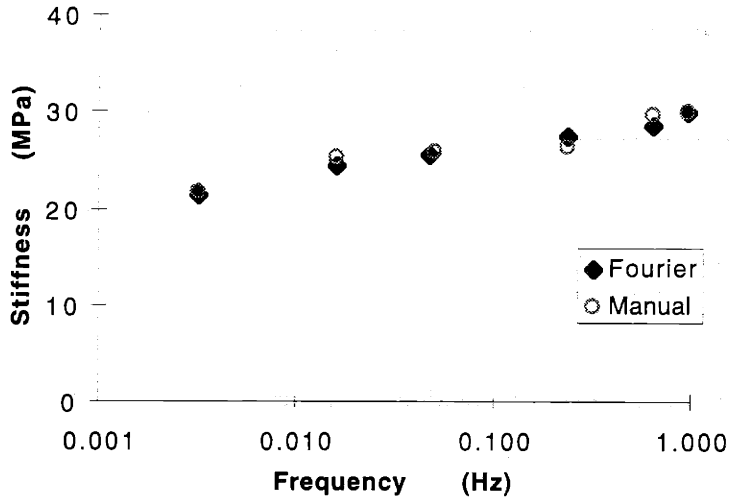

Figure A.7: Comparison of two methods used to calculate the dynamic stiffness. "Fourier" refers to the procedure of normalizing the fourier magnitudes at the fundamental frequency for the load measurement to that of the displacement measurement and scaling the result with the appropriate area and thickness measurements, transducer scaling factors, and the gravitational constant. "Manual" refers to the process of measuring the peak-to-peak load and displacement tracings with a ruler (Wescott R405-12", Korea) from a strip chart recording followed by scaling with the same factors as above. Discrepancies range from 0.7% at 0.86Hz and 3.7% at 0.55Hz.

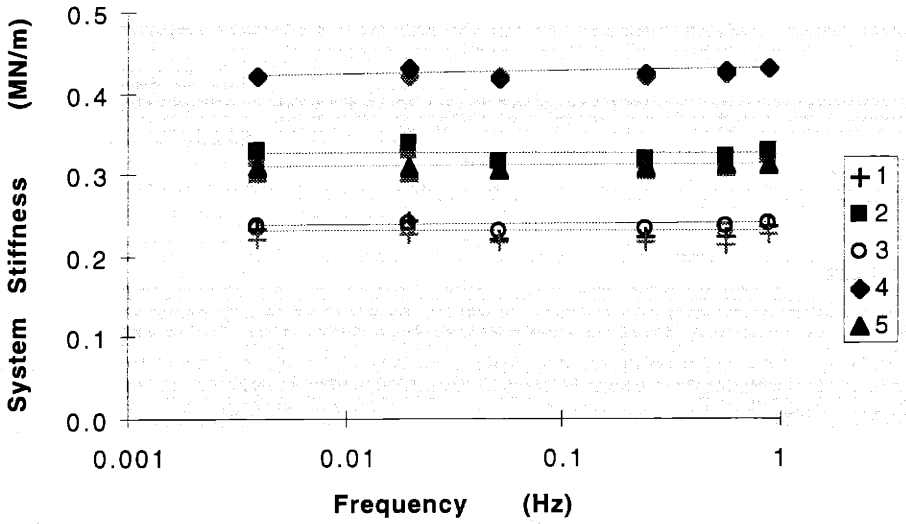

Figure A.8: Tissue Compression System test-position stiffness, without cartilage.

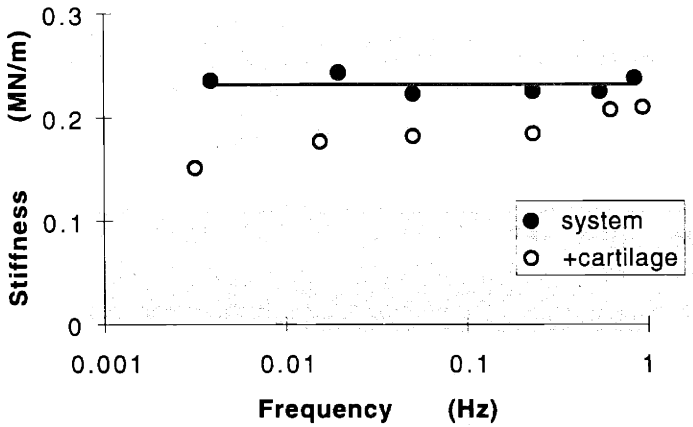

Figure A.9: Frequency-dependent stiffness of cartilage (same 4mm-diameter subject of Figures A.1 through A.6) and the TCS (position 1). With increasing frequency the tissue becomes stiffer, exhibiting incompressibility, indicating that the apparent stiffness is that of the system.

Appendix B

The spatial pattern of glycosaminoglycan depletion in cultured cartilage explants treated with 100ng/ml IL-1ß.

Epiphyseal cartilage explants cultured under 10%-strain static axial compression in the presence (photomicrographs B.1-B.3) and absence (B.4) of 100ng/ml interleukin-1ß. Samples (3mm diameter and 2mm thick) were incubated on an orbital shaker with daily media (± IL-1ß) changes. At the end of the culture period each sample was chemically fixed in 10% neutral-buffered formalin, sectioned to 5µm, and stained with aqueous 0.1% toluidine blue O. Diffusion-filtered brightfield photomicrographs were taken at 5X magnification using Kodak Gold 400 film.

Histological preparations highlight the pervading vasculature (large areas without stain), chondrocytes (tiny points without stain) and the vast proteoglycan-rich extracellular matrix for which Toluidine blue O stains a purple-bluish hue. The culture conditions specific to these samples constrained the diffusion of IL-1ß to the radial direction. IL-1ß, present in the media, enters the bulk tissue at the radial edge.

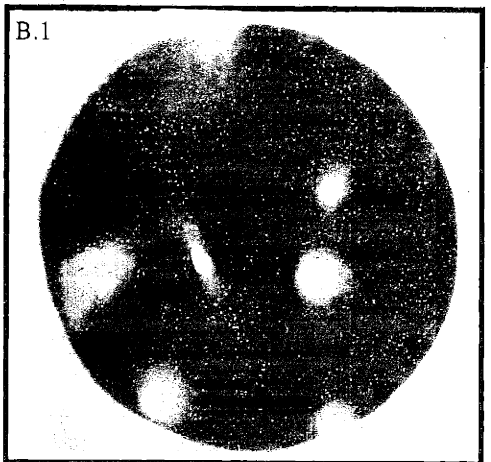

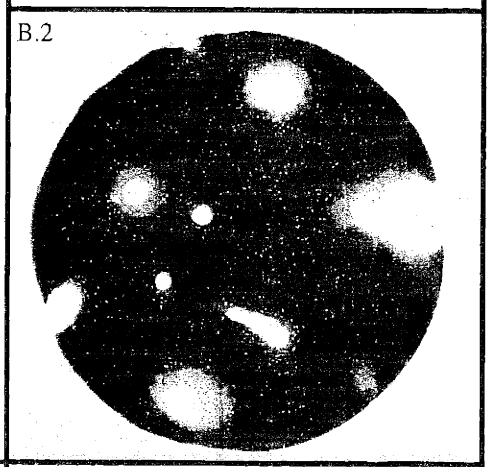

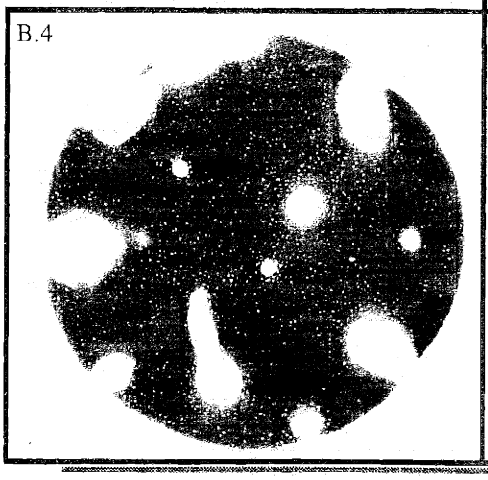

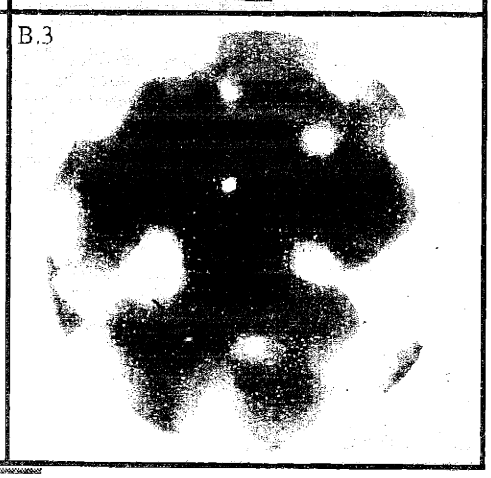

Photo	Culture Time (Days)	Treatment (±IL-1ß)
B.1	1	+
B.2	3	+
B.3	5	+
B.4	5	-

The initiation of glycosaminoglycan degradation, indicated by the absence of stain, occurs in the perivascular regions (Figure B.1). With time (Figures B.2 and B.3), the path of degradation extends outward into the bulk extracellular matrix in a front-like fashion. For reference, the untreated sample (Figure B.4) exhibits perivascular dye-loss, but this "degradation", through inspection of other histological samples, appears to be delayed and its progression has been observed to move slowly relative to interleukin-1ß-induced degradation.

Note that the diffusion path of IL-1ß has been demonstrated to differ from the spatial pattern of glycosaminoglycan release.

These experiments were performed by Dr. Biswal, who graciously shared his results for their inclusion in this thesis (Biswal 1996).

Appendix C

Absolute biochemical and stiffness measurements of tissue explants reported in the Results section.

Untreated Controls:

Experiment **3**: Untreated Controls (ulna-derived tissue)

Equilibrium Stiffness (MPa)

Sample	Day 0	Day 1	Day 2	Day 3	Day 4	Day 5
1	1.21	1.05	0.92	0.89	0.91	0.84
2	1.17	1.10	0.99	0.95	0.92	0.89
3	1.24	1.16	1.05	0.99	0.98	0.90
4	1.38	1.22	1.15	1.08	1.10	1.04
5	1.15	1.47	1.01	1.09	0.95	1.00

0.02Hz Dynamic Stiffness

	Day 0	Day 1	Day 2	Day 3	Day 4	Day 5
1	14.74	14.78	12.13	11.76	13.66	13.52
2	15.93	17.04	14.91	12.86	14.32	13.57
3	13.97	15.12	13.73	12.04	13.19	12.03
4	17.06	16.90	15.05	15.49	16.27	18.08
5	15.86	27.86	24.62	18.28	14.75	18.30

0.05Hz Dynamic Stiffness

	Day 0	Day 1	Day 2	Day 3	Day 4	Day 5
1	17.21	17.31	15.00	13.93	16.66	16.54
2	17.58	18.60	16.44	12.86	16.77	16.53
3	18.19	18.93	17.22	16.29	17.59	16.90
4	20.44	20.10	18.19	18.19	19.64	22.29
5	20.69	31.48	28.18	22.14	18.17	21.70

0.23Hz Dynamic Stiffness

	Day 0	Day 1	Day 2	Day 3	Day 4	Day 5
1	19.43	19.03	16.37	15.26	17.76	20.21
2	19.64	20.06	18.21	12.86	18.11	19.49
3	20.53	20.97	19.06	17.95	18.89	19.99
4	23.17	22.49	21.00	20.82	21.14	21.57
5	22.80	34.58	30.58	23.23	19.40	25.51

0.55Hz Dynamic Stiffness

	Day 0	Day 1	Day 2	Day 3	Day 4	Day 5
1	20.28	19.74	17.09	15.71	18.77	20.77
2	20.36	20.95	19.00	12.86	19.25	20.29
3	21.68	22.30	20.01	18.44	20.04	20.66
4	24.32	24.17	21.91	21.51	22.41	22.53
5	24.06	35.93	32.18	25.39	20.34	25.91

0.88Hz Dynamic Stiffness

	Day 0	Day 1	Day 2	Day 3	Day 4	Day 5
1	20.77	20.06	17.72	16.53	20.14	22.01
2	20.72	21.34	19.44	12.86	20.36	21.23
3	22.13	22.78	20.66	19.37	20.91	21.64
4	24.44	24.73	22.63	22.04	23.11	23.63
5	24.45	35.87	32.93	25.42	21.09	26.67

GAG Content (µg)

1	1326	1308	1291	1279	1264	1252
2	1263	1249	1234	1222	1209	1198
3	1258	1245	1232	1220	1207	1196
4	1093	1078	1067	1056	1044	1034
5	1095	1084	1071	1060	1050	1040

Exp. **4**: Untreated Controls (ulna-derived tissue)

Equilibrium Stiffness (MPa)

	Day 0	Day 1	Day 2	Day 3	Day 4	Day 5
	0.68	0.64	0.62	0.55	0.56	0.47
	1.00	0.97	0.92	0.79	0.75	0.62
	0.89	0.81	0.82	0.76	0.67	0.58
	0.54	0.52	0.48	0.43	0.39	0.36
	0.91	0.83	0.76	0.77	0.63	0.54

0.02Hz Dynamic Stiffness

	Day 0	Day 1	Day 2	Day 3	Day 4	Day 5
	14.59	12.96	12.37	11.91	12.73	11.41
	18.14	18.16	17.21	15.75	17.28	15.09
	16.74	15.40	14.84	15.92	15.85	15.69
	10.03	9.43	9.00	7.97	8.08	7.21
	16.97	14.55	13.79	12.21	13.82	12.55

0.05Hz Dynamic Stiffness

	Day 0	Day 1	Day 2	Day 3	Day 4	Day 5
	17.79	15.70	15.32	15.23	15.67	14.94
	21.84	22.10	21.52	20.34	21.46	18.61
	23.40	21.37	20.90	20.82	20.86	20.43
	14.44	13.09	12.44	10.71	11.02	9.93
	22.51	20.09	19.03	17.33	17.84	16.16

0.23Hz Dynamic Stiffness

	Day 0	Day 1	Day 2	Day 3	Day 4	Day 5
	19.59	18.49	18.18	17.81	17.97	16.91
	24.43	25.18	24.67	22.97	24.49	21.17
	27.15	25.36	24.96	24.82	24.53	23.70
	15.63	16.24	15.39	14.29	13.31	11.92
	25.67	23.07	21.67	19.97	20.72	18.64

0.55Hz Dynamic Stiffness

	Day 0	Day 1	Day 2	Day 3	Day 4	Day 5
	21.18	19.50	19.70	19.12	19.20	18.09
	25.80	25.83	26.23	24.22	24.98	22.39
	28.83	26.62	26.89	26.62	26.23	25.50
	18.25	17.42	17.03	15.58	14.46	13.01
	27.37	24.22	23.51	21.39	22.21	20.19

0.88Hz Dynamic Stiffness

	Day 0	Day 1	Day 2	Day 3	Day 4	Day 5
	22.57	20.41	20.82	19.93	19.55	18.40
	27.12	26.65	27.36	24.97	25.80	22.68
	30.47	27.73	28.05	27.28	26.61	26.01
	19.24	18.21	17.76	16.24	14.78	13.28
	28.32	25.38	24.53	22.44	22.79	20.56

GAG Content (µg)

	687.2	668.4	652.2	629.4	603.6	576.0
	809.2	794.6	778.5	755.9	724.4	680.7
	802.8	784.7	767.0	748.3	732.3	708.3
	637.3	611.4	584.2	555.1	523.2	484.5
	776.2	748.6	722.1	691.1	652.5	608.5

Exp. **14/15**: Controls (FPG-derived tissue)

Equilibrium Stiffness (MPa)

	Day 0	Day 1	Day 2	Day 3	Day 4
	0.64	0.66	0.64	0.63	0.45
	0.84	0.74	0.70	0.83	0.64

	7.89	7.80	6.33	6.26	6.86
	7.55	7.37	6.78	6.65	6.81

	8.36	8.32	6.59	6.71	7.47
	8.26	8.04	7.11	7.18	7.56

	9.04	9.01	7.12	7.00	7.99
	8.92	8.71	7.64	7.47	8.16

	9.74	8.84	7.77	7.50	8.41
	9.61	8.94	8.22	8.00	8.59

	9.67	8.83	7.91	7.72	8.68
	9.67	9.07	8.52	8.26	8.87

GAG Content (µg)

	1491	1462	1436	1409	1387
	1486	1478	1468	1458	1447

	1895	1861	1825	1792	1758
	1980	1972	1962	1949	1935

Samples treated with 100ng/ml interleukin-1ß:

Experiment **6** (ulna-derived tissue)

Sample	Day 0	Day 1	Day 2	Day 3	Day 4	Day 5	Day 6
	Equilibrium Stiffness (MPa)						
1	0.66	0.62	0.58	0.37	0.25	0.11	0.10
2	0.83	0.80	0.75	0.50	0.29	0.15	0.11
3	0.49	0.38	0.34	0.10	0.05	0.05	0.07
4	0.76	0.75	0.70	0.41	0.26	0.15	0.09
5	0.71	0.55	0.50	0.34	0.18	0.11	0.02
	0.02Hz Dynamic Stiffness						
1	9.54	7.61	7.37	5.85	4.40	3.19	2.91
2	12.58	11.43	11.56	8.39	6.20	4.02	3.09
3	9.25	6.68	5.86	3.05	2.45	2.04	2.00
4	12.08	11.11	10.38	7.12	5.31	4.03	3.16
5	12.22	10.73	9.98	7.54	5.28	4.14	2.76
	0.05Hz Dynamic Stiffness						
1	12.65	11.26	11.15	8.28	6.00	4.09	3.07
2	15.35	14.56	14.43	11.03	7.75	5.08	3.17
3	11.41	8.82	8.23	4.07	2.76	2.07	1.89
4	14.67	13.93	13.38	9.58	6.84	4.87	3.44
5	14.50	12.91	13.47	9.59	6.81	5.32	2.26
	0.23Hz Dynamic Stiffness						
1	14.61	13.58	14.24	10.62	7.63	4.64	2.60
2	17.54	17.13	17.49	13.39	9.45	5.90	2.80
3	13.68	10.99	10.67	4.63	2.36	1.73	1.34
4	17.18	17.02	17.02	12.19	8.58	5.67	2.98
5	17.34	15.52	15.52	12.45	8.39	4.90	1.70
	0.55Hz Dynamic Stiffness						
1	15.38	15.27	15.65	11.57	8.43	4.89	2.26
2	18.18	18.30	18.86	14.74	10.52	6.70	2.52
3	14.53	11.98	11.65	4.80	2.34	1.60	1.10
4	18.15	18.38	18.33	13.32	9.58	5.96	2.89
5	18.35	16.87	16.66	13.51	9.06	4.58	1.31
	0.88Hz Dynamic Stiffness						
1	16.59	15.81	16.30	12.14	8.49	5.06	2.21
2	19.44	18.85	19.64	15.19	10.90	6.99	2.47
3	15.43	12.36	12.24	4.99	2.22	1.45	1.02
4	19.03	18.84	18.96	13.61	9.75	5.97	2.91
5	18.45	17.35	17.35	14.04	9.23	4.29	1.04
	GAG Content (µg)						
1	736	675	635	508	367	215	87
2	727	670	625	498	338	208	84
3	671	532	479	311	163	93	70
4	686	653	609	479	319	194	91
5	597	525	488	420	298	186	89

Exp. **19** (FPG-derived tissue)

Sample	Day 0	Day 1	Day 2	Day 3	Day 4	Day 5
	0.004Hz Dynamic Stiffness					
1	5.42	4.97	5.12	3.29	2.42	1.76
2	5.90	5.26	5.45	3.20	1.65	0.98
3	6.62	5.94	6.45	4.32	3.05	1.85
4	6.88	6.18	5.59	3.06	1.76	1.22
5	7.83	7.67	8.74	6.51	5.88	4.83
	0.02Hz Dynamic Stiffness					
1	13.32	12.95	11.36	10.18	7.55	6.42
2	11.76	11.57	9.84	8.04	4.64	2.44
3	14.96	14.57	13.05	12.01	8.47	5.36
4	10.17	9.77	7.83	5.85	3.67	2.61
5	15.78	16.16	15.12	14.70	13.11	11.14
	0.05Hz Dynamic Stiffness					
1	16.78	16.42	15.36	14.28	11.30	8.90
2	13.55	13.25	12.24	10.41	6.83	4.29
3	17.05	16.88	15.39	14.64	10.98	7.94
4	11.21	10.57	8.78	6.83	4.49	3.30
5	19.62	19.01	18.23	17.86	16.24	14.34
	0.23Hz Dynamic Stiffness					
1	17.76	17.62	16.97	15.53	13.57	10.79
2	14.58	14.12	13.21	11.15	7.67	4.91
3	18.05	17.25	16.58	15.20	12.67	8.55
4	12.59	11.62	9.78	7.22	5.17	3.74
5	22.16	21.37	20.95	19.72	19.16	16.59
	0.55Hz Dynamic Stiffness					
1	18.38	18.68	15.36	14.28	14.36	11.34
2	14.93	15.13	12.24	10.41	8.01	5.12
3	18.48	18.27	15.39	14.64	13.33	8.92
4	13.10	12.56	8.78	6.83	5.50	3.90
5	23.11	23.11	18.23	17.86	20.40	17.86
	0.88Hz Dynamic Stiffness					
1	19.55	19.55	18.44	17.78	14.85	11.88
2	15.65	15.76	14.21	12.06	8.29	5.21
3	19.43	19.21	17.86	16.59	13.69	9.12
4	13.70	13.00	10.76	8.08	5.80	3.92
5	23.91	24.13	23.10	21.86	20.90	18.67
	GAG Content (µg)					
1	1344	1331	1308	1279	1140	989
2	974	960	931	791	569	405
3	937	925	905	878	717	546
4	1331	1249	1042	831	578	417
5	860	851	830	806	742	625

Samples treated with 10TRU/ml hyaluronate lyase:

Experiment **13** (ulna-derived tissue)

Equilibrium Stiffness (MPa)

Sample	Day 0	Day 1	Day 2	Day 3	Day 4	Day 5	Day 6
1	1.27	1.07	1.17	0.72	0.59	0.57	0.38
2	1.40	1.29	1.25	1.02	0.86	0.80	0.55
3	1.01	0.86	0.93	0.88	0.73	0.55	0.33
4	1.25	1.18	1.24	0.84	1.01	0.85	0.57
5	1.00	0.94	0.87	0.72	0.61	0.68	0.49
	0.02Hz Dynamic Stiffness						
1	5.58	4.83	5.30	3.83	2.41	3.80	2.30
2	5.71	4.97	5.06	4.60	3.32	4.30	3.18
3	6.23	5.72	5.94	4.65	3.90	4.79	3.72
4	9.21	8.21	7.73	7.48	6.93	7.43	5.40
5	10.94	8.93	8.48	6.98	5.44	5.62	5.81
	0.05Hz Dynamic Stiffness						
1	7.24	6.58	7.63	5.79	4.09	4.30	3.51
2	6.17	6.95	7.33	6.75	4.91	5.48	4.77
3	8.75	7.72	9.00	7.54	6.02	6.60	5.22
4	13.70	13.06	12.68	12.49	10.72	10.03	7.21
5	13.19	12.08	11.71	10.03	8.67	7.97	7.96
	0.23Hz Dynamic Stiffness						
1	7.43	7.36	8.31	7.63	4.89	6.42	5.17
2	8.45	8.13	8.13	9.41	6.32	7.51	6.52
3	10.17	9.99	10.66	11.29	8.01	8.85	6.78
4	16.53	15.76	15.50	18.68	13.34	13.29	8.93
5	14.17	13.02	12.25	12.74	10.29	10.35	9.64
	0.55Hz Dynamic Stiffness						
1	8.42	7.63	8.76	6.84	5.16	6.48	5.52
2	9.76	8.70	8.56	8.51	6.64	7.49	6.91
3	11.29	10.50	11.33	10.22	8.49	9.11	7.12
4	18.15	16.75	16.48	16.67	14.20	13.83	9.81
5	15.63	14.16	13.37	11.12	10.65	10.53	9.98
	0.88Hz Dynamic Stiffness						
1	9.07	8.23	8.95	6.99	6.16	6.44	5.77
2	10.49	9.36	9.04	8.89	7.68	7.65	7.29
3	11.96	10.97	11.76	10.73	9.34	9.17	7.46
4	18.93	17.45	16.69	17.09	15.36	13.91	10.84
5	16.56	15.00	14.02	11.55	11.44	10.92	10.48
	GAG Content (µg)						
1	973	944	888	806	729	669	572
2	900	864	826	769	719	661	591
3	1094	1055	1010	947	854	762	640
4	1020	991	928	868	793	722	589
5	907	868	812	745	687	625	569

Exp. **14/15** (FPG-derived tissue)

Equilibrium Stiffness (MPa)

Day 0	Day 1	Day 2	Day 3	Day 4	Day 5
0.79	0.65	0.50	0.38	0.30	0.19
0.71	0.58	0.46	0.37	0.28	0.18
0.02Hz Dynamic Stiffness					
9.70	8.28	7.59	6.78	6.40	5.69	4.79	3.99	3.49
10.00	8.92	8.71	8.41	8.08	7.46	7.05	6.40	5.98
13.34	10.76	10.21	9.04	8.35	7.99			
0.05Hz Dynamic Stiffness								
10.81	9.84	8.81	7.95	7.55	6.51	5.69	4.73	3.82
11.31	10.30	10.02	9.67	9.33	9.13	8.17	5.24	7.06
14.75	12.18	11.71	10.39	9.77	9.49			
0.23Hz Dynamic Stiffness								
11.85	10.79	9.64	9.09	8.56	7.68	6.16	4.98	4.29
12.26	11.28	10.88	10.68	10.40	10.12	9.11	8.50	7.56
15.97	13.32	12.69	11.62	10.86	10.68			
0.55Hz Dynamic Stiffness								
12.09	11.34	10.10	9.70	9.31	8.07	6.84	5.52	4.61
12.41	11.85	11.52	11.52	11.30	10.40	9.81	9.20	8.04
16.40	14.22	13.23	12.63	11.89	11.08			
0.88Hz Dynamic Stiffness								
12.43	11.18	10.41	9.98	9.57	8.24	7.26	5.64	4.77
12.66	12.39	11.81	12.02	11.46	10.61	10.20	9.33	8.30
16.69	14.69	13.74	13.10	12.30	11.54			
GAG Content (µg)								
946	843	724	611	508	441			
1047	936	843	741	656	583			
1639	1512	1368	1240	1123	995	822	671	547
1941	1833	1724	1613	1511	1413	1233	1070	931
1676	1565	1439	1325	1211	1107	968	953	953

Samples treated with 0.1U/ml chondroitinase-ABC or 0.0025X trypsin:

Experiment **7 Ch'ase** (ulna-derived tissue)

Equilibrium Stiffness (MPa)

Sample	Day 0	Day 1	Day 2	Day 3	Day 4
	0.18	0.02	0.02	0.03	
	0.20	0.02	0.02	0.01	0.04
	0.81	0.77	0.65	0.41	0.14
	0.71	0.61	0.47	0.19	0.06
	0.87	1.01	0.73	0.53	0.42
0.02Hz Dynamic Stiffness					
	3.10	1.86	1.63	1.82	1.55
	2.99	1.76	1.57	1.97	1.97
	12.35	7.85	5.28	3.79	2.78
	12.40	8.26	5.57	3.62	2.76
	12.07	8.77	7.67	5.80	4.95
0.05Hz Dynamic Stiffness					
	3.64	1.30	1.42	1.63	1.16
	3.67	1.26	1.23	1.57	1.67
	14.62	11.70	8.78	5.78	2.85
	14.51	10.25	7.18	4.58	2.91
	13.51	10.80	6.60	7.49	5.81
0.23Hz Dynamic Stiffness					
	3.83	0.70	0.69	1.00	0.90
	3.78	0.63	0.65	1.11	1.07
	17.13	13.47	10.58	6.66	4.04
	17.20	12.38	8.46	5.25	2.60
	15.61	12.73	11.65	5.25	6.38
0.55Hz Dynamic Stiffness					
	4.07	0.49	0.54	0.71	0.73
	4.03	0.39	0.34	0.90	1.03
	18.29	15.10	11.41	7.32	4.32
	18.47	13.67	9.31	5.74	2.59
	16.22	13.55	11.96	5.22	6.68
0.88Hz Dynamic Stiffness					
	4.28	0.33	0.46	0.59	0.55
	4.13	0.32	0.24	0.78	0.92
	19.10	15.40	12.07	7.92	4.43
	19.29	14.02	9.75	5.88	2.62
	17.05	13.97	12.42	9.52	6.77

Exp. **25** Trypsin (FPG-derived tissue)

0.004Hz Dynamic Stiffness

Day 0	Day 1	Day 2	Day 3	Day 4	Day 5
7.09	4.63	3.58	2.84	2.57	1.96
5.65	3.67	2.94	2.64	2.30	1.44
4.77	2.68	2.07	1.46	1.40	1.37
4.31	2.73	2.13	1.69	1.42	1.39
5.83	4.91	4.26	3.32	3.03	2.46
0.02Hz Dynamic Stiffness					
10.27	7.34	6.26	5.21	3.23	4.00
11.40	8.35	6.91	5.65	4.27	4.49
9.45	6.33	5.01	3.73	2.95	2.62
10.03	6.84	5.33	3.88	2.77	2.11
15.01	10.65	8.59	6.44	5.32	4.05
0.05Hz Dynamic Stiffness					
10.50	8.09	6.89	6.04	4.97	4.75
12.16	9.70	8.20	7.05	6.33	5.98
10.42	7.55	6.18	4.85	4.52	3.19
10.96	8.48	6.84	5.11	4.00	2.64
16.83	12.79	10.81	8.43	6.57	4.62
0.23Hz Dynamic Stiffness					
11.10	8.87	7.63	6.72	5.62	4.90
13.17	10.79	9.25	8.13	7.44	6.68
11.43	8.49	7.16	5.82	5.03	3.29
12.74	10.03	8.03	6.21	4.48	2.84
19.00	14.35	11.98	9.23	6.98	4.88
0.55Hz Dynamic Stiffness					
10.83	9.40	6.89	6.04	6.05	5.02
12.80	11.44	8.20	7.05	7.94	6.86
11.49	9.17	6.18	4.85	5.22	3.40
13.88	10.80	6.84	5.11	4.67	2.89
19.37	15.21	10.81	8.43	7.08	5.04
0.88Hz Dynamic Stiffness					
10.99	9.62	8.42	7.56	6.31	4.98
12.92	11.75	10.24	9.06	8.34	6.94
11.86	9.38	8.05	6.64	5.46	3.32
14.32	11.08	9.89	6.99	4.93	2.75
19.67	14.94	12.93	9.65	7.05	4.41
GAG Content (µg)					
1290	988	768	603	499	398
1437	1139	958	800	669	566
1381	1018	827	645	524	409
1269	991	806	588	472	355
1343	1028	847	665	540	425

Appendix D

A quick and simple assessment of chondrocyte viability utilizing fluorescein diacetate and propidium iodide

Studies addressing questions of cartilage physiology frequently involve organ culture models. In evaluating the tissue response due to harvesting procedures or any controlled perturbation the question of cell viability often arises. Fortunately, there are several methods available to probe the cell state; including fluorescent vital dye staining, biochemical assessment of lactate deyhrogenase activity, and morphological changes as observed through immunocytochemical methods.

Developing a rapid, yet accurate, method for the detection of viable cells was the primary objective of this study. Fluorescent staining was chosen as the most suitable means by which to assess viability. Aside from the facts that (1) fluorescent staining is procedurally less complicated than LDH-assessment and morphological studies and (2) the results are readily interpretable, the preponderance of positive results exhibited in the literature clearly supported this choice as most suitable for meeting our objective.

Of the several dyes available for assessing "live" cells, we chose fluorescein diacetate. In short, fluorescein diacetate (FDA) is recognized as a fluorescent indicator of intracellular esterase activity. FDA is membrane permeable in its intact form. Intracellular esterases hydrolyze the molecule into the highly fluorescent and quasi-membrane-impermeant fluorescein anion. Presumably, such activity occurs during normal cytosolic metabolic processes and therefore its detection infers that the cell is "alive" and functioning normally. We chose ethidium bromide (EB) and propidium iodide (PI) for the detection of "dead" cells. They were selected because the available literature indicated each had at least two functionally requisite traits: both were efficient markers of DNA and both were reportedly impermeable to cellular membranes (Gray and Morris 1987; Jayapal et al. 1991; Keilhoff and Wolf 1993; Smith and Smith 1989). Presumably, a "dead" cell would have a compromised cell membrane thereby allowing propidium iodide and ethidium bromide to permeate the membrane barrier and stain the nuclei. By intercalating the bases of DNA, PI and EB elicit an intense red-orange fluorescence.

Fluorescein diacetate combined with ethidium bromide has been used as a "live-dead" viability stain for isolated pancreatic cells (Gray and Morris 1987). Likewise, live-dead assays consisting of fluorescein diacetate and propidium iodide have been utilized (Keilhoff and Wolf 1993; Smith and Smith 1989). Furthermore, other studies (Farnum et al. 1990) indicate fluorescent viability staining techniques could be applied to chondrocytes embedded in their extracellular matrix.

Fluorescein diacetate (Sigma F-7378) was dissolved in dimethyl sulfoxide (DMSO) (Fisher Scientific D128-500) to a stock concentration of 1 mg/ml. Similarly, 1.0mg propidium iodide (Sigma P4170) was dissolved in 10ml phosphate-buffered saline (PBS); and ethidium bromide (Sigma E-8751) was diluted to a stock concentration of 1 mg/ml in DMSO. All stock solutions were protected from light and stored at 4°C (which is below the freezing point of DMSO). Within twenty-four hours of photomicroscopy the stock solutions of FDA and EB were further diluted in HBSS to 5 ng/ml. PI was diluted to 5µg/ml in PBS (typically 200µl of the stock solution into 4ml of PBS). One-to-two milliliters of each working solution was pipetted into an individual well in a 24-well culture dish. Approximately 5ml of saline (HBSS) in a petri dish was placed on the observation platform on the microscope. Cartilage samples were thinly sliced (schematically depicted in Figure D.1), stained (typically for one minute) in a working solution, and placed into the bath for observation. A Nikon Diaphot-TMD inverted phase microscope and Nikon N2000 camera were used to take photomicrographs. A mercury-xenon lamp provided the epifluorescent light source. Bright field (lamp intensity 9-11) and fluorescent images were captured on Kodak Gold 100 speed film.

The objectives of this study were to (1) ensure fluorescein diacetate stains viable cells and propidium iodide or ethidium bromide stains non-viable cells and (2) to compare the performance of fluorescein diacetate, propidium iodide, and ethidium bromide to calcein-AM and ethidium homodimer-1, Molecular Probes' cell viability kit (L-3224).

A comprehensive documentary of all the available evidence is beyond the scope of this thesis. Let it suffice that the results indicate:

1. The methods described above are suitable for FDA detection of viable cells in thinly prepared tissue slices (preparations B, C, or D in Figure D.1). Refer to Figures 4.2 (sample prepared like "prep C") and 4.3 (prep D).
2. FDA is equally accurate as calcein-AM in determining chondrocyte viability. For comparison to the results of #1, a sample stained with calcein-AM and ethidium homodimer-1 is presented in Figure D.2. Incubation for at least 5 minutes is necessary for eliciting positive results with calcein-AM, although periods of up to 30 minutes have been noted. FDA indicates viability within one minute of incubation.
3. FDA does not homogeneously distribute in "full-thickness" tissue samples (preparation A). Figures D.3 (stained as prep A, sectioned to prep B for photomicroscopy) and D.4 (stained as prep A, sectioned to prep B for photomicroscopy) depict the limited-diffusion of FDA into a full-thickness tissue sample. Figure D.5 (stained as prep B) serves as a control in that it is the same tissue as D.4, but the thin section was incubated for one minute in FDA. Other data, not shown, indicates the diffusion calcein-AM is inhibited also. A working hypothesis is that the peripheral cells are behaving as "sinks" for these esterase substrates and are actively

transporting them into the cell preventing the homogeneous distribution of FDA and calcein-AM.

4. There are several applications for which these methods are useful.
   - For starters, indicating chondrocyte viability of samples cultured as described in this thesis is a good application (see Figure 4.3).
   - Cartilage that was shipped on ice for four days was found to exhibit a normal amount of esterase activity (Figure D.6).
   - Injuriously compressed cartilage samples, of which protocols and experiments are described in glorious detail elsewhere (Quinn 1996), demonstrated widespread catastrophe and a high density of non-physiological ethidium bromide staining (Figure D.7 and D.8, bright field and fluorescent images, respectively)
5. Propidium iodide is more suitable than ethidium bromide for identifying non-viable cells. There is evidence that both propidium iodide and ethidium bromide can penetrate intact cell membranes. However, over incubation times of five minutes the presence of propidium iodide is decidedly less than that of ethidium bromide. Furthermore, in contrast to the low fluorescent intensity of propidium iodide stained cells after five minutes of incubation, the magnificent fluorescence localized in "naturally" (as a result of explantation or injurious compression) or artificially (chemically induced with exposure to DMSO or ethanol) compromised cells after only one minute is quite astonishing.

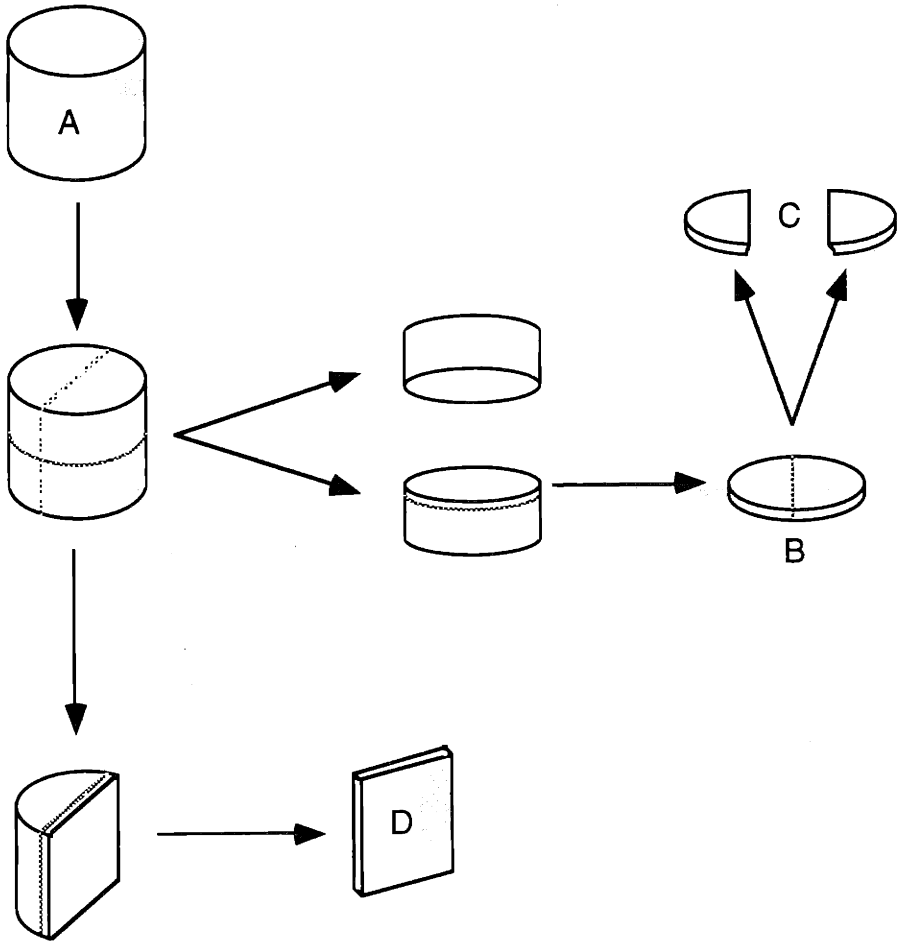

Figure D.1: **Preparation of cartilage explants**
The full thickness cartilage explant, A, (typically 4mm in diameter and 2mm in thickness) is bisected transverse to its longitudinal axis. This process is done by hand utilizing forceps and a standard razor blade. From the "inside" face of either half a thin (~100μm?) section is shaved yielding a disc, B. This configuration is the most typical of all samples studied under the microscope and is sufficiently thin so a presentable bright-field image can be captured. Additionally, these discs provide good resolution for fluorescent images. This configuration, though not easy to prepare initially, is reproducible with some practice. For studies involving the comparison of fluorescein diacetate and propidium iodide (or ethidium bromide) vs. calcein-AM and ethidium homodimer-1 the B-disc was bisected along its diameter, yielding pieces we'll collectively call C. This provides a means for directly comparing staining methods. Alternatively, tissue samples were prepared into rectangular cross-sections by bisecting the full thickness explant along its longitudinal axis and slicing off a thin section, D, from an inside edge. This orientation proved useful in examining injuriously compressed samples (which were compressed parallel to the longitudinal axis) and samples that were cultured in axial confinement.

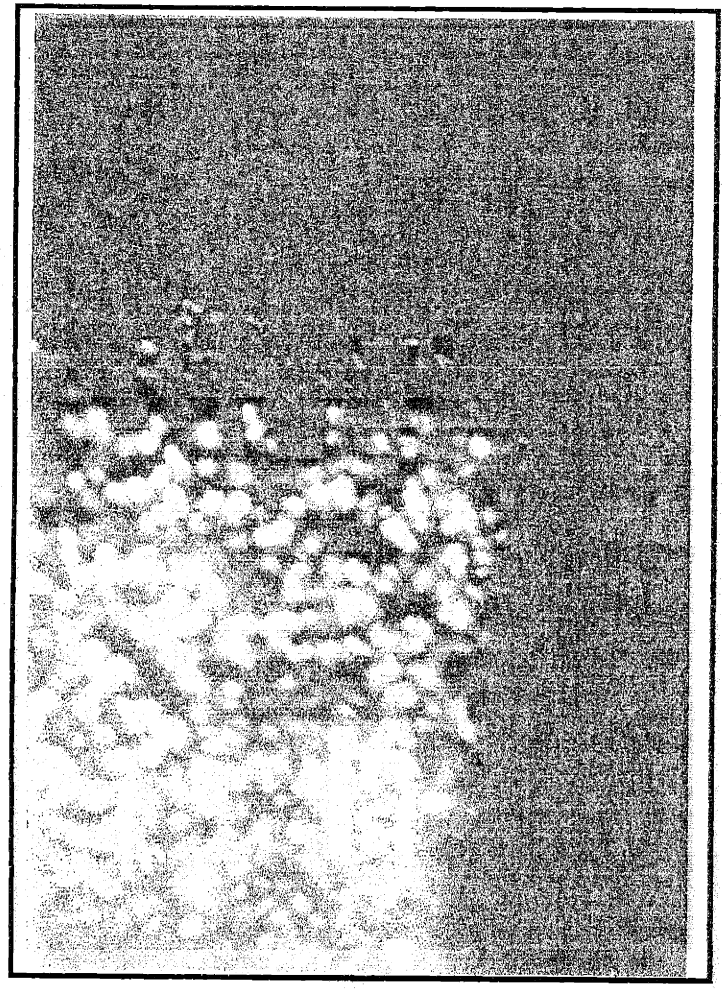

Figure D.2: Viability Kit from Molecular Probes®

Cartilage cultured 24 hours then sectioned (prep C) and immersed in 2μM calcein-AM and 4μM EtHd-1 for 5 minutes. 50X magnification.

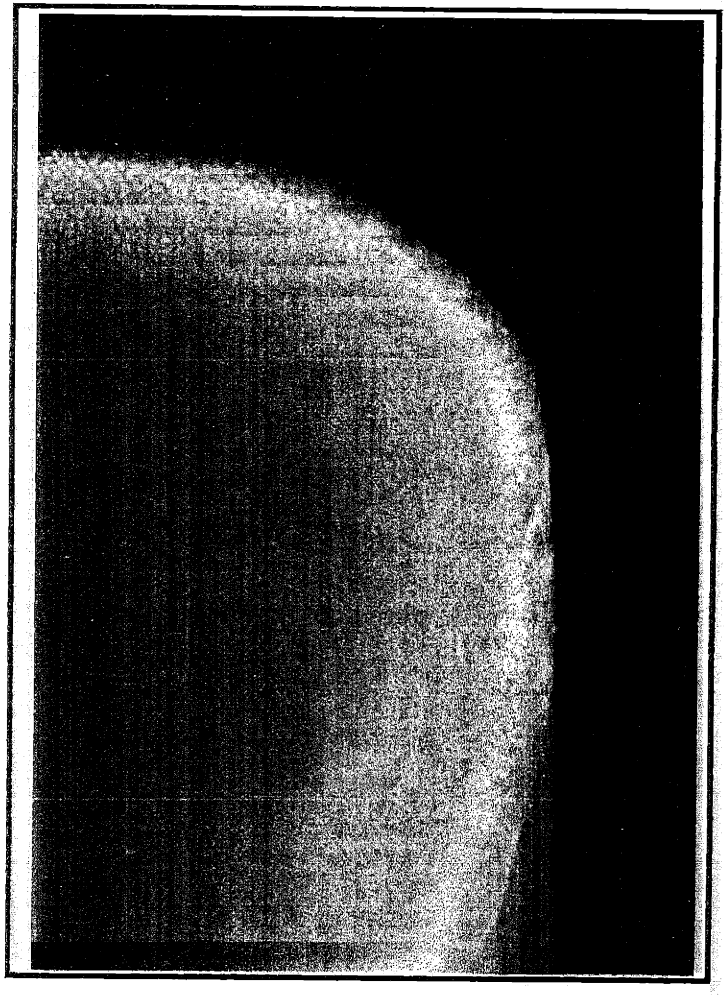

Figure D.3: Fluorescein Diacetate Diffusion 30 minutes

Cartilage sample (4mm-diameter, 2mm-thick) from the calf femoropatellar groove cultured in free-swelling conditions for 13 days. Next, it was incubated in 5ng/ml FDA for 30 minutes (prep A) and sliced (prep B) for microscopy. 10X magnification.

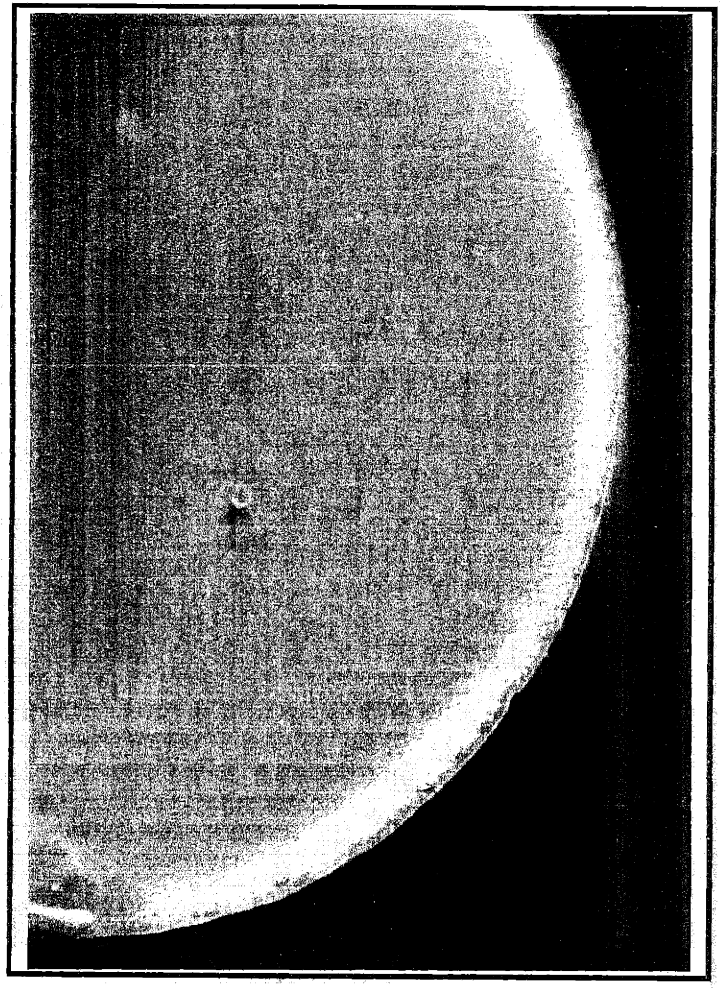

Figure D.4: FDA Diffusion 24 Hours
Cartilage sample (4mm-diameter, 2mm-thick) from the calf femoropatellar groove cultured in free-swelling conditions for 2 days. Next, it was incubated in 5ng/ml FDA for 24 hours (prep A) and then sliced (prep B) for microscopy. 10X magnification.

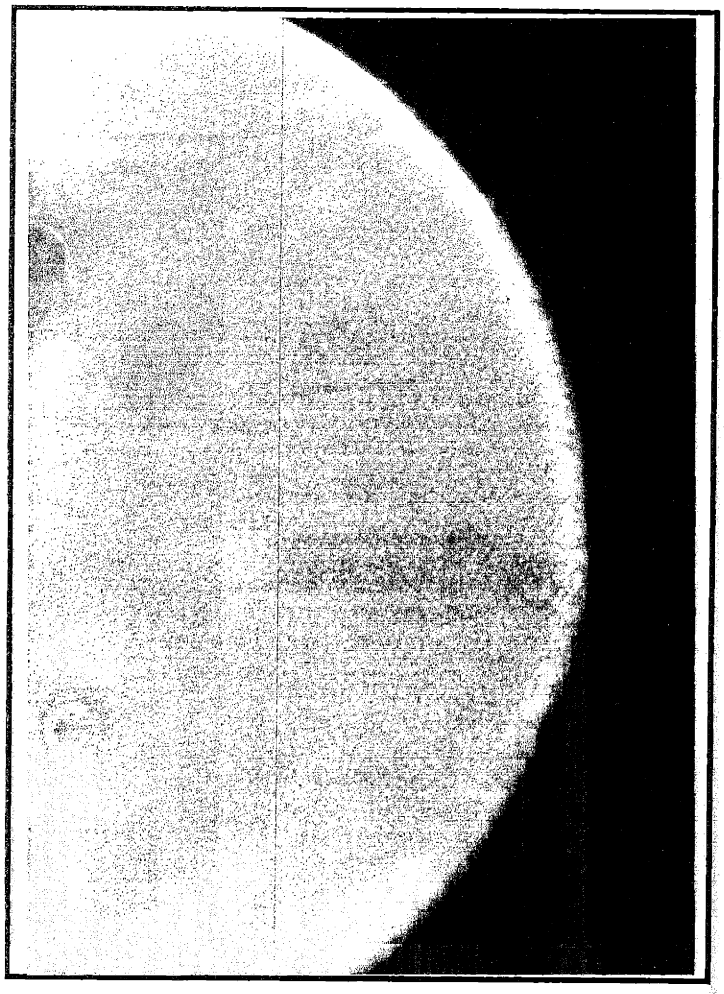

Figure D.5: FDA Diffusion (Conrol)
Same sample as in Figure D.4, but the section was immersed in 5ng/ml FDA for one minute. Note that the presence of viable cells throughout the explant has been confirmed. 10X magnification.

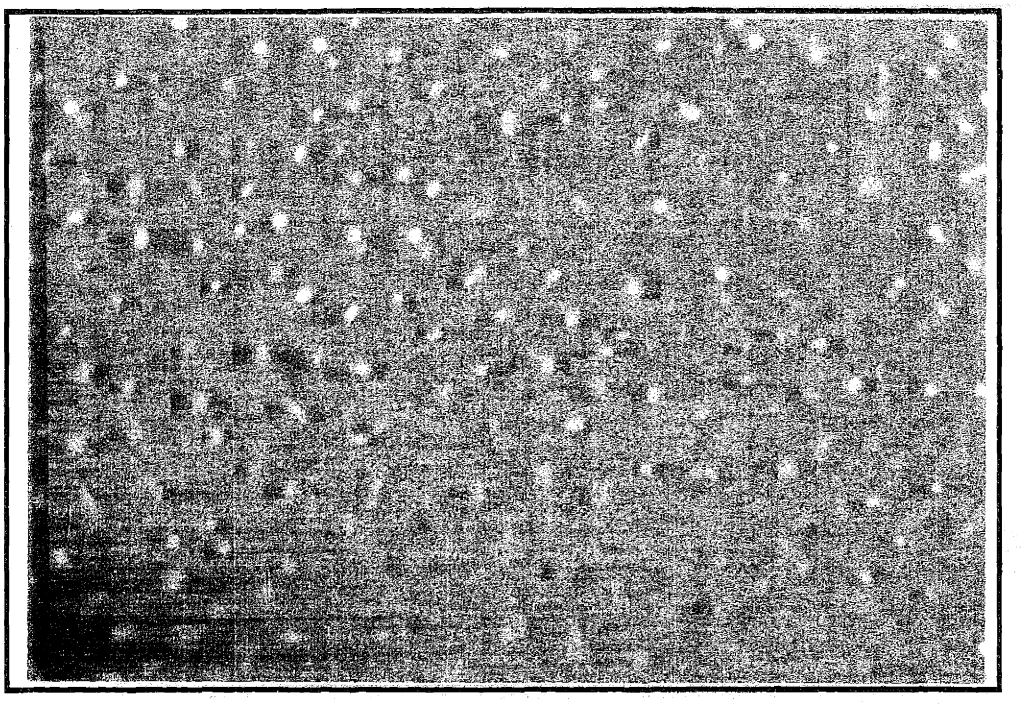

Figure D.6: Cartilage sample harvested from the adult bovine femoral-head. The totally encapsulated joint was received "on ice" four days after the animal was slaughtered. A section from near the articular surface was prepared (prep B) and immersed in 5ng/ml FDA. 50X magnification.

Figure D.7: Injuriously Compressed Cartilage
Calf femoropatellar groove cartilage (4x2mm) explant cultured eight days in free-swelling conditions; on the eighth day the sample was subjected to three cycles of one-hour at 50% compression, one-hour free-swelling. Rapid strain rates were used in compressing the sample. This bright field image indicates a ruptured ECM. 25X magnification

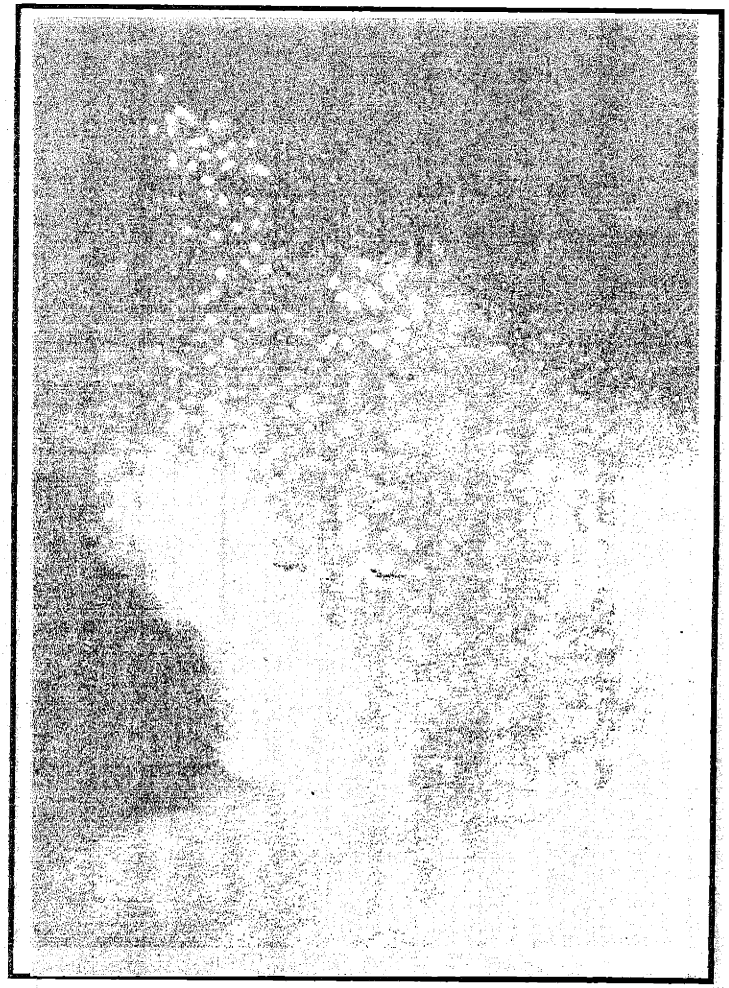

Figure D.8: Injuriously Compressed Cartilage
Same sample as Figure D.7, fluorescent image. Immersed (prep D) in 5ng/ml FDA & EB for 1 minute. 25X magnification

Appendix E

Mechanical properties of tissue-engineered cartilage constructs

The study of tissue-engineered cartilage constructs provided a novel approach in investigating the contribution of changes in glycosaminoglycan content to mechanical properties. In contrast to inducing the degradation of glycosaminoglycans in cartilage explants, cell-polymer constructs provided the unique opportunity to monitor glycosaminoglycan synthesis and the evolution of a mechanically functional extracellular environment.

A complete discussion of construct cultivation techniques is described by Freed and Vunjak-Novakovic (Freed and Vunjak-Novakovic 1995). However, a brief introduction is necessary. Cultivation utilized biodegradable polyglycolic acid scaffolds (void volume of 97%), the same material used in absorbable surgical sutures. Bovine chondrocytes were seeded throughout the polymer substrate and cultured in a bioreactor which simulated "microgravity". The three-dimensional environment of the construct, essential for maintaining the chondrocyte phenotype, in conjunction with simulated microgravity has been demonstrated to promote the morphogenesis of tissue. Histological and biochemical assessments indicate the production of collagen and glycosaminoglycans with time in cultivation.

The extent to which these matrix macromolecules are developed into a mechanically functional network is unknown. The objective of this preliminary study was to monitor the dynamic stiffness over the first 33 days of cultivation, a time period of significant growth as seen histologically and biochemically.

Constructs were sampled from the bioreactors at three time points (12, 26, and 33 days) and prepared into discs (~4mm-diameter, 2-3mm-thick) using a cylindrical holder and a razor blade. The construct discs were loaded into polysulfone compression chambers and equilibrated in a phosphate-buffered saline (Gibco 14190-144) supplemented with a cocktail of protease inhibitors (10mM Na_2EDTA, 10mM benzaamidine-HCl, 10mM N-ethylmaleimide, 1mM phenylmethanesulfonyl chloride). The dynamic stiffness was measured over a range of frequencies at an offset level of 10% -18% compressive strain, dependent upon the initial thickness of the individual sample. The peak-to-peak amplitude of the imposed displacement wave was between 1-2% strain.

The dynamic stiffness is reported in Figure E.1. After twelve days of cultivation the dynamic stiffness was on the order of 1MPa and appeared to be independent of frequency. Although this indicated some intrinsic resiliency, because the stiffness was independent of frequency, fluid flow was apparently unrestricted at the highest frequency tested (0.86Hz). By the 26th day of cultivation the development of a frequency-dependent dynamic stiffness was apparent.

The low-frequency response did not change, but the dynamic stiffness increased with frequency and plateaued at ~2MPa. Seven more days of cultivation elevated the low-frequency stiffness but had no effect on the high-frequency stiffness.

The spectral development of the dynamic stiffness, in frequency-dependence and magnitude, is correlated with increases in both glycosaminoglycan and collagen content (Figure E.2). The attendant accumulation of these structural elements had obvious effects on the ability of the constructs to withstand compression and redistribute tissue fluid. Both collagen and glycosaminoglycans contribute to the mechanical properties of the hydrated gel-like constructs; presumably, the proteoglycans entangle themselves in the collagen network. Solid phase redistribution and exudation of tissue fluid is a result of compression, the latter consequence increases the density of fixed charges and increases the swelling tendency of the tissue. Since the constructs were tested in an "unconfined" fashion, the contribution of collagen to the dynamic stiffness is significant. It restrains the swelling tendency of the proteoglycans and therefore limits the degree to which the constructs "bulge" in the radial direction. The interpretation of the individual effects of the development of collagen and glycosaminoglycans is difficult because of the unconfined nature of these mechanical measurements. Nevertheless, now there is mechanical evidence of enhanced structural integrity that correlates with the previously established histological and biochemical indices of growth.

The only apparent difference between the stiffness measured for the 26-day and 33-day constructs occurs at the low frequency limit. Although there is a 1.5-fold increase in the ~0.002Hz stiffness, the increase in the biochemical measurements of glycosaminoglycan or collagen is relatively small. Although the content of structural molecules is important, the degree to which the matrix molecules interact with one-another (e.g., chemical binding reactions or stearic obstructions) must be considered. The construct's resistance to compression could possibly be enhanced if the collagen network had evolved such that it either (a) more efficiently entrapped the proteoglycans, (b) the degree of cross-linking among the collagen fibers increased (thereby increasing the construct's tensile strength), or (c) the extracellular matrix was more uniformly distributed throughout the sample (constructs stained with safronin-O appear more spatially-uniform with time). It is difficult to speculate as to why the higher frequency stiffness measurements are similar. Could it be that flow restrictions remain unchanged even when the matrix has been significantly re-organized?

Another consideration is that the difference in the low-frequency measurements is attributable to a procedural artifact. Note that for the data in Figure E.1 the frequencies that were tested change from one time-point to the next; the 26-day stiffness was measured at 0.002Hz and the 33-day at 0.004Hz. The different testing frequencies, which were unintentionally changed, might have significantly altered the apparent frequency response of the constructs. Thus, since it

was not directly compared, we cannot exclude the possibility that the 0.004Hz stiffness of 26-day and 33-day constructs were actually equal.

Comparison of the dynamic stiffness of cartilage constructs to that of normal cartilage is important, especially given that tissue morphogenesis is of clinical significance. Figure E.3 depicts the dynamic stiffness of femoropatellar groove-derived cartilage explants (4mm-diameter, ~2mm-thick) with that of the 33-day constructs. The constructs are significantly less stiff than cartilage explants. Although the mechanical development of the tissue constructs has been observed up to 33 days in cultivation, it is obvious that the construct extracellular matrix is lacking the fluid restrictions of normal cartilage.

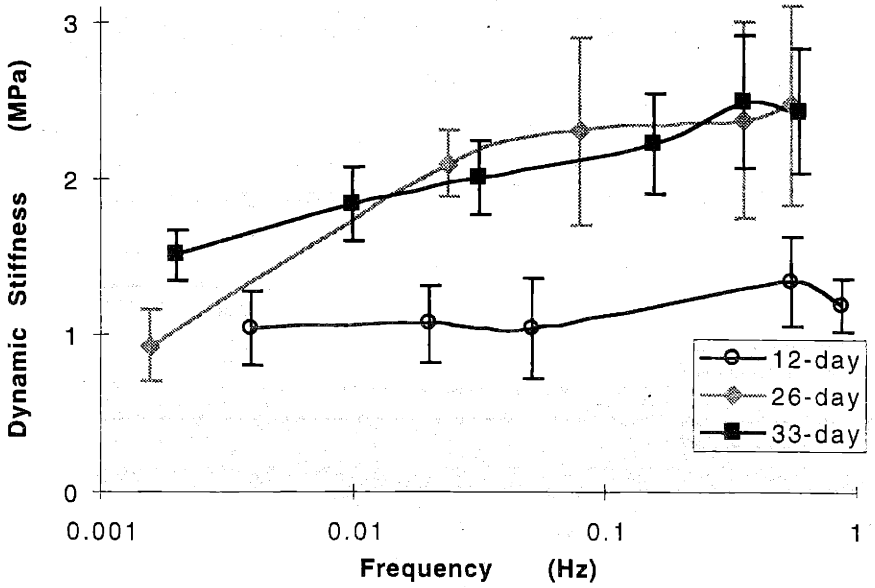

Figure E.1: The dynamic stiffness of tissue-engineered cartilage constructs was observed to change with cultivation time. Samples were removed from their bioreactors at three time points and prepared into cylindrical discs (~4mm-diameter, 2-3mm-thick); constructs were sampled at 12 days (n=4), 26 days (n=3), and 33 days (n=5).

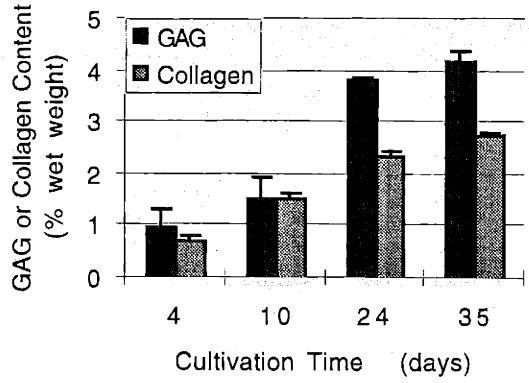

Figure E.2: Biochemical measurements of glycosaminoglycan and collagen content (mean of three samples plus the standard deviation of the mean, relative to the wet weight of the sample). Time points 4, 10, and 24 are of one study and time point 35 if of a second study. Samples were assayed immediately after harvesting and were never cultured in media. Collagen content, which represents types I and II, was determined by the hydroxyproline assay and glycosaminoglycan content was assessed with the DMB assay. The data, from other samples that were not studied mechanically, is provided to illustrate the increase in glycosaminoglycan and collagen fractions with cultivation time (manuscript in preparation, authored by L. Freed and G. Vunjak-Novakovic). The authors report that in normal cartilage they found typical values of 10.7±3.6% collagen and 8.9±2.1% glycosaminoglycan contents.

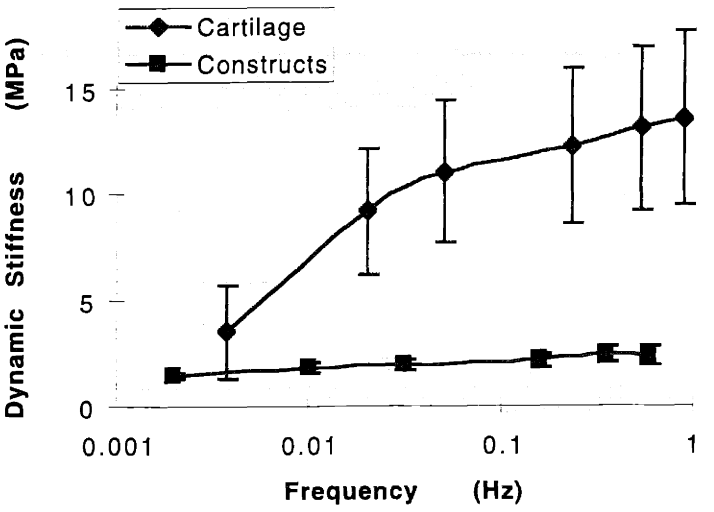

Figure E.3: The dynamic stiffness of untreated cartilage explants (n=23) and 33-day tissue-engineered cartilage constructs (n=5). Calf femoropatellar groove cartilage was prepared into 4mm-diameter, 2mm-thick discs and cultured for two days in the TCS before the stiffness measurement. The construct data is from Figure E.1.

References

Armstrong, C., Lai, W., and Mow, V. (1984). "An Analysis of the unconfined compression of articular cartilage." *J Biomech Eng*, 106, 165-173.

Arner, E., and Pratta, M. (1989). "Independent effects of interleukin-1 on proteoglycan breakdown, proteoglycan synthesis, and prostaglandin E2 release from cartilage organ culture." *Arthritis and Rheumatism*(32), 288-297.

Bader, D., Kempson, G., Egan, J., Gilby, W., and Barrett, A. (1992). "The effects of selective matrix degradation on the short-term compressive properties of adult human articular cartilage." *Biochimica et Biophysica Acta*(1116), 147-154.

Bedard, P.-A., and Golds, E. (1993). "Cytokine-induced expression of mRNAs for chemotactic factors in human synovial cells and fibroblasts." *Journal of Cellular Physiology*(154), 433-441.

Biswal, S. (1996). "The combined effects of interleukin-1ß and mechanical compression on the spatiotemporal distribution of glycosaminoglycans in calf epiphyseal cartilage," Doctor of Medicine, Harvard and MIT, Cambridge.

Bonasser, L., Paguio, C., Frank, E., Jeffries, K., Moore, V., Lark, M., Caldwell, C., Hagmann, W., and Grodzinsky, A. (1994). *Effects of matrix metalloproteinases on cartilage biophysical in vitro and in vivo*, The Annals of the New York Academy of Sciences.

Buckwalter, J., Hunziker, E., Rosenberg, L., Coutts, R., Adams, M., and Eyre, D. (1988). "Articular cartilage: composition and structure." Injury and Repair of the Musculoskeletal Soft Tissue, 405-425.

Bullough, P. (1992). "The Pathology of Osteoarthritis." Osteoarthritis: Diagnosis and Medical/Surgical Management, R. Moskowitz, D. Howell, V. Goldberg, and H. Mankin, eds., WB Saunders Co, Philadelphia PA, 39-69.

Campbell, I., Golds, E., Mort, J., and Roughley, P. (1986). "Human articular cartilage secretes characteristic metal-dependent proteinases upon secretion by mononuclear cell factor." *Journal of Rheumatology*(13), 20-27.

Chang, D. (1992). "Coupled effects of human interleukin-1ß protein and mechanical forces on the physical and metabolic properties of cartilage explants," Master of Science, MIT, Cambridge.

Cho, N. (1996). "Analysis of the Tissue Compression System." , MIT, Cambridge.

Clinton, S., Fleet, J., Loppnow, H., Salomon, R., Clark, B., Cannon, J., Shaw, A., Dinarello, C., and Libby, P. (1991). "Interleukin-1 gene expression in rabbit vascular tissue in vivo." *American Journal of Pathology*, 138(4), 1005-1014.

Demczuk, S., Baumberger, C., Mach, B., and Dayer, J. (1987). "Expression of human IL-1 alpha and beta messenger RNAs and IL-1 activity in human peripheral blood mononuclear cells." *J Mol Cell Immunol*(5), 255.

Dinarello, C. (1991). "Interleukin-1 and interleukin-1 antagonsim." *Blood*, 77(8), 1627-1652.

Duff, G., Dickens, E., Wood, N., and al, e. (1988). "Immunoassay, bioassay and in situ hybridisation of monokines in human arthritis." Progress in Leucocyte Biology, M. Powanda, J. Oppenheim, M. Kluger, and C. Dinarello, eds., Liss, New York, 387-392.

Farndale, R., Buttle, D., and Barrett, A. (1986). "Improved quantification and discrimination of sulphated glycosaminoglycans by use of dimethylmethylene blue." *Biochim Biophys Acta*(883), 173-177.

Farnum, C., Turgai, J., and Wilsman, N. (1990). "Visualization of living terminal hypertrophic chondrocytes of growth plate cartilage in situ by differential interference contrast microscopy and time-lapse cinematography." *Journal of Orthopaedic Research*, 8(5), 750-763.

Ferry, J. (1970). *Viscoelastic Properties of Polymers*, Wily, NY.

Frank, E., and Grodzinsky, A. (1987). "Cartilage electromechanics-II: a continuum model of cartilage electrokinetics and correlation with experiments." *J Biomechanics*, 20(6), 629-639.

Frank, E., Grodzinsky, A., Koob, T., and Eyre, D. (1987). "Streaming potential: a sensitive index of enzymatic degradation." *Journal of Othopaedic Research*, 5(4).

Freed, L., and Vunjak-Novakovic, G. (1995). "Cultivation of cell-polymer tissue constructs in simulated microgravity." *Biotechnology and Bioengineering*, 46, 306-313.

Goldring, M., and Goldring, S. (1991). "Cytokines and cell growth control." *Critical Reviews in Eukaryotic Gene Expression*, 1(4), 301-326.

Gray, D., and Morris, P. (1987). "The use of fluorescein diacetate and ethidium bromide as a viability stain for isolated Islets of Langerhans." *Stain Technology*, 62(6).

Gray, M., Pizzanelli, A., Grodzinsky, A., and Lee, R. (1988). "Mechanical and physicochemical determinants of the chondrocyte biosynthetic response." *Journal of Orthopaedic Research*, 6(6), 777-792.

Heinegard, D., and Oldberg, A. (1989). "Structure and biology of cartilage and bone matrix noncollagenous macromolecules." *FASEB J*(3), 2042-2051.

Hirsch, C. (1944). *Acta Chir. Scand. Suppl.*(83).

Hubbard, J., Steinberg, J., Bednar, M., and Sledge, C. (1988). "Effect of purified human interleukin-1 on cartilage degradation." *Journal of Orthopaedic Research*, 6(2), 180-187.

Hughes, C., Murphy, G., and Hardingham, T. (1991). "Metalloprotease digest of cartilage proteoglycan: pattern of cleavage by stromelysin and susceptibility to collagenase." *Biochemical J*(297), 733-739.

Hunziker, E., Hermann, W., and Schenk, R. (1982). "Improved cartilage fixation by ruthenium hexamine trichloride (RHT)." *J Ultrstruct Res*(81), 1-12.

Hunziker, E., Hermann, W., and Schenk, R. (1983). "Ruthenium hexamine trichloride (RHT) - mediated interaction between plasmalemmal components and pericellular matrix proteoglycans is responsible for the preservation of chondrocytic plasma membranes in situ during cartilage fixation." *J Histochem Cytochem*, 31(6), 717-727.

Jayapal, V., Sharmila, K., Selvibai, G., Thyagarajan, S., Shanmugasundaram, N., and Subramanian, S. (1991). "Fluorescein diacetate and ethidium bromide staining to determine the viability of Mycobacterium smegmatis and Escherichia coli." *Lepr Rev*, 62, 310-314.

Jurvelin, J., Saamanen, A.-M., Arokoski, J., Helminen, H., Kiviranta, I., and Tammi, M. (1988). "Biomechanical properties of the canine knee articular cartilage as related to matrix proteoglycans and collagen." *Engineering in Medicine*, 17(4), 157-162.

Keilhoff, G., and Wolf, G. (1993). "Comparison of double fluorescence staining and LDH-test for monitoring cell viability in vitro." *Neuropharmacology and Neurotoxicology*, 5(2), 129-132.

Kempson, G., Muir, H., Swanson, S., and Freeman, M. (1970). "Correlations between stiffness and the chemical constituents of cartilage on the femoral head." *Biochim. Biophys. Acta*(215), 70-77.

Kempson, G., Tuke, M., Dingle, J., Barrett, A., and Horsfield, P. (1976). "The effects of proteolytic enzymes on the mechanical properties of adult articular cartilage." *Biochimica et Biophysica Acta*(428), 741-760.

Kim, Y.-J. (1989). "Radially Unconfined Compression of Poroelastic Media with Axisymmetric Boundary Conditions," Master of Science, M.I.T., Cambridge.

Lai, A. (1993). "Effects of recombinant human interleukin-1 beta and mechanical compression of the physical and metabolic properties of calf epiphyseal cartilage," Doctor of Medicine, Harvard and MIT, Cambridge.

Lee, R., Frank, E., Grodzinsky, A., and Roylance, D. (1981). "Oscillitory Compression Behavior of Articular Cartilage and its Associated Electromechanical Properties." *J Biomech Eng*, 103(November), 280-292.

MacNaul, K., Chartrain, N., Lark, M., Tocci, M., and Hutchinson, N. (1990). "Discoordinate expression of stromelysin, collagenase, and tissue inhibitor of metalloproteinases-1 in rheumatoid synovial fibroblasts." *J Biol Chem*(265), 17238-17245.

Maroudas, A. (1979). "Physicochemical Properties of Articular Cartilage." Adult Articular Cartilage, M. Freeman, ed., Pitman Medical Publishing Co Ltd., Kent, England, 215-290.

Morales, T., and Hascall, V. (1989). "Effects of interleukin-1 and lipopolysaccharides on protein and carbohydrate metabolism in bovine articular cartilage and organ culture." *Connective Tissue Research*, 19, 255-275.

Ohya, T., and Kaneko, Y. (1970). "Novel hyaluronidase from streptomyces." *Biochim. Biophys. Acta*(198), 607-609.

Parsons, J., and Black, J. (1987). "Mechanical behavior of articular cartilage Quantitative changes with enzymatic alteration of the proteoglycan fraction." *Bull Hosp Jt Dis Orthop Inst*, 47(1), 13-30.

Quinn, T. (1996). "Articular Cartilage: Matrix Assembly, Mediation of Chondrocyte Metabolism, and Response to Compression," Doctoral, Harvard University and the Massachusetts Institute of Technology, Cambridge.

Rosenberg, L., Hellman, W., and Kleinschmidt, A. (1975). "Electronmicroscopic studies of proteoglycan aggregates from bovine articular cartilage." *J Biol Chem*(250), 1877-1883.

Sah, R., Grodzinsky, A., Plaas, A., and Sandy, J. (1992). *Articular Cartilage and Arthritis*, Raven Press, Ltd., New York.

Schmidt, M., Mow, V., Chun, L., and Eyre, D. (1990). "Effects of proteoglycan extraction on the tensile behavior of articular cartilage." *Journal of Orthopaedic Research*, 8(3), 353-363.

Smith, A., and Smith, H. (1989). "A comparison of fluorescein diacetate and propidium iodide staining and in vitro excystation for determining giardia intesinalis cyst viability." *Parasitology*, 99, 329-331.

Smith, R., Allison, A., and Schurman, D. (1989). "Induction of articular cartilage degradation by recombinant interleukin 1α and 1ß." *Connective Tissue Research*, 18, 307-316.

Thompson, S. (1966). *Selected Histochemical and Histopathological Methods*, Springfield.
Thurston, C., Hardingham, T., and Muir, H. (1975). "The kinetics of degradation of chondroitin sulphates and hyaluronic acid by chondroitinase from proteus vulgaris." *Biochem. J.*(145), 397-400.

Wood, D., Ihrie, E., and Hammermann, D. (1985). "Release of interleukin-1 from human synovial tissue in vitro." *Arthritis and Rheumatism*(28), 853-862.

Wuthier, R. (1968). "Lipids of mineralizing epiphyseal tissues in the bovine fetus." *Journal of Lipid Research*, 9, 68-78.